2007

Development of Fluorescent Chemosensors Based on Energy Transfer in End-Capped Pi-Conjugated Systems

Huating Zhang
Louisiana State University and Agricultural and Mechanical College, hzhang7@lsu.edu

DEVELOPMENT OF FLUORESCENT CHEMOSENSORS BASED ON ENERGY TRANSFER IN END-CAPPED π-CONJUGATED SYSTEMS

A Thesis

Submitted to the Graduate Faculty of the
Louisiana State University and
Agricultural and Mechanical College
in partial fulfillment of the
requirement for the degree of
Master of Science

in

The Department of Chemistry

By
Huating Zhang
B.S., Shangxi Medical University, 2001
May, 2007

DEDICATION

To my parents,

Runlin Zhang, Yan’E Qian

To my husband,

Youjun Yang

ACKNOWLEDGMENTS

Mom and Dad, thank you giving me life, love, education. Thank you, all my sisters, for your unconditional supports all the time.

Next, I would like to thank my research advisor, Dr. Evgueni E. Nesterov, for affording me the opportunity to work in his group. Thank you for guiding me in my research and for always being there to help and support me. I would also like to thank the members (past and present) of the Nesterov Research Group.

Special thanks are extended to Dr. Garno and Dr. Taylor for being my committee members.

I thank Hairong for help with MALDI-TOF and mostly importantly for your friendship. I'd also like to recognize Jieren Li for your encouragement all the time. I am very appreciated.

I'd also like to thank Dr. Crowe and Dr. Hammer for your excellent teaching.

Last, I want to thank my husband for help with everything.

TABLE OF CONTENTS

DEDICATION……..ii

ACKNOWLEDGMENTS……iii

LIST OF FIGURES……..……..v

LIST OF SCHEMES……..……vi

LIST OF ABBREVIATIONS……..…….....vii

ABSTRACT…….……..ix

I. THE HISTORY OF CONJUGATED POLYMERS ……..…....1

II. APPLICATIONS OF CPS IN SENSORY SYSTEMS UTILIZING ENERGY TRANSFER…….3

III. EXPERIMENTAL DESIGN…….....…....6

IV. RESULTS AND DISCUSSION…….....…....9
- A. Synthetic Attempts toward **1**……..……..……10
- B. Synthesis of Fragment A……11
- C. Synthesis of Fragment B……13
- D. Attempts to Couple All Three Fragments……..15
- E. Attempt with the Hexyl Substituted Derivative……..22
- F. Synthesis of Silica Supported Conjugated Polymer ……23
- G. Synthesis of a Monomer for a Water Soluble Boronic Acid Functionalized Conjugated Polymer…….……..25
- H. Synthesis of Long Wavelength (Near-Infrared) Dye……27

V. CONCLUSION……..29

VI. EXPERIMENTAL……..…30

REFERENCES…….…….....….....40

APPENDIX: CHARACTERIZATION DATA..……...42

VITA…….83

LIST OF FIGURES

Figure 1. Structure of polyacetylene……..…….……1

Figure 2. Structures of common conjugated polymers…….……1

Figure 3. The basics of semiconductor……..……...2

Figure 4. The above poly(phenylene enthynylene) displays a dominant terminus emission resulted from fast energy migration from backbone……..4

Figure 5. Mechanistic difference between Forster and Dexter energy transfer……5

Figure 6. General design of molecular sensor self-assembled on solid support…….7

Figure 7. ^{1}H NMR spectrum of Fragment A in $CDCl_3$……..12

Figure 8. Absoption and emission spectra of fragment B in $CHCl_3$……...…15

Figure 9 MALDI-TOF of compound **18**…….……15

Figure 10. ^{1}H NMR of the Fragment B in $CDCl_3$……16

Figure 11. ^{1}H NMR of **22** in $CDCl_3$……19

Figure 12. Overlay of the spectra of **20**, **21** and fragment C……19

Figure 13. Absorption and emission of **22** in $CHCl_3$……20

Figure 14. ^{1}H NMR spectrum of **24** in $CDCl_3$……...…….21

Figure 15. Comparasion of the absorption and emission **24** and **20**……21

Figure 16. ^{1}H NMR of **35** in $CDCl_3$……23

Figure 17. Overlay of the absorption and emission spectra of **20** and **36**……..24

Figure 18. Comparison of the solution fraction and the silica particle fraction……..25

LIST OF SCHEMES

Scheme 1. The geometry change of polythiophene ……..4

Scheme 2. Designed sensor **1** and its signaling mechanism……..9

Scheme 3. The self assembling of terminal alkene……10

Scheme 4. Retrosynthetic analysis of compound **1**……..10

Scheme 5. Sonogashira Coupling catalyzed by Pd(II) catalyst……11

Scheme 6. Mechanism of the Sonogashira coupling. (request permission)……..11

Scheme 7. Synthesis of fragment A……..……12

Scheme 8. Synthesis of Fragment B……13

Scheme 9. Synthesis of a tetramer analog (**22**) of compound **1**…….17

Scheme 10. Synthetic Attempts toward **1**……20

Scheme 11. Toward the synthesis of *n*-Hexyl substituted oligomers……22

Scheme 12. Synthesis of silica based conjugated polymer sensor **44**……..…26

Scheme 13. Retrosynthetic analysis of polymer **45**…….27

Scheme 14. Attempts to synthesize monomer **42**……..27

Scheme 15. New route for the synthesis of monomer **48**……..28

Scheme 16. Synthesis of long wavelength dye…….28

LIST OF ABBREVIATIONS

$B(OH)_2$	Boronic acid
Br	bromide
Br_2	bromine
$CDCl_3$	Deuterated chloroform
$CHCl_3$	Chloroform
CN	nitrile
COOH	carboxylic acid
CP	Conjugated Polymer
CuI	Cupper (I) iodide
DCM	Dichloromethane
E-PAD	Electronic Paper Display
Et	Ethyl
h	hours
Hex	Hexyl
I	iodide
I_2	iodine
i-Pr_2NH	di-isopropylamine
K_2CO_3	potassium carbonate
KOH	potassium hydroxide
LED	Light Emitting Diode
MALDI-TOF	Matrix-Assisted Laser Desorption/Ionization Time-Of-Flight
Me	Methyl
MeMgI	Methyl Magnisium iodide
MeO	Methoxy
MeOH	Methanol
min	minutes
$Na_2S_2O_4$	Sodium hydrosulfite
Na_2SO_3	Sodium sulfite
$NaIO_4$	Sodium periodate
n-BuLi	*n*-butyllithium
NH_2	Amino
NMR	Nuclear Magnetic Resonance
NR_3	Triarylamine
OH	Hydroxyl
OLED	Oganic Light Emitting Diode
$P(t\text{-}Bu)_3$	Tritertbutylphosphine
PAn	Polyaniline
$Pd(PhCN)_2Cl_2$	Bis(benzonitrile)palladium(II) chloride
$Pd(PPh_3)_4$	Tetrakis(triphenylphosphine)palladium(0)
Ph	Phenyl
PPE	Poly(phenyleneethynylene)

PPh_3	Triphenylphosphine
ppm	parts per million
PPy	Polypyrrole
PT	Polythiophene
PTSA	para-Toluenesulphonic acid
R	Alkyl
rt	room temperature
SH	thiol
TBDMS	Tertbutyldimethylsilyl
TIPS	Triisopropylsilyl
TMS	Trimethylsilyl
Ts	Tosylate
TsCl	Tosylate chloride
UV-Vis	Ultra violet-visible

ABSTRACT

A novel sensory platform based on conjugated polymer was developed, that consists of a monodispersed oligo(phenylene ethynylene) backbone, end-capped with a terminal alkene for further attachment to a solid surface at one terminus, and an anthracene based receptor group at the other terminus. Energy transfer from backbone to end-cap was observed by absorption spectroscopy and fluorescence spectroscopy. Other ongoing projects described herein include the synthesis of longer-chain analogues of the above platform, the synthesis of silica microspheres based conjugated polymer sensory platform and the synthesis of long wavelength (NIR) dye for *in vivo* amyloid screening studies.

I THE HISTORY OF CONJUGATED POLYMERS

The Nobel Prize in Chemistry in 2000 was awarded to Heeger, MacDiarmid and Shirakawa to acknowledge their discovery and development of conductive polymer, an oxidized polyacetylene (Figure 1), synthesized from polymerization of acetylene. They found that polyacetylene will become $1x10^{10}$ times more conductive after oxidation by I_2, a process called doping. This metal-like property has drastically changed our conventional understanding towards plastic material, to which conductive polymer belongs.[1]

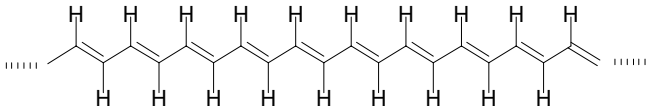

Figure 1. Structure of polyacetylene.

A variety of different conductive polymers were developed and have found wide practical applications in electronic and optical devices, light emitting diodes (LED), corrosion protection, photovoltaic cells and sensory devices, photodetectors, field-effect transistors, etc.[2] A few representative examples such as poly(phenylene vinylene) (PPV), poly(phenylene ethynylene) (PPE), polythiophenes (PT), polypyrrole (PPy) and polyaniline (PAn) are shown in Figure 2.

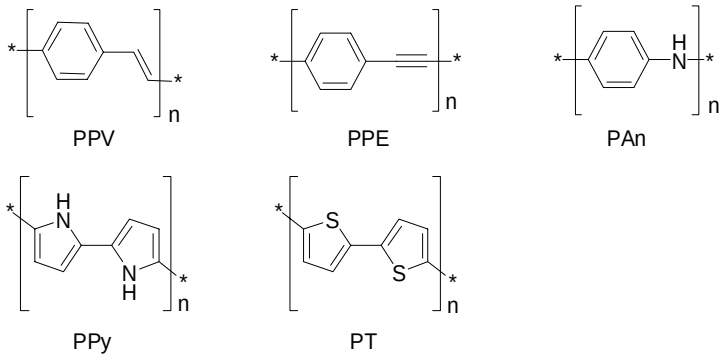

Figure 2. Structures of common conjugated polymers.

However, scientists currently show greater enthusiasm towards the less conductive, undoped form of conjugated polymers since conjugated polymer was found to display electroluminescence after voltage is applied. This property has rendered conjugated polymers as effective candidates for polymer light emitting diodes (PLED). Compared to their traditional inorganic LED analogs, PLED has significant advantages. First, ink-jet printing technology can be applied for processing plastic soluble polymers. Second, the devices can be flexible. The research toward the development of flexible large area display and Electronic Paper Display (E-PAD) are intensively sought-after.[3] The electroluminescent property originates from the fact that conjugated polymers are semiconductors. Upon excitation, an electron of the valence band of conjugated polymer is excited to the conduction band. The resulting vacancy in the valence band is termed "hole". This bound electron-hole pair, excited state of conjugated polymer, is called "exciton" and it generates fluorescence because the recombination of the electron and hole leads to the emission of a photon. By varying the structure of conjugated polymer, the wavelength of emission covers a wide range of the spectrum from ultra-violet, to visible, to near infrared.

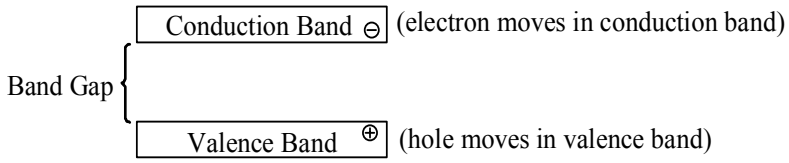

Figure 3. The basics of the electronic structure of a semiconducting polymer.

II APPLICATIONS OF CPs IN SENSORY SYSTEMS UTILIZING ENERGY TRANSFER

In recent years, conjugated polymer-based sensory systems have attracted attention due to their signal amplification effects after T. M. Swager proposed the concept of a molecular wire in 1995.[4] Signal amplification originates from the transport properties of conjugated polymers. Transport properties refer to the fact that binding of the analyte to one or a minimal number of receptors in conjugated polymers is enough to result in a measurable macro-property disturbance. Electrical conductivity (resistivity) and fluorescence (based on fast energy migration) are two properties most readily monitored.

Electrical conductivity is very sensitive to the molecular structures and conformation changes of the conjugated polymers and can be precisely monitored by relatively simple instrumentation. For example, polypyrrole is 10 thousand times more conductive compared to its *N*-methyl analog.[5] The sterics induced by the *N*-methyl group cause the adjacent pyrrole rings not to be co-planar, and consequently this affects the delocalization of the electrons in the poly pyrrole backbone. The effective delocalization is also dependent on the conformational change of the backbone caused by binding to analytes. An example is polythiophene with a crown-ether macrocycle tethered to two adjacent thiophene units. In the presence of alkali metal ions, depending on the macrocycles present, different thiophene units adopt a planar geometry. Upon coordination with metal ions, adjacent thiophene units will no longer be co-planar. This twisted geometry leads to significant conductivity alternation.[6]

The end group of a polymer is generally not taken into consideration. However, the end group of a rigid-rod conjugated polymer can play an important role in signal amplification. After excitation by light, the exciton rapidly migrates to an end group, which has a lower band-gap.

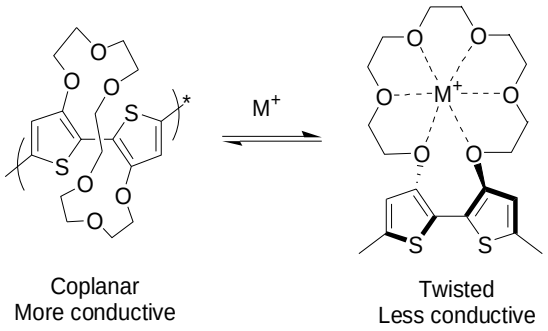

Scheme 1. The geometry change of polythiophene upon coordination with alkali metal ions.

Recombination of electrons and holes leads to longer wavelength emission. It was reported that the emission from the end capped group can be dominant.[7] For example, an anthracene end-cap in the following conjugated polymer has a lower band-gap compared to its PPE backbone. Emission from the anthracene comprises 95% of total emission, which results from the fast energy migration from the polymer backbone to the low band-gap terminus (Figure 4).[8]

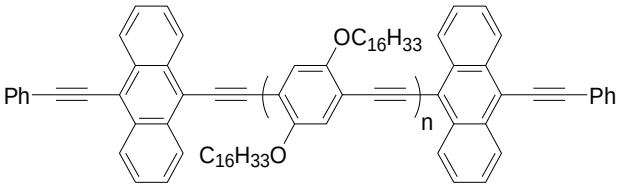

Figure 4. The above poly(phenylene ethynylene) displays a dominant anthracene emission resulting from fast energy migration from the backbone.

There are two possible pathways for the energy migration in conjugated polymers: Förster energy transfer[9] or Dexter Energy Transfer.[10] Förster energy transfer can happen both intramolecularly and intermolecularly since it is a through-space energy transfer based on a dipole-induced dipole mechanism. The efficiency is proportional to $1/R^6$, where R is the distance between the donor and acceptor. In solid state applications such as fluorescent polymer thin films, Förster energy transfer is the dominant process due to the decreased intermolecular

distances. Dexter Energy Transfer occurs via an exchange mechanism, which can be seen as a simultaneous exchange of a pair of electrons occurring through interacting molecular orbitals. It requires strong electronic coupling between the donor and acceptor to compete with the Förster energy transfer process. The mechanistic difference between Förster and Dexter energy transfers is shown in Figure 5.

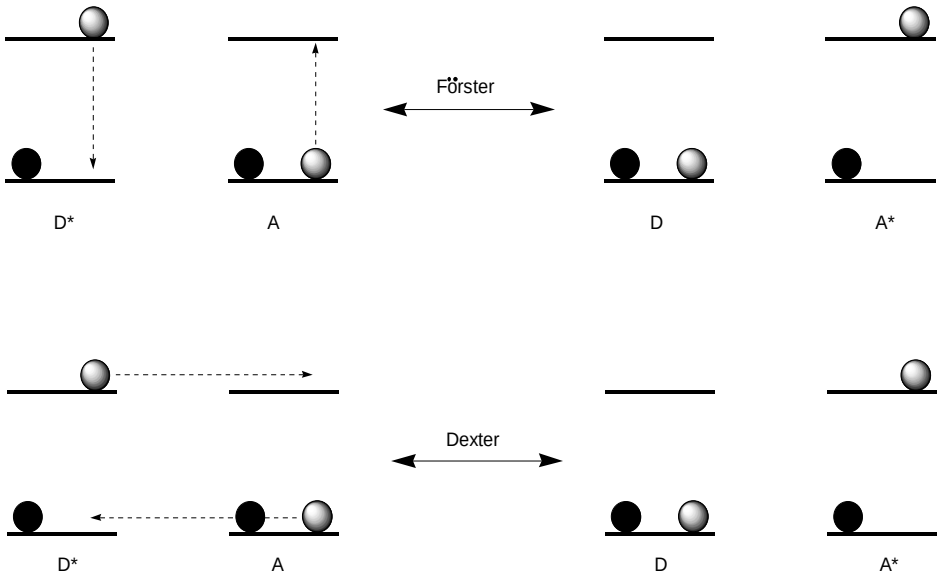

Figure 5. Mechanistic difference between Förster and Dexter energy transfer, where D is Donor, A is Acceptor, D* is the excited state of Donor and A* is the excited state of Acceptor.

Much research has been carried out to further address the energy migration mechanism in different situations. The aim of our research is to study the factors that have an effect on the photophysical properties of specially designed, conjugated polymer/oligomer and influence energy transfer pathways in these systems.

III EXPERIMENTAL DESIGN

The development of sensitive and selective templates for real-time detection of various analytes is of crucial importance for various fields including clinical, environmental and food applications, etc.[11] Fluorescence-based techniques are desirable due to their high sensitivity. Recently, substantial progress has been made in the development of small-molecule fluorescent sensors for the selective detection of a wide array of analytes ranging from ions or small molecules to large biomolecules utilizing different chemical reactions, supramolecular interactions and other non-bonding interactions between the sensor and the analyte.[12] The signaling processes are generally restricted to dilute solutions of sensors in various solvents. However, solution-based detection is harder to implement into practical devices. In contrast, solid-state fluorescent sensors can be conveniently applied in instrumentation. In addition, they are well-suited for vapor sensing.[13] However, aggregation of the fluorescent sensors in the solid state usually leads to much diminished fluorescence.[14] Furthermore, the analyte-sensor interaction is limited mostly to the film surface, since it is difficult for the analyte to diffuse into the solid film.[15] Due to these reasons, small-molecule-based solid devices are challenging to be used in practical sensing applications. Compared to small-molecule sensors, conjugated polymers (CPs) have apparent advantages such as bright fluorescence in the solid state and analyte binding amplification resulting from their excitation transport properties.

From a practical viewpoint, it is preferable for a sensory signal to exhibit a new emission at a different wavelength rather than display fluorescence quenching or enhancement of the original signal to facilitate detection. Many CP-based fluorescent turn-on sensors have been reported to date, but most of them do not operate in solid state.[15] Herein, we are designing a novel approach to building turn-on or color-changing solid-state fluorescent sensors, based on attenuation of

energy transfer in conjugated systems utilizing the self-assembled monolayer technique (Figure 6).

The core of the strategy lies in the design of the conjugated polymer system. The sensor is composed of a rigid-conjugated monodisperse oligomer core (oligophenylene ethynylene) end-

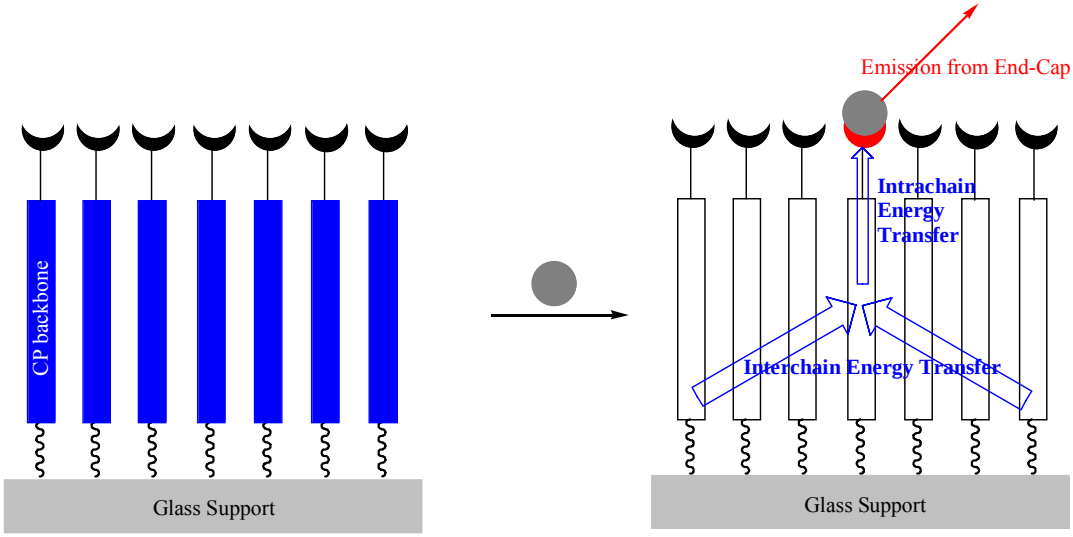

Figure 6. General design of a molecular sensor self-assembled on a solid support. Binding of an analyte results in lowering the band gap at the receptor terminus, thus directing energy migration towards the end group and enhancing its fluorescence.

capped with an anthracene based sensing group at one terminus, and a silicon-terminated linkage at the other end. The latter group can be used to covalently attach these molecules to a glass substrate through self-assembly (Scheme 3). The terminal sensing group is a π-conjugated moiety bearing a receptor for selective attachment or coordination binding with a specific analyte. Upon appropriate UV-Vis irradiation, the oligomer backbone will be selectively excited. In dilute solution, the exciton migration will occur intramolecularly both by through-bond (Dexter-type) and through-space (Förster-type) mechanisms. Efficiency will strongly depend on the relative position of the band-gap of the backbone and the HOMO-LUMO gap of the end group.

In a particular case where they are approximately equal before binding the analyte, the energy transfer towards the end group is not favorable. Short wavelength fluorescence from the oligomer backbone will be predominant. Analyte binding will lower the energy gap of the termini. At this moment, exciton migration towards the end cap will be favorable and lead to a much enhanced fluorescence emission from the end group located at a longer wavelength compared to the emission from the backbone. One can also envision an opposite situation. Prior to analyte binding, the band gap at the terminus is relatively low, therefore leading to significant emission from the end-cap. Upon binding the analyte, the energy gap of the end-cap increases, energy migration becomes less favorable, and shorter-wavelength emission from the backbone will be enhanced. In any case, the analyte binding will lead to a fluorescence wavelength change, making quantitative analytical detection accurate and simple.

The molecular sensors will be combined into a solid-state sensor device through self-assembling. The self-assembling of alkanethiol on gold surfaces is well established. Detections of various analytes including metal ions, biologically important molecules, and vapors, based on such strategies were reported.[16] However, gold usually leads to fluorescence quenching, thus forcing the use of less sensitive optical and electrochemical techniques as analyte binding transduction schemes. Recently, Reinhoudt et al. reported the self-assembling on a glass surface for sensing studies where fluorescence was not quenched by the glass support.[17]

IV RESULTS AND DISCUSSION

Compound **1** was the initially designed target of our mono-dispersed oligomer sensing platform (Scheme 2). The anthracene end-cap is functionalized with an aldehyde group for chemosensing of cysteine and homosysteine[18] Cysteine and homocysteine are the chemical stimuli which can result in the band-gap variation through reaction with an aldehyde to give a thiazolidine ring. Changes from an electron-withdrawing aldehyde group to an electron donating thiazolidine functionality increase the HOMO-LUMO gap of the end-cap so that the emission from the end-cap would decrease and that of the backbone should be enhanced. In addition to the fundamental significance of demonstrating the validity of this chemosensing platform, the choice of these particular analytes was also dictated by practical considerations. Cysteine and homocysteine are important biomolecules. Elevated levels of homocysteine are an indication of cardiovascular and Alzheimer's disease. Deficiency of cysteine is related to various diseases such as slow growth, edema, lethargy, liver damage, muscle and fat loss etc. Therefore, development of a reliable practical methodology is of crucial importance for cysteine and homocysteine detection.

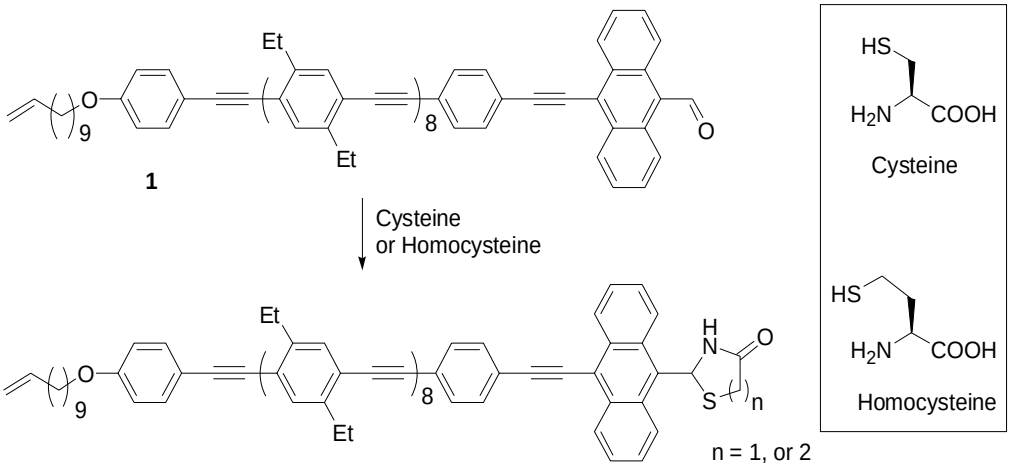

Scheme 2. Designed sensor **1** and its interaction with cysteine and homocysteine.

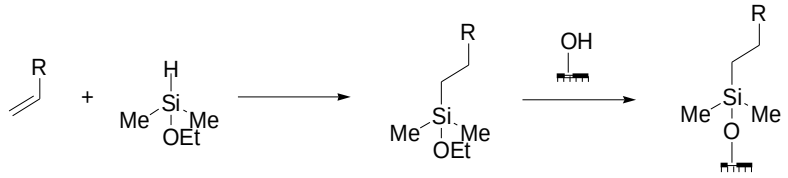

Scheme 3. An approach to chemical transformation of terminal alkenes for their self-assembly on a glass surface.

A. Synthetic Attempts toward 1.

A retrosynthetic analysis revealed that compound **1** might be assembled from three different fragments (Scheme 4) using palladium-catalyzed Sonogashira coupling (Scheme 5).[19] The catalytic cycle of Sonogashira coupling is shown in Scheme 6.

My contribution focused on the synthesis of the Fragment A and Fragment B, and assembling the target molecule by coupling between the different fragments. Fragment C was synthesized by Dr. Evgueni Nesterov.

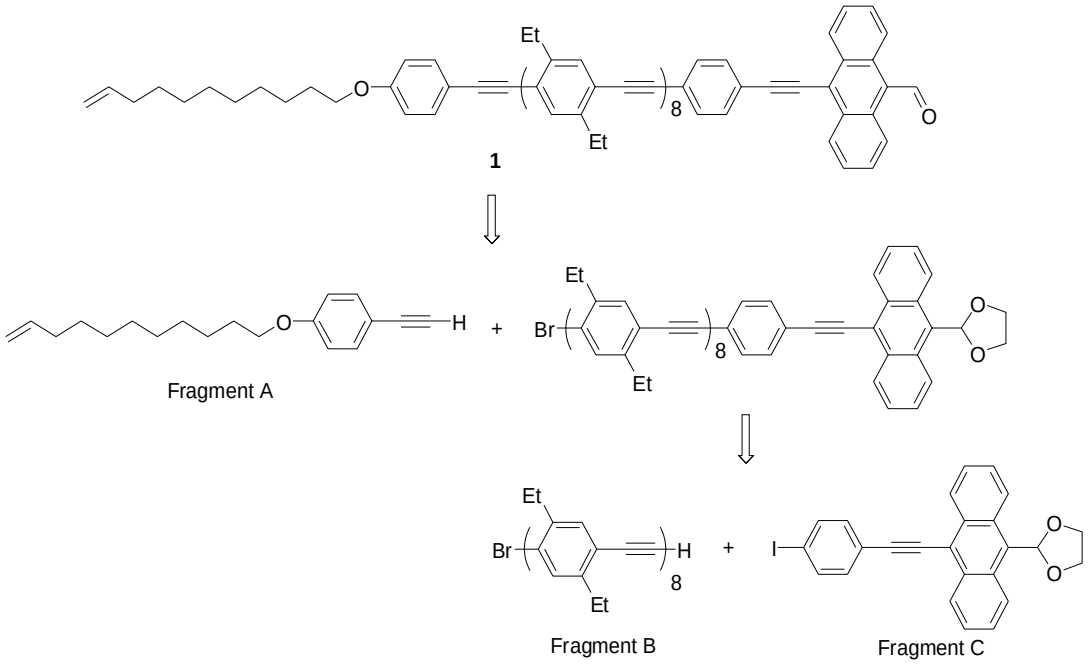

Scheme 4. Retrosynthetic analysis of compound **1**.

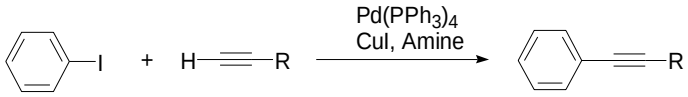

Scheme 5. An example of Sonogashira Coupling catalyzed by Pd(0) catalyst.

B Synthesis of Fragment A

10-Undecen-1-ol (**2**) reacted with TsCl in the presence of pyridine to afford **3** in 62% yield. Williamson alkylation of 4-iodophenol by tosylate **3** in the presense of K_2CO_3 furnishes **4** in 91% yield (Scheme 7). Sonogashira coupling between **4** and TMS-acetylene gives **5** in 99% yield. Desilylation of **5** by KOH in MeOH furnished the desired fragment **A** in 85%

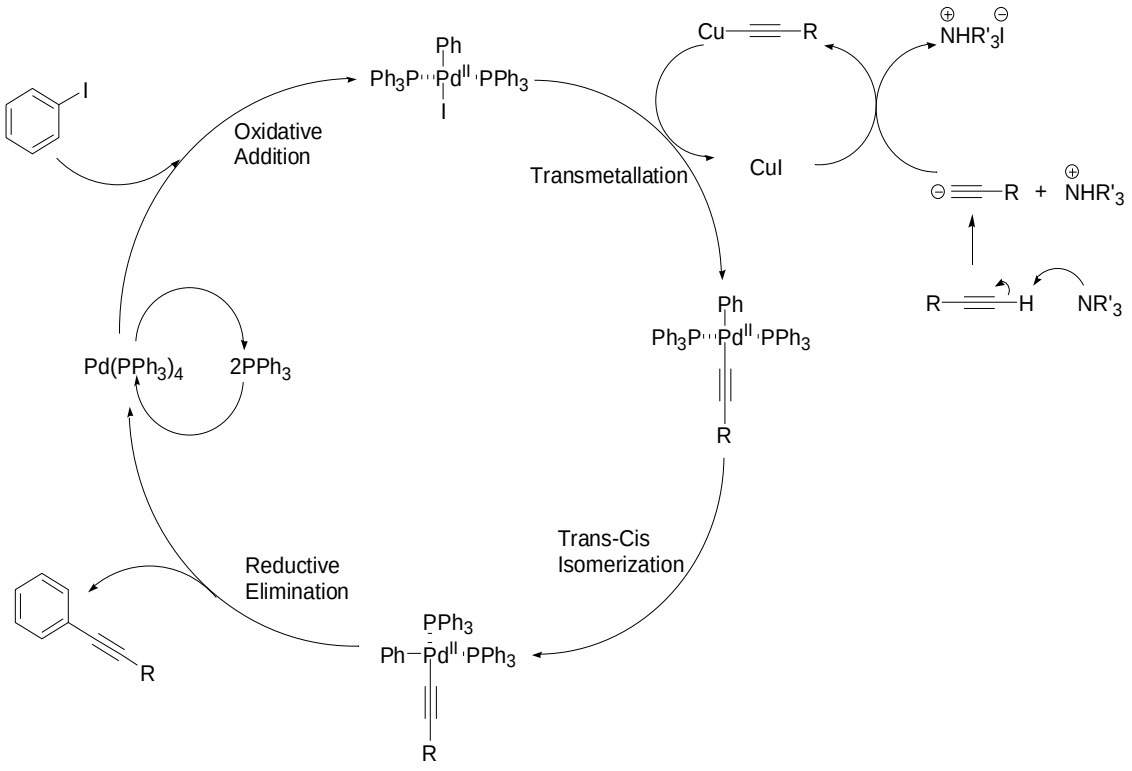

Scheme 6. Mechanism of the Sonogashira coupling.

yield. The ^{1}H NMR of fragment A is shown in Figure 7. The terminal alkyne proton has a resonance at 3.00 ppm. The three protons on the mono-substituted alkene group shows up at 5.0 ppm (2H) and 5.8 ppm (1H) respectively. The two protons on the methylene group next to the

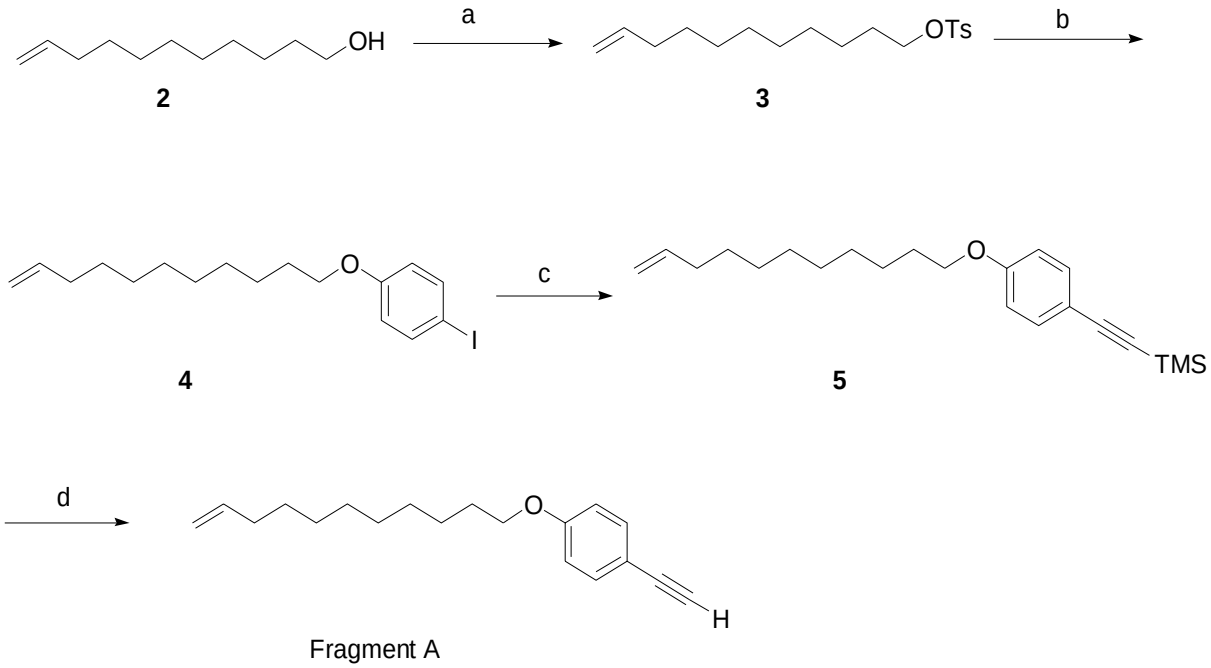

Scheme 7. a) TsCl, Pyridine, 0ºC for 2h, r.t. for 16 h, 63%, b) 4-iodophenol, K_2CO_3, 100ºC, 50 h, 91%, c) TMS-acetylene, $Pd(PPh_3)_4$, CuI, *i*-Pr_2NH,55ºC, 30 h, 99%, d) KOH, r.t., 40 min, 85%.

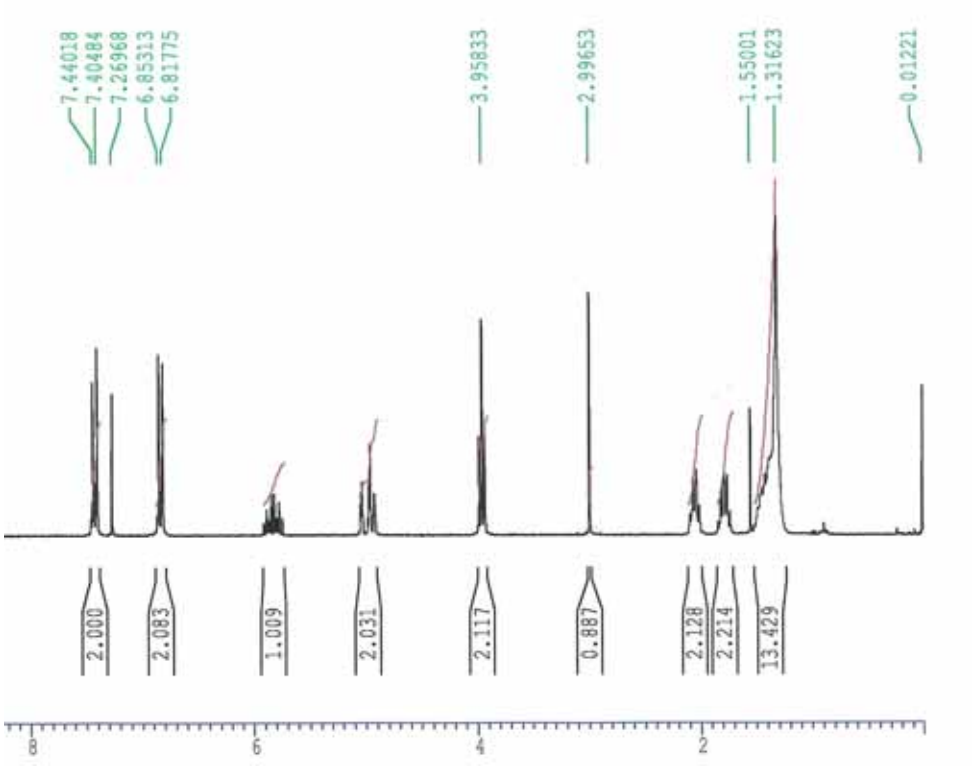

Figure 7. ^1H NMR spectrum of Fragment A in $CDCl_3$. The resonance of the alkyne proton is located at 3.00 ppm.

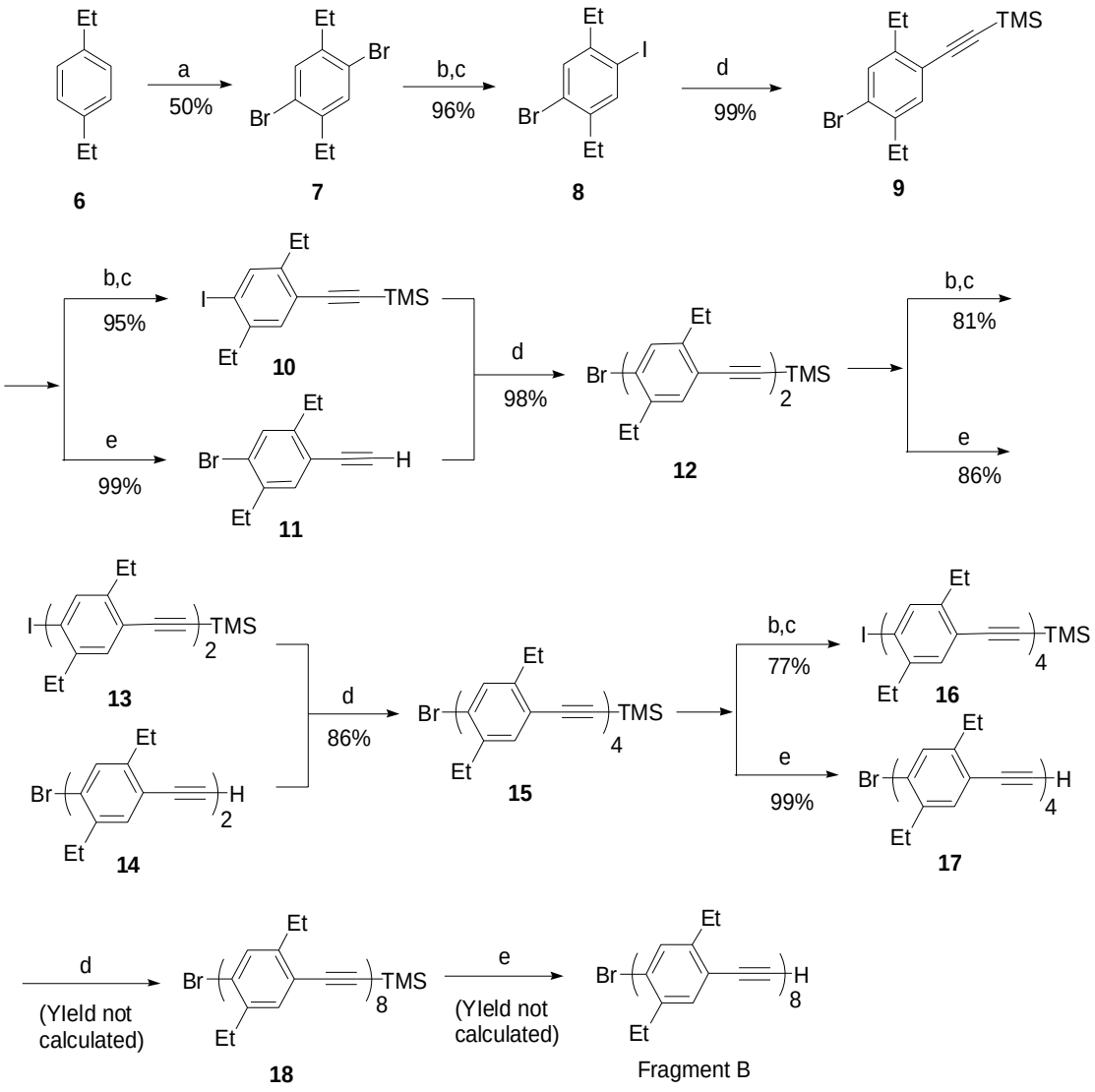

Scheme 8. Synthesis of Fragment B. a) Br_2, cat. I_2, 0ºC, 17 h, b) *n*-BuLi, -78º C, 1 h, c) I_2, -78ºC – r. t., overnight, d) TMS-acetylene, $Pd(PPh_3)_4$, CuI, *i*-Pr_2NH, 55ºC, 24 h, e) KOH, r.t., 40 min.

oxygen atom locate at 3.96 ppm. Aromatic protons show as two doublets at 6.8 ppm and 7.4 ppm. All the remaining protons from the alkyl chains locate in a range from 1.3 ppm to 2.1 ppm.

C Synthesis of Fragment B

para-Diethylbenzene **6** was brominated to afford **7** in 50% yield. Monolithiation with 1 equiv of *n*-BuLi followed by quenching with I_2 gave monoiodo compound **8** in 96% yield (Scheme 8). Sonogashira coupling between **8** and TMS-acetylene catalyzed by $Pd(PPh_3)_4$ and

CuI in the presence of diisopropylamine afforded **9** in 99% yield. To achieve a high yield, the reaction should be carried out at a relatively low (~55ºC) temperature. Under these conditions,the coupling selectively occurred at the more reactive iodine center. A similar strategy was utilized throughout the rest of the synthesis to achieve highly regioselective mono-alkynylation by Sonogashira coupling. Half of **9** was lithiated, followed by iodination, to generate **10** in 95% yield. The other half of **9** was desilylated by KOH in MeOH to produce **11** in 99% yield. Sonogashira coupling between **10** and **11** furnished **12** in 98% yield. The same procedures were followed to synthesize tetramer **15** and octamer **18** (Scheme 8). The structure of compound **18** was confirmed via MALDI-TOF. The exact mass of **18** was calculated to be 1400.72 and $[M+H]^+$ was found to be 1401.41 (Figure 9). However, due to the fact that **18** is very sticky and has very poor solubility in common organic solvents, purification via standard chromatography was not successful and **18** could not be recovered. A byproduct—a result of homocoupling of two acetylene—has similar solubilities in different solvents compared to **18** and could not be removed. Still the impure sample of **18** was subjected to desilylation by KOH in MeOH to effect fragment B. Multiple attempts to use chromatography to purify fragment B resulted in a very small fraction of relatively pure sample. Most of the product was lost in the column since no solvents could elute it down. The ^{1}H NMR spectra of fragment B is shown in Figure 10, and its UV-Vis and fluorescence spectra are shown in Figure 8. Fragment B displays a strong absorption in $CHCl_3$ with maximum at 370 nm, corresponding to the oligo(phenylene enthynylene) backbone. It is strongly fluorescent and displays an intense maximum at 415 nm with a shoulder peak at 440 nm due to aggregation.

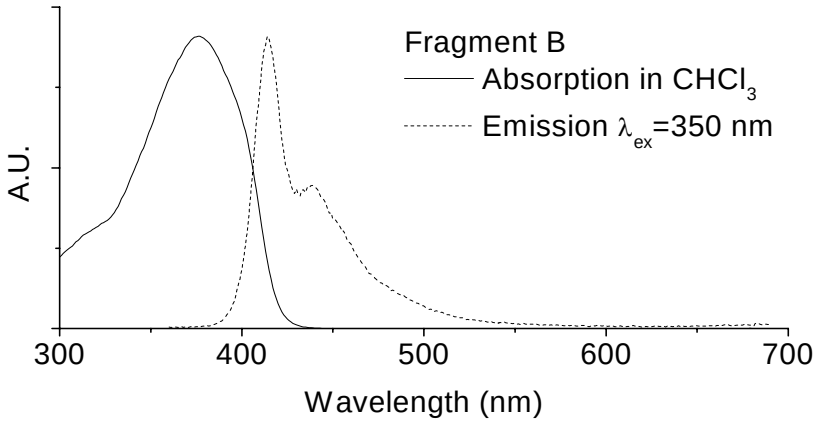

Figure 8. Absoption and emission spectra of fragment B in $CHCl_3$.

D Attempts to Couple All Three Fragments

The more soluble tetramer **16** was used to prepare Compound **22**, an analogue of

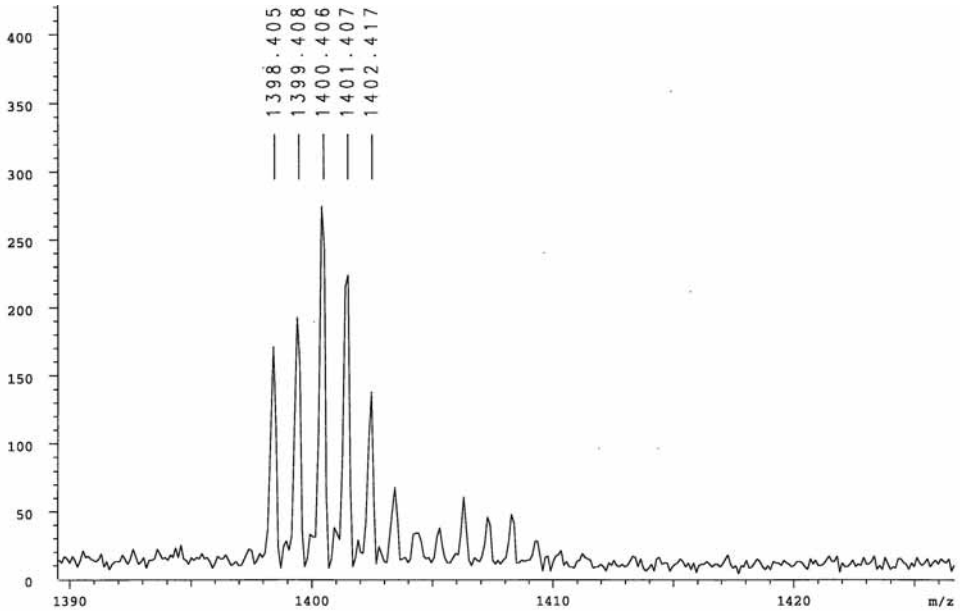

Figure 9 MALDI-TOF of compound **18**. A molecular peak $[M+H]^+$ is found at 1401.41.

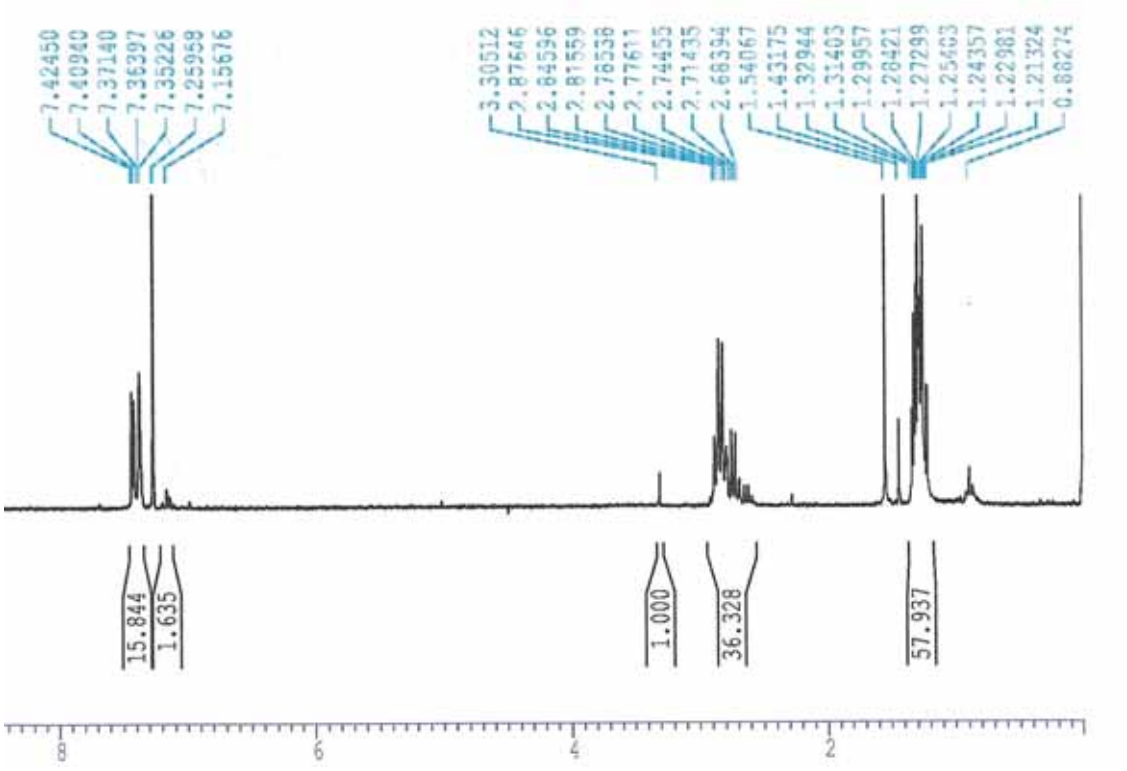

Figure 10. ^{1}H NMR of the Fragment B in $CDCl_3$. Singlet at 3.30 ppm corresponds to the terminal alkyne H.

compound **1** (Scheme 9). Compound **19** was obtained in 56% yield. TMS on **19** was removed by treating with KOH in MeOH to yield **20** in 92% yield. This was followed by coupling with fragment A to furnish compound **21** in 53% yield. Ethylene glycol acetal protection of aldehyde was removed by a catalytic amount of PTSA to generate **22** in 51% yield (Scheme 9). The ^{1}H NMR of **22** is shown in Figure 11. The aldehyde peak is located at 11.55 ppm. The terminal monosubstituted alkene peaks are located at 4.97 (2H) and 5.85 (1H) ppm. The presence of the resonances from both alkene and aldehyde confirmed the attainment of compound **22**. Sensing studies in solutions are currently ongoing. They will be followed by preparations of solid-state devices through self-assembling on a glass surface.

Compound **20** (Figure 12A) shows a strong absorption at ca. 375 nm. The corresponding emission maximum is located at 408 nm, and an additional shoulder peak from aggregation is

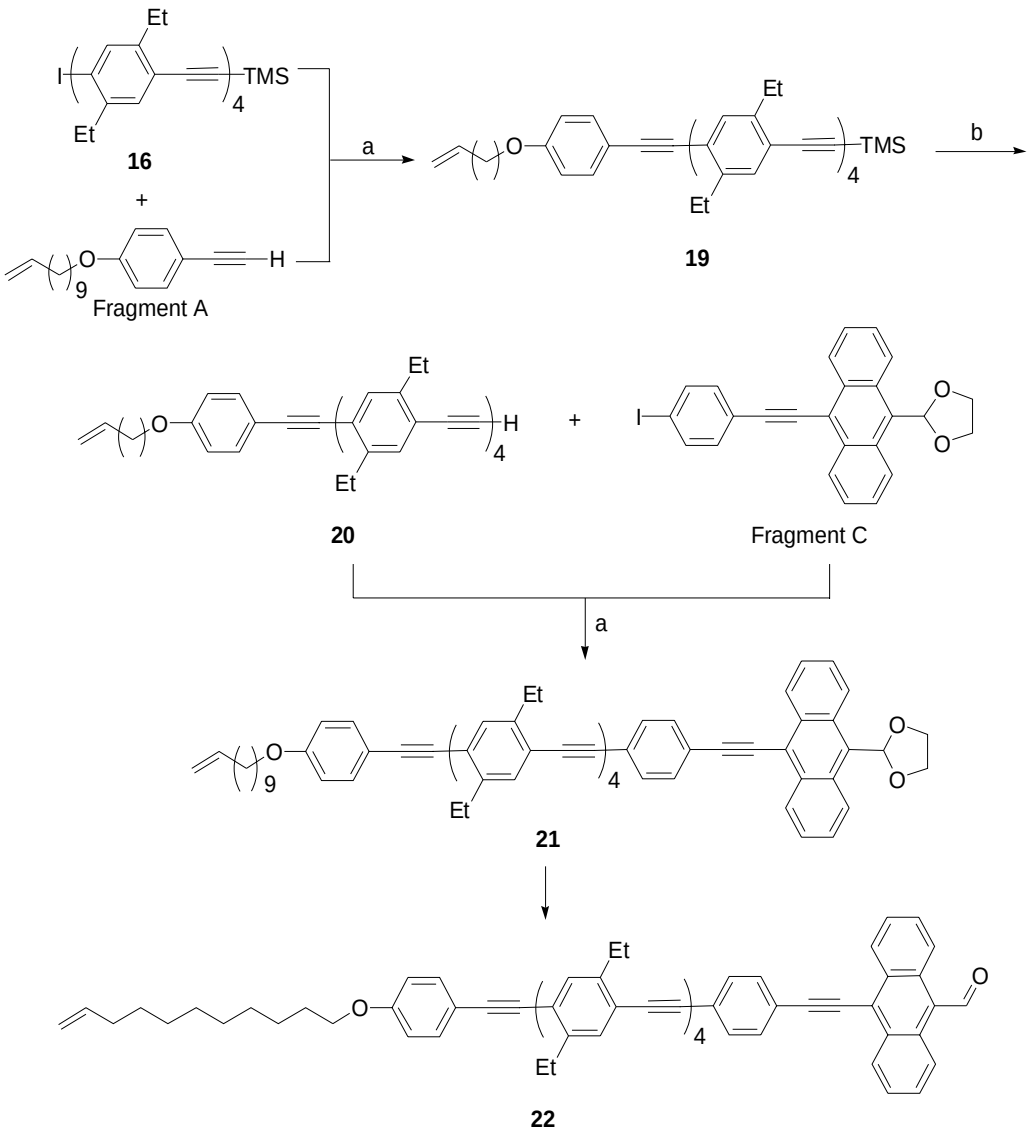

Scheme 9. Synthesis of a tetramer analog (**22**) of compound **1**. a) $Pd(PPh_3)_4$, CuI, Toluene:*i*-Pr_2NH(7:3), 55ºC, 24h, b) PTSA, rt, 12 h.

located at 430 nm. The absorption of fragment C (Figure 12B) has a strong absorption maxima corresponding to the vibronic transitions at 407 and 431 nm respectively. The emission of fragment C also shows a vibronic structure with maximum of 439 nm and a less intensive peak at

466 nm. It is interesting to point out that the absorption of fragment C (acceptor) and emission of compound **20** (donor) overlap very well (Figure 12C). This indicates that the energy transfer from the oligomer backbone to the anthracene moiety through the through-space dipole-induced dipole Förster mechanism will prevail in compound **21**. Indeed, the emission of **21** mostly comes from the anthracene end group (Figure 12D). The excitation wavelength was chosen to be 350 nm, which excites the backbone efficiently but not the anthracene unit. The absorption spectrum of **21** appears to be a superposition of absorption spectra of its constituents, fragment C and compound **20** (Figure 12D). This can be attributed to the weak electronic interactions between the tetramer core and the end group in **21**. With these weak electronic couplings, we can assume that the Förster through-space energy transfer mechanism seems to be predominant for compound **21**. The absorption and emission of the aldehyde-terminated compound **22** displays a significant red shift compared to **21** (Figure 13). This is due to the incorporation of the electron withdrawing carbonyl group onto the end-cap. As in the previous case, the efficiency of energy transfer is very high, resulting in predominance of the end-group emission. With the apparent smaller spectral overlap in this case, there is a good probability for the Dexter through-bond mechanism to contribute significantly into energy transfer. However, more studies are required to fully support this conclusion.

Encouraged by the successful synthesis of **22**, I tried the synthesis using the less soluble octamer (**18**). However, iodination of **18** to its more reactive iodide analog was unsuccessful under the same condition. I changed the catalyst from $Pd(PPh_3)_4$ to a more reactive system, $Pd(PhCN)_2Cl_2$ with P(*t*-Bu)$_3$.[20] Considering the large molecular weight, extended reaction time was applied when coupling with Fragment A. As a result, compound **23** is obtained in a form of a sticky yellow residue. Desilylation of **23** generated **24** smoothly. However, further attempts to

couple **24** with fragment C were not successful (Scheme 10). ^{1}H NMR spectrum of **24** is shown in Figure 14.

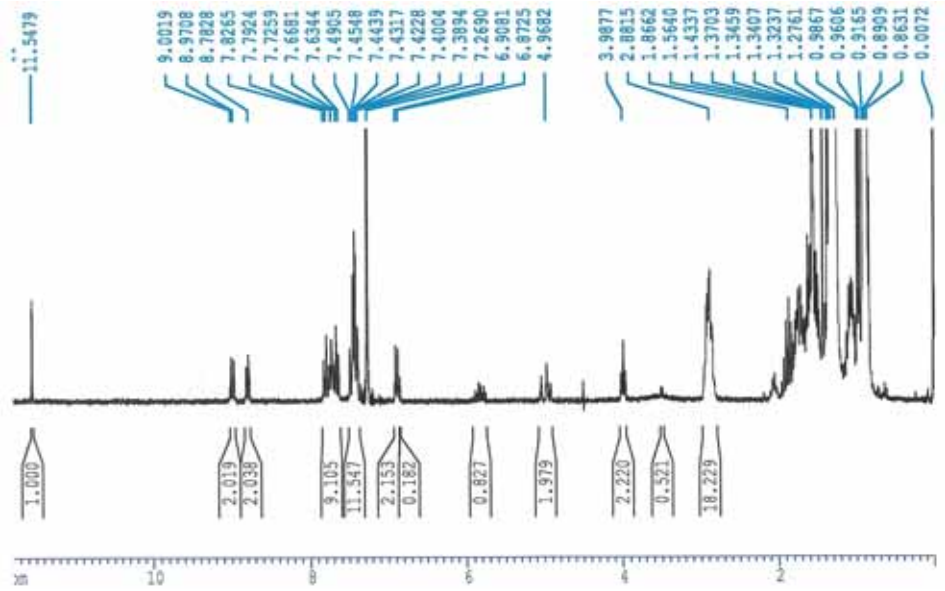

Figure 11. ^{1}H NMR of **22** in $CDCl_3$. Peak at 11.55 ppm is the resonance of the aldehyde proton. Resonances of the terminal alkene protons are located at 4.97 ppm and 5.85 ppm.

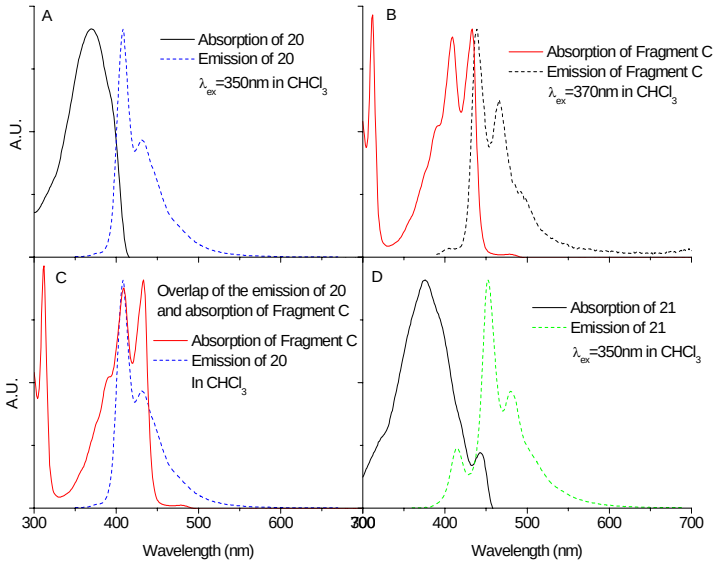

Figure 12. A) Absorption and emission of **20** in $CHCl_3$, B) Absorption and emission of fragment C in $CHCl_3$, C) Overlay of the emission of **20** and absorption of fragment C in $CHCl_3$, D) Absorption and emission of **21** in $CHCl_3$ showing that the emission is mainly from terminal anthracene moiety.

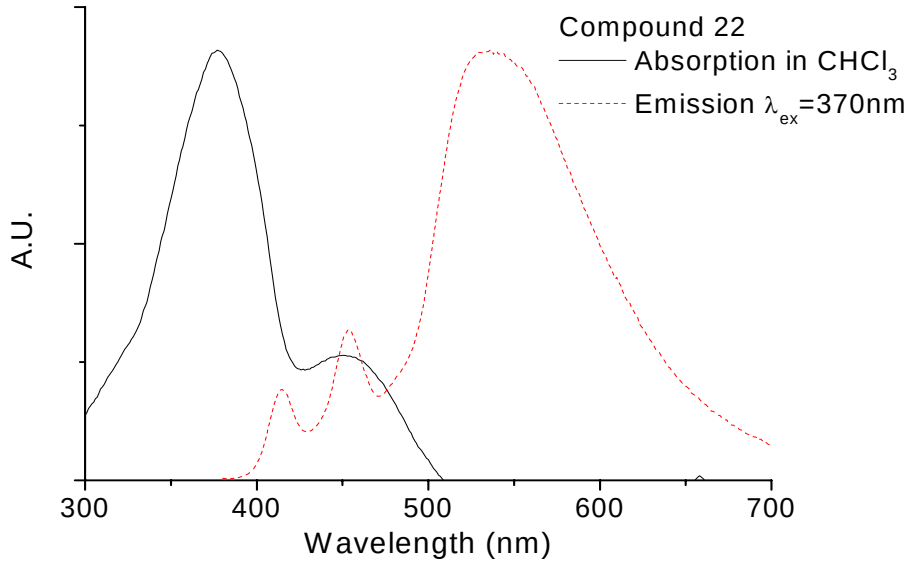

Figure 13. Absorption and emission of **22** in $CHCl_3$.

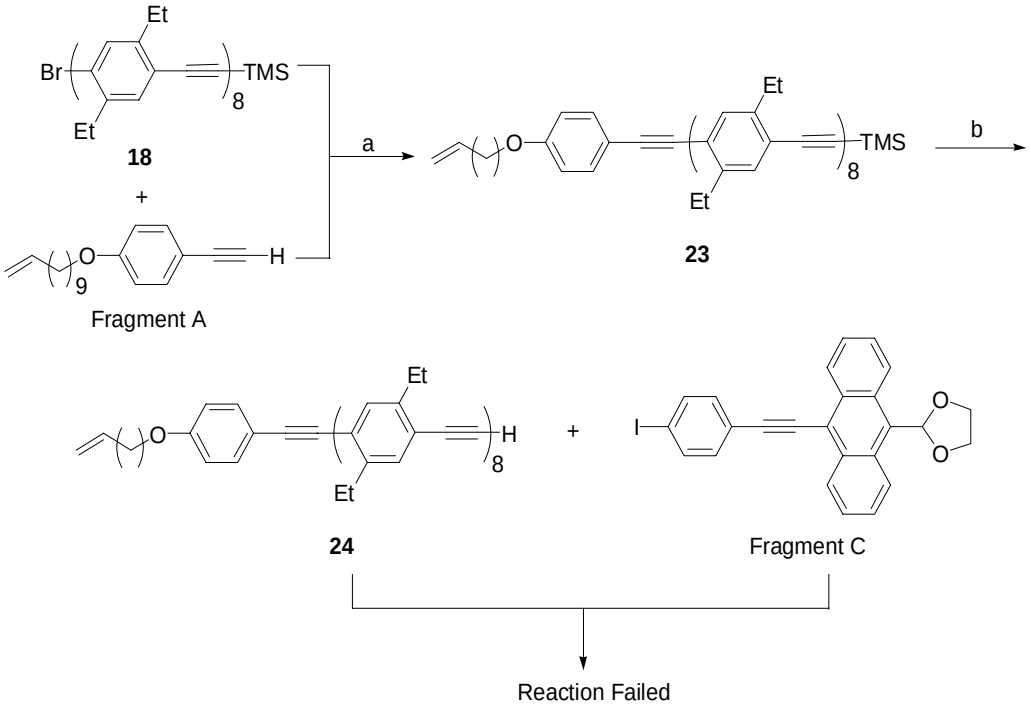

Scheme 10. Synthetic attempts toward **1**. a) $Pd(PhCN)_2Cl_2$, P(*t*-Bu)$_3$, i-Pr_2NH, CuI, 65ºC, 48 h, b) KOH/MeOH, rt, 1 h.

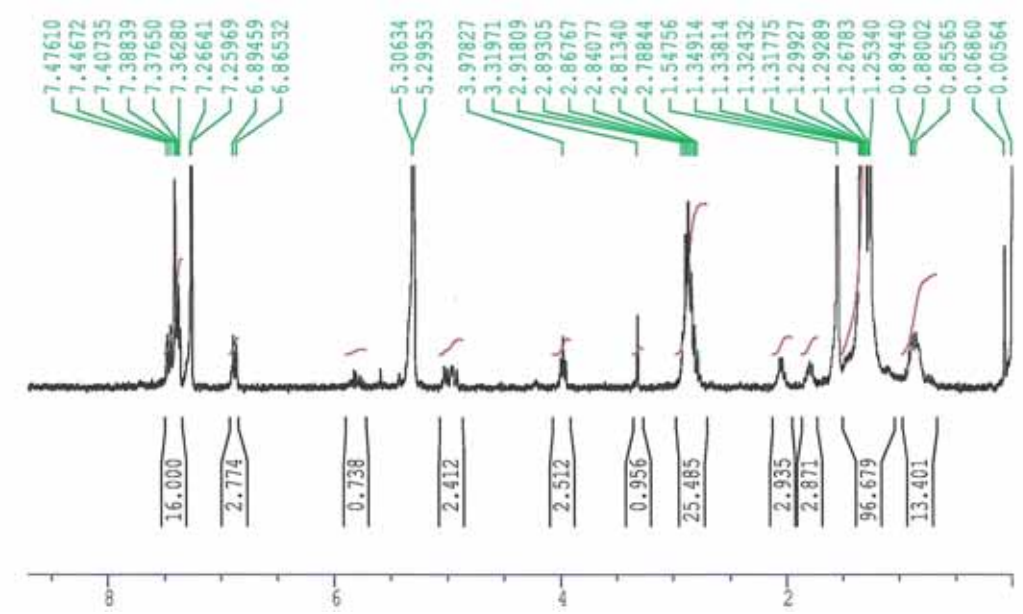

Figure 14. ^{1}H NMR spectrum of **24** in $CDCl_3$. The alkyne proton appears at 3.32 ppm. Terminal alkene protons are located at ca. 5.00 ppm and 5.83 ppm. The peak at 5.30 ppm is from DCM, which is trapped in the gel-like **24** and cannot be removed. The ^{1}H NMR spectrum was collected at elevated temperature to improve **24**'s solubility in $CDCl_3$.

We found that the absorption and emission spectra of **24** red are shifted by ca. 15 nm. This is in a good agreement with the fact that **24** has extended π-electron conjugation (Figure 15).

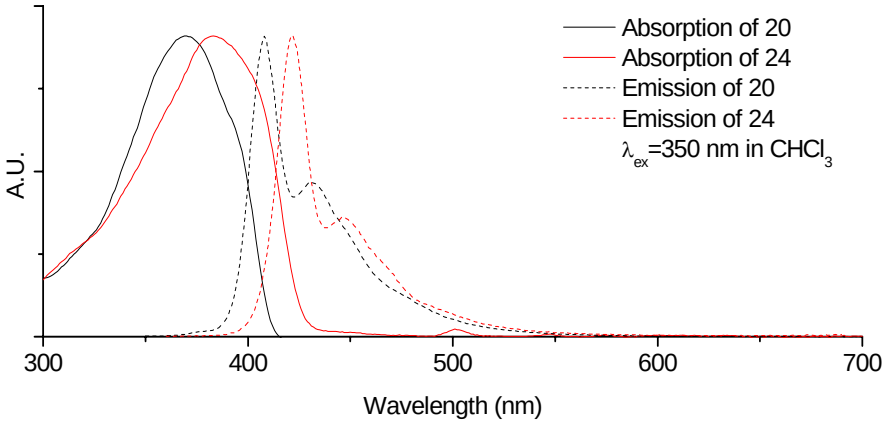

Figure 15. Comparison of the absorption (solid lines) and emission (dashed lines) of **24** and **20** in $CHCl_3$.

E Attempt with the Hexyl Substituted Derivative

It is well-known that long alkyl chains increase the solubility of compounds in common organic solvents. To increase the solubility of oligomers in organic solvents and further facilitate

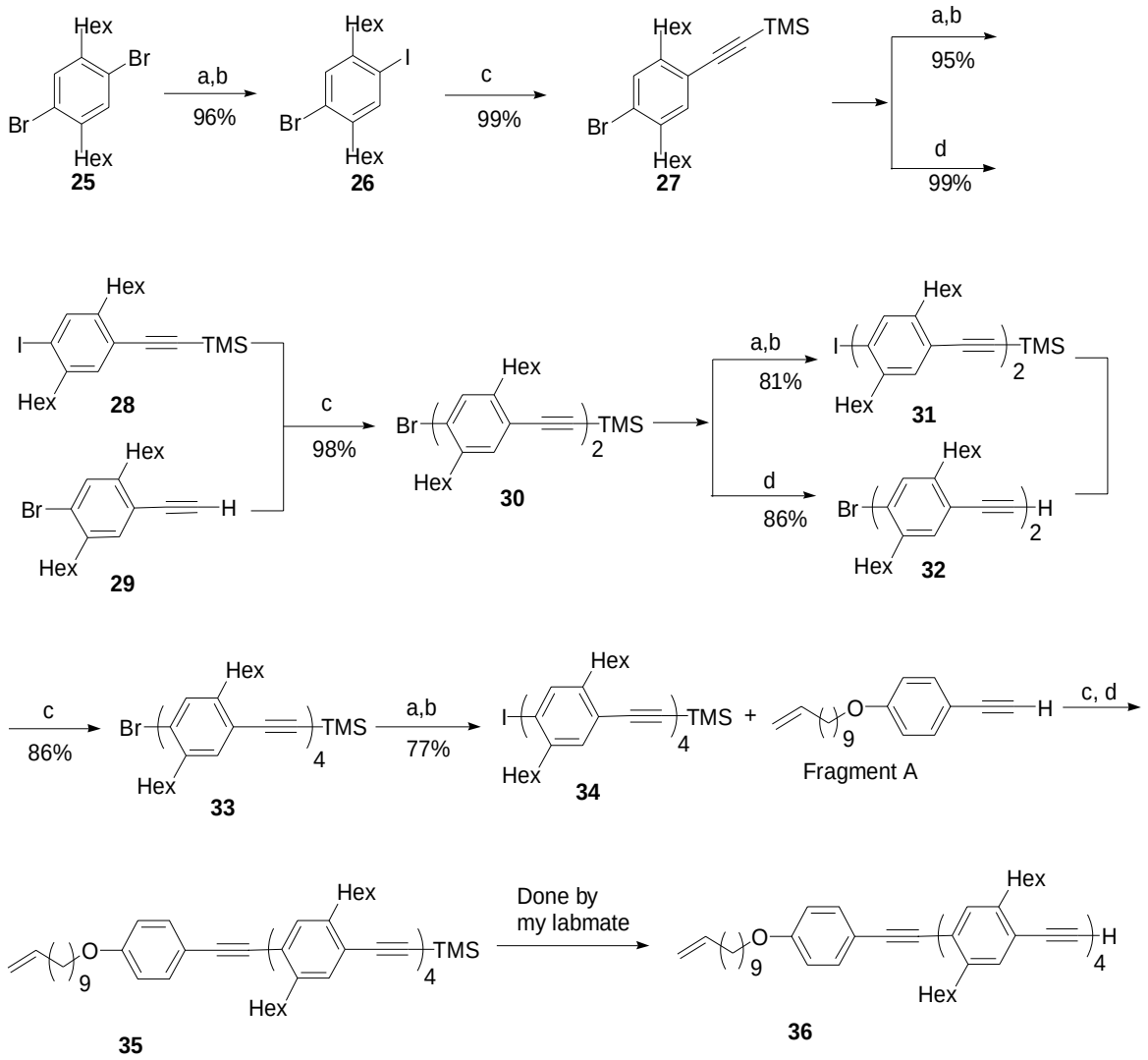

Scheme 11. Toward the synthesis of *n*-Hexyl substituted oligomers.

the coupling of different fragments, we tried to use *p*-dihexylbenzene instead of the diethyl counterpart (Scheme 11). The same procedures as for the synthesis with diethylbenzene described above were used. After the tetramer **35** was synthesized, I transferred the project to

another student in my group. The ^{1}H NMR spectrum of **35** is shown in Figure 16. Hexyl groups indeed increased the solubility of the compounds and made them very soluble even in such a non-polar solvent as hexane. Importantly, the use of the longer hexyl side chain did not seem to affect electronic conjugation in the oligomers. Figure 17 shows that the ethyl and hexyl analogs (**20** and **35**) have very close absorption and emission spectra in $CHCl_3$.

F Synthesis of Silica Supported Conjugated Polymer

An alternative approach to the oligomer self-assembly-based one described above was to synthesize the end-capped conjugated polymer chains starting from the low molecular weight precursor pre-attached to the solid support. This approach seemed to allow avoiding problems

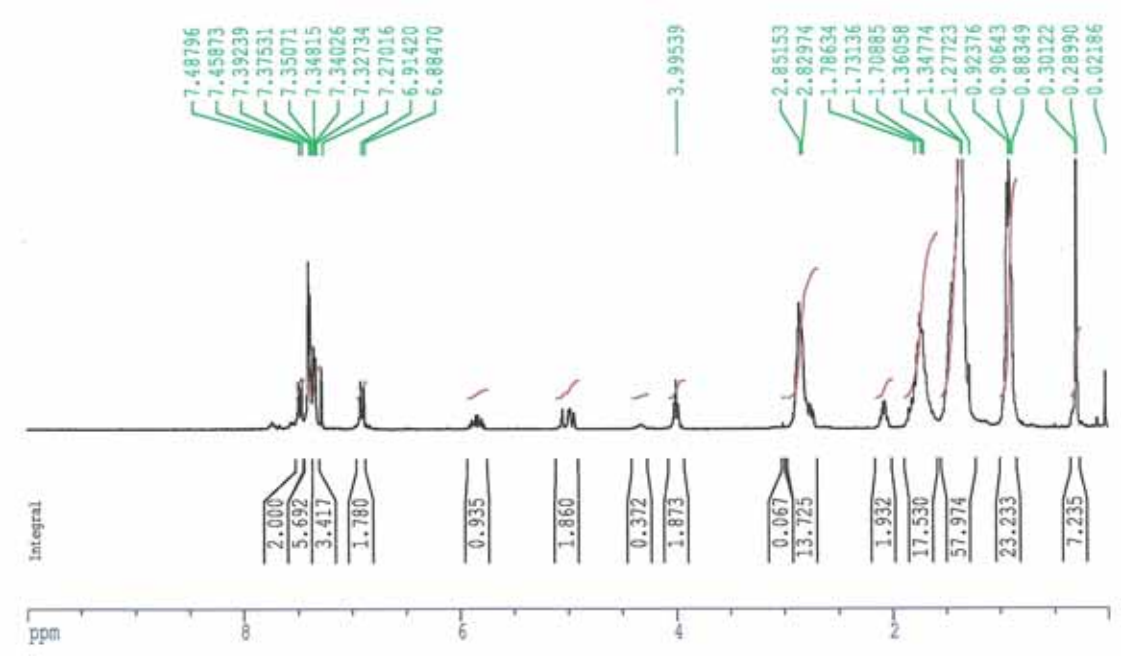

Figure 16. ^{1}H NMR of **35** in $CDCl_3$. Terminal TMS (9H) is located at 0.29 ppm, and the terminal alkene (3Hs) is at 4.99 ppm and 5.84 ppm.

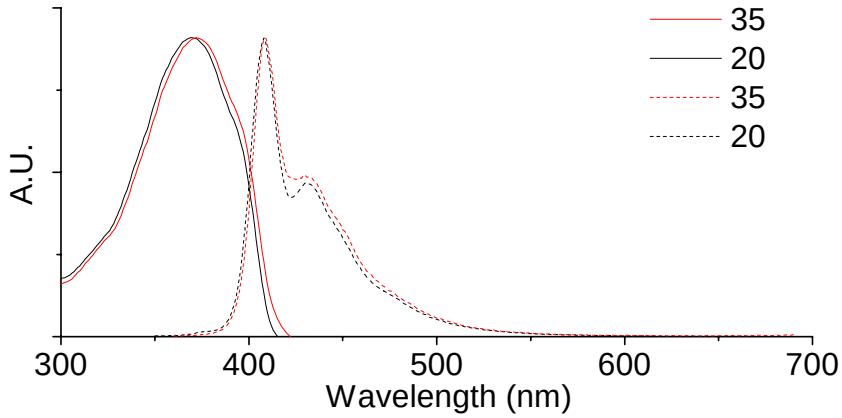

Figure 17. Overlay of the absorption (solid lines) and emission (dashed lines, excited at 350 nm) spectra of **20** and **36** clearly shows that alkyl substituents on the phenylene group do not exhibit a strong influence on the photophysical properties of the oligomer backbone.

with low solubility of oligomers. So we attempted it as well, using 0.33μm silica microspheres. Compound **37** reacted with commercially available 3-(trimethoxysilyl)propylamine (**38**) to yield the amide **39** in 72% yield (Scheme 12). Special precaution should be taken for column purification of **39** since it readily reacts with silica gel unless column is pre-treated with triethylamine. Compound **39** was attached to the surface of silica particles to generate **40**, which has a terminal aryl iodide functionality. This could serve to initiate a Sonogashira-Coupling based polymerization of monomer **41**. After carrying out the polymerization reaction for 24 h, a solution of end-capping reagent (fragment C) was added to the resulting mixture. This afforded highly fluorescent microparticles **43** bearing short conjugated polymer chains. GPC studies of the solution fraction **42** found the *number averaged molecular weight* $\overline{\mathrm{Mn}} \approx 1800$, which corresponds to a chain of *ca*. 10 repeating units, with a polydispersity of 1.65. The overlay of the emission spectra of the solution fraction and the silica particle clearly showed that the backbone emission of **42** has almost the same emission maximum as the particle fraction. This also

confirms that the GPC data were also valid in estimating the short polymer chains attached to the silica particles. The project was then transferred to my labmate and further studies are ongoing.

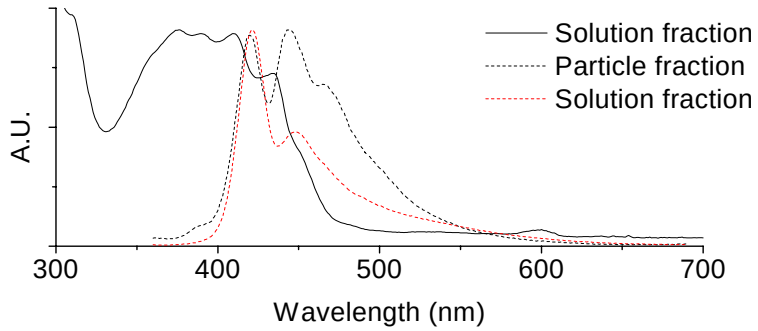

Figure 18. Comparison of the UV-Vis and fluorescence spectra of solution fraction and the silica particle fraction.

G Synthesis of a Monomer for a Water Soluble Boronic Acid Functionalized Conjugated Polymer

My task was to synthesize monomer **48** which will be used to prepare a water soluble polymer (**45**) with pendant boronic acid groups for ultra-sensitive vicinal glycol detection (Scheme 13). para-Xylene (**49**) was brominated to afford **50** in a 70% yield. Benzylic bromination of **50** with NBS gave **51** in 73% yield. Nucleophilic substitution of the benzylic bromide by Na_2SO_3 leads to **52** in 77% yield. However, **52** did not couple with TMS-acetylene to yield the desired monomer **48**. It is likely that the benzylic sulfonate groups hinder the Sonogashira coupling. In an alternative approach, coupling between **51** and TMS-acetylene did not yield the desired bis-acetylene, but the tetrasubstituted product **53** (Scheme 14). We are currently exploring the coupling between **50** and TIPS acetylene. TIPS is chosen to replace TMS due to its better robustness. Compound **54** was obtained in almost 99% yield. I am currently working on the NBS bromination of the compound **54**. Once **55** has been obtained, Na_2SO_3 will be used to displace the benzylic bromides to furnish **56**. Further desilylation will generate desired monomer **48** (Scheme 15).

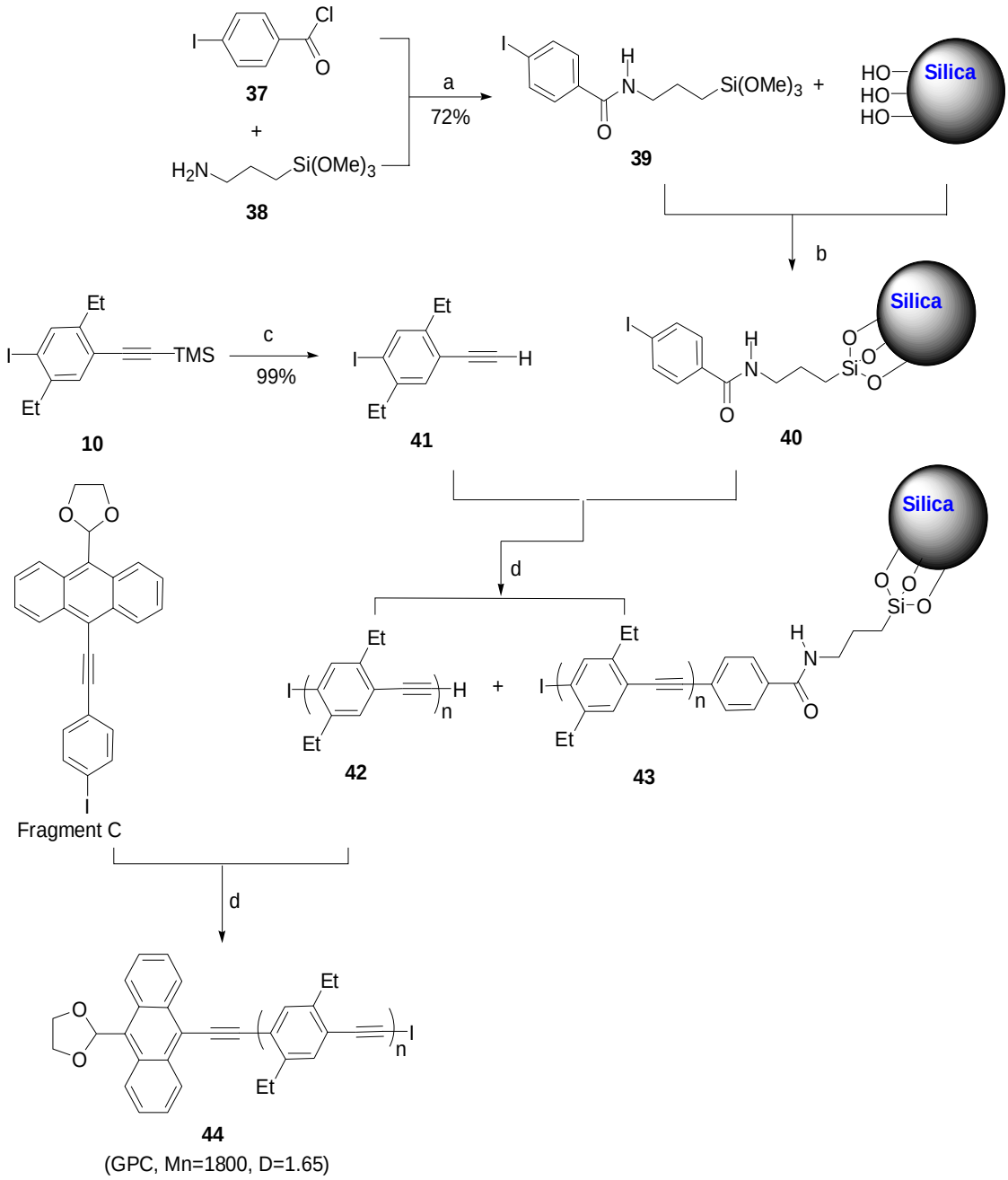

Scheme 12. Synthesis of a silica microsphere supported conjugated polymer system. a) DCM, 0ºC, 1 h, b) Toluene, reflux, 4h, c) KOH, MeOH, rt, 1 h, d) $Pd(PPh_3)_4$, CuI, *i*-Pr_2NH, 60ºC, 24 h.

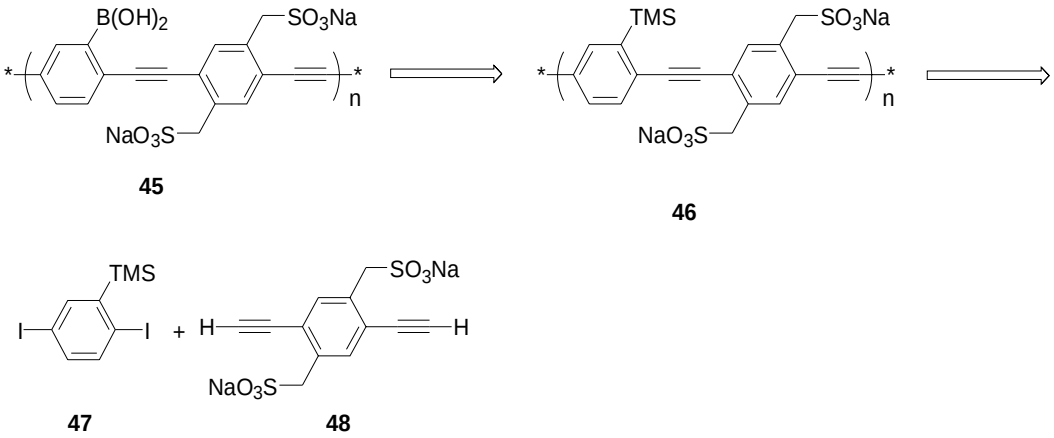

Scheme 13. Retrosynthetic analysis of polymer **45**.

H Synthesis of Long Wavelength (Near-Infrared) Dye

Compound **60** is synthesized following a literature procedure.[21] It is further protected with TBDMS to yield **61** in 55% yield. Stirring with malononitrile in the presence of $TiCl_4$ in anhydrous pyridine yields trace amounts of **62**. Reaction optimization is ongoing and deprotection of **62** by fluoride will furnish the expected long wavelength dye (Scheme 16).

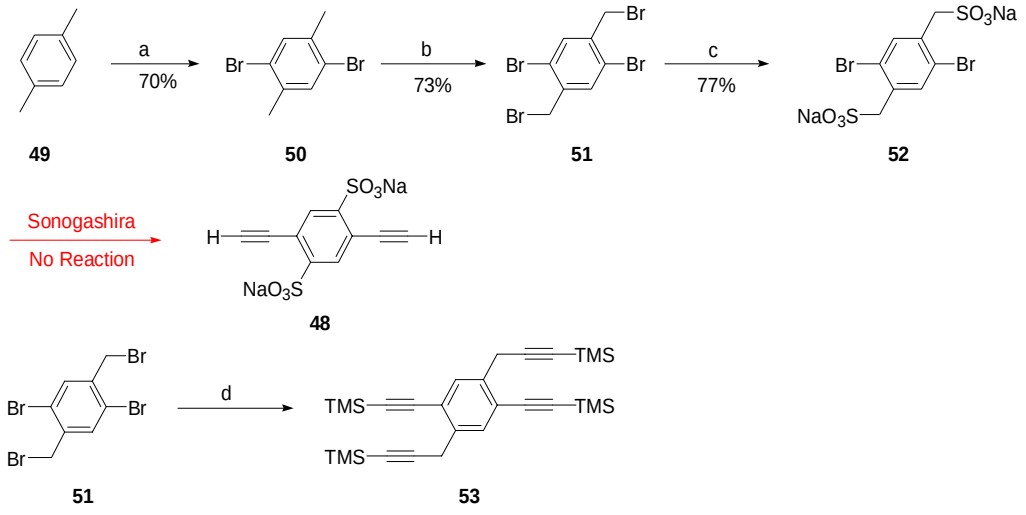

Scheme 14. Attempts to synthesize monomer **47**. a) Br_2, I_2, 0ºC, 24 hr, b) NBS, CCl_4, reflux, 24 h, c) Na_2SO_3, EtOH/H_2O, TBAB, reflux, d) TMS-acetylene, $Pd(PPh_3)_4$, CuI, *i*-Pr_2NH, 60ºC, 24 h, e) TIPS-acetylene, $Pd(PPh_3)_4$, CuI, *i*-Pr_2NH, 85ºC, 22 h, f) KOH, rt, 1h.

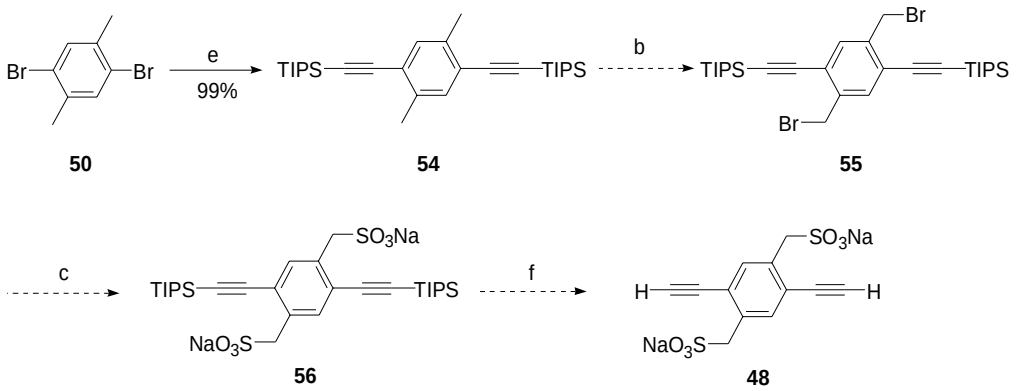

Scheme 15. New route for the synthesis of monomer **47**.

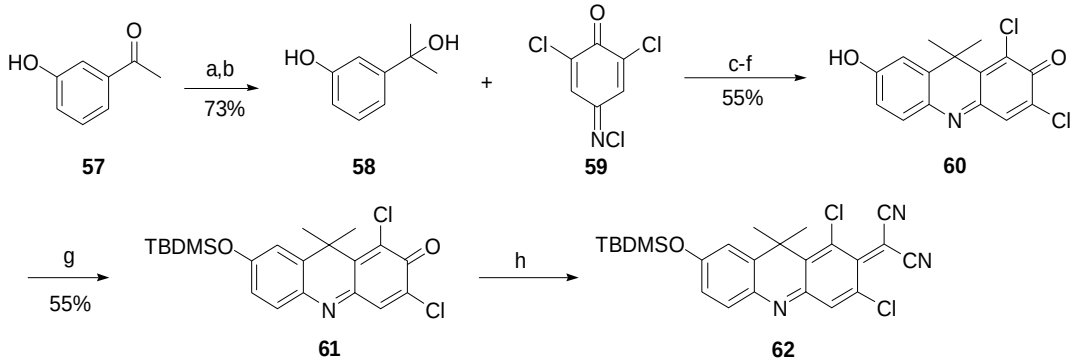

Scheme 16. Synthesis of long wavelength dye. a) MeMgI, rt, 6 h, b) H^+, c) NaOH, 0ºC, 1.5 h, d) $Na_2S_2O_4$, rt, 30 min, e) HCl, reflux, 1.5 h, f) $NaIO_4$, rt, 30 min, g) TBDMSCl, imidazole, rt, 24 h, h) $CH_2(CN)_2$, pyridine, $TiCl_4$, 0ºC, 15 h.

V CONCLUSION

The synthesis of a monodispersed oligo(phenylene ethynylene) backbone, end-capped with a terminal alkene for further attachment to a solid surface at one terminus, and an anthracene based receptor group at the other terminus, was successfully accomplished. Efficient energy transfer from backbone to end-cap was observed by absorption spectroscopy and fluorescence spectroscopy in agreement with the initial experimental design. The synthesis of a longer-chain analogue of the above platform, silica microspheres based conjugated polymer sensory platform and the synthesis of long wavelength (NIR) dye for *in vivo* amyloid screening were described.

VI EXPERIMENTAL

Compound **3**. 10-Undecen-1-ol (5.0 g, 29.4 mmol) was added in a 300 ml three-neck round bottom flask and dissolved in pyridine (20 mL). A solution of TsCl (8.4 g, 44.0 mmol) in pyridine (20 mL) was added dropwise with constant stirring at the ice bath temperature. Mixture was maintained at 0ºC under N_2 atmosphere for 2 h before it was warmed up to rt. The mixture was stirred for another 19 h followed by addition of H_2O (150 mL). Then, the reaction mixture was stirred for another 1 h before extraction with EtOAc (3 × 75 mL). Combined organic layers were washed with 1% HCl (5 × 50 mL) and distilled water (5 × 50mL), and dried over Na_2SO_4. Solid was removed by suction filtration. The resulting solution was concentrated under reduced pressure to give compound **3** (6.0 g) in 63 % yield. Data for compound **3**: ^{1}H NMR ($CDCl_3$, 400 MHz) δ 7.79 (d, *J* = 8.4 Hz, 2H), 7.34 (d, *J* = 8.4 Hz, 2H), 5.84-7.77 (m, 1H), 4.99 (d, *J* = 17.1 Hz, 1H), 4.93 (d, *J* = 10.2 Hz, 1H), 4.02 (t, *J* = 6.53 Hz, 2H), 2.04-1.20 (m).

Compound **4**. A 250 ml round bottom flask was charged with 4-iodophenol (2.0 g, 9.3 mmol), compound **3** (6 g, 18.5 mmol), K_2CO_3 (2.6 g, 18.5 mmol) and KI (30.7 mg, 1.9 mmol). Methylethylketone (100 mL) was added. The reaction mixture was refluxed for 50 h under N_2 atmosphere. Inorganic salts were removed by suction filtration. The organic solvent was removed under reduced pressure. The residue was dissolved in DCM and washed with 10% NaOH solution and distilled water. The organic layer was separated and dried over $MgSO_4$. The resulting organic solution was concentrated under reduced pressure to give crude product, which was subjected to column chromatography (silica gel, Hexane) to give compound **4** (3.4 g) in 91% yield. Data for compound **4**: ^{1}H NMR ($CDCl_3$, 250 MHz) δ 7.54 (d, *J* = 8.9 Hz, 2H), 6.68 (d, *J* = 8.9 Hz, 2H), 5.92-5.73 (m, 1H), 5.05-4.91 (m, 2H), 3.91 (t, *J* = 6.5 Hz, 2H), 2.10-1.25 (m).

Compound **5**. A mixture of compound **4** (3.2 g, 8.5 mmol), TMS-acetylene (1.7 g, 16.9 mmol), $Pd(PPh_3)_4$ (147 mg, 0.13 mmol) and CuI (24.4 mg, 0.13 mmol) were charged in a sealed flask and dissolved in 70 mL of Toluene:*i*-Pr_2NH (v/v 7:3). The mixture was stirred at 55ºC for 30 h. The resulting mixture was passed through a short column (silica gel) to remove metal catalyst and inorganic salts. Concentration under reduced pressure affords compound **5** (2.9 g) in 99% yield. Data for compound **5**: ^{1}H NMR ($CDCl_3$, 250 MHz) δ 7.39 (d, *J* = 8.7 Hz, 2H), 6.81 (d, *J* = 8.7 Hz, 2H), 5.90-5.73 (m, 1H), 5.50-4.92 (m, 2H), 3.95 (t, *J* = 6.5 Hz, 2H), 2.10-1.32 (m), 0.24 (s, 9H).

Fragment **A**. Compound **5** (2.9 g, 8.2 mmol) was dissolved in THF (175 mL) and added dropwise into a solution of KOH (2.4 g, 42.3 mmol) in MeOH (200 mL) with constant stirring. The resulting mixture was stirred for an additional 40 min at rt. The solution was poured into water (300 mL) and extracted with ether. The combined ether layers were washed successively with water (200 mL), saturated NH_4Cl solution (100 mL), brine (100 mL) and water (3 × 100 mL), and dried over Na_2SO_4. Solution was concentrated under reduced pressure and the residue was subjected to column chromatography (silica gel, Hexane) to give fragment **A** (1.9 g) in 85%. Data for fragment **A**: ^{1}H NMR ($CDCl_3$, 250 MHz) δ 7.42 (d, *J* = 8.5 Hz, 2H), 6.83 (d, *J* = 8.5 Hz, 2H), 5.90-5.73 (m, 1H), 5.50-4.92 (m, 2H), 3.96 (t, *J* = 6.5 Hz, 2H), 2.99 (s, 1H), 2.13-1.20 (m).

Compound **8**. A solution of *n*-BuLi (145 mL of 1.6 M solution in Hexane, 0.23 mol) was added dropwise to a solution of compound **7** (63 g, 0.23 mol) in THF (900 ml) with constant stirring at the dry ice/Acetone bath temperature. After addition was complete, the resulting mixture was stirred for another 3 h followed by addition of a solution of I_2 (71.3 g, 0.28 mol) in THF (250 mL). The resulting mixture was stirred for another 1 h at -78°C and allowed to warm to rt overnight. The solution was concentrated to 30% of the initial volume, and 20% $Na_2S_2O_3$

solution in H_2O was added till the mixture turned yellow. Water (300 mL) was added, and the reaction mixture was extracted with DCM. Organic layers were washed successively with dilute $Na_2S_2O_3$, brine, and water before drying over Na_2SO_4. Solvents were removed under reduced pressure. Compound **8** (70 g) was obtained after recrystallization from EtOH. Data for compound **8**: ^{1}H NMR (Acetone-d_6, 250 MHz) δ 7.77 (s, 1H), 7.48 (s, 1H), 2.84-2.68 (m, 4), 1.22-1.15 (m, 6H).

Compound **9** was prepared following the synthetic procedure for compound **5**. The following amounts of reagents were used: compound **8** (35.7 g, 0.11 mol), TMS-acetylene (10.3 g, 0.11 mol), $Pd(PPh_3)_4$ (1.8 g, 1.6 mmol) and CuI (0.31 g, 1.6 mmol) in 400 mL of Toluene:*i*-Pr_2NH (v/v 7:3). The crude product was purified by column chromatography (silica gel, Hexane) to give compound **9** (32 g) in 98% yield. Data for compound **9**: ^{1}H NMR ($CDCl_3$, 250 MHz) δ 7.36 (s, 1H), 7.26 (s, 1H), 2.77-2.64 (m, 4H), 1.25-1.18 (m, 6H), 0.25 (s, 9H).

Compound **10** was iodinated following the synthetic procedure for compound **8**. The following amounts of reagents were used: compound **9** (16.22 g, 52.5 mmol), *n*-BuLi (40 mL of 1.6 M solution in Hexane, 64 mmol), I_2 (18 g, 69.8 mmol). Crude product was purified by column chromatography (silica gel, Hexane) to give compound **10** (17.7 g) in 95% yield. Data for compound **10**: ^{1}H NMR ($CDCl_3$, 250 MHz) δ 7.65 (s, 1H), 7.26 (s, 1H), 2.72-2.64 (m, 4h), 1.25-1.15 (m, 6H), 0.26 (s, 9H).

Compound **11** was prepared following the synthetic procedure for the fragment **A**. The following amounts of reagents were used: compound **9** (16.22 g, 52.5 mmol), KOH (9.9 g, 0.16 mol). The product was purified by column chromatography (silica gel, Hexane) to give

compound **11** (12.3 g) in 99% yield. Data for compound **11**: ^{1}H NMR ($CDCl_3$, 250 MHz) δ 7.38 (s, 1H), 7.30 (s, 1H), 3.26 (s, 1H), 2.80-2.65 (m, 4H), 1.25-1.18 (m, 6H).

Compound **12** was prepared following the synthetic procedure for compound **5**. The following amounts of reagents were used: compound **11** (12.4 g, 52.5 mmol), compound **10** (17.0 g, 47.7 mmol), $Pd(PPh_3)_4$ (0.83 g, 0.72 mmol) and CuI (0.14 g, 0.72 mmol) in 300 mL of Toluene:*i*-Pr_2NH (v/v 7:3). The product was purified by column chromatography (silica gel, Hexane) to give compound **12** (21.6 g) in 98% yield. Data for compound **12**: ^{1}H NMR ($CDCl_3$, 250 MHz) δ 7.42 (s, 1H), 7.36 (s, 1H), 7.34 (s, 1H), 7.33 (s, 1H), 2.90-2.65 (m, 8H), 1.34-1.19 (m, 12H), 0.27 (s, 9H).

Compound **13** was prepared following the synthetic procedure for compound **8**. The following amounts of reagents were used: compound **12** (10 g, 21.5 mmol), *n*-BuLi (16.1 mL of 1.6 M solution in Hexane, 25.8 mmol) and I_2 (7.3 g, 28.6 mmol). The product was purified by column chromatography (silica gel, Hexane) to give compound **13** (8.9 g) in 81 % yield. Data for compound **13**: ^{1}H NMR (Acetone-d_6, 250 MHz) δ 7.80 (s, 1H), 7.45 (s, 1H), 7.43 (s, 1H), 7.35 (s, 1H), 2.90-2.65 (m, 8H), 1.30-1.19 (m, 12H), 0.26 (s, 9H).

Compound **14** was prepared following the synthetic procedure for the fragment A. The following amounts of reagents were used: compound **12** (10.3 g, 22.2 mmol), KOH (3.7 g, 66.7 mmol). The product was purified by column chromatography (silica gel, Hexane) to give compound **14** (7.5 g) in 86% yield. Data for compound **14**: ^{1}H NMR (Acetone-d_6, 250 MHz) δ 7.53 (s, 1H), 7.48 (s, 1H), 7.45 (s, 1H), 7.40 (s, 1H), 3.96 (s, 1H), 2.90-2.73 (m, 8H), 1.31-1.20 (m, 12H).

Compound **15** was prepared following the synthetic procedure for compound **5**. The following amounts of reagents were used: compound **13** (7.5 g, 14.6 mmol), compound **14** (6.3 g, 16.1 mmol), $Pd(PPh_3)_4$ (0.3 g, 0.22 mmol) and CuI (0.042 g, 0.22mmol) in 100 mL of Toluene:*i*-Pr_2NH (v/v 7:3). The product was purified by column chromatography (silica gel, Hexane:$CHCl_3$ 95:5) to give compound **15** (9.8 g) in 86% yield. Data for compound **15**: ^1H NMR ($CDCl_3$, 300 MHz) δ 7.42-7.33 (m, 8H), 2.92-2.72 (m, 16H), 1.35-1.22 (m, 24H), 0.27 (s, 9H).

Compound **16** was prepared following the synthetic procedure for compound **8**. The following amounts of reagents were used: compound **15** (4.6 g, 5.9 mmol), ICH_2CH_2I (2.3 g, 8.3 mmol) as a replacement for I_2, *n*-BuLi (5.1 mL of 1.6 M solution in Hexane, 8.2 mmol). The product was purified by column chromatography (silica gel, Hexane:$CHCl_3$=50:50) to give compound **16** (3.8 g) in 77% yield. Data for compound **16**: ^1H NMR ($CDCl_3$, 300 MHz) δ 7.71 (s, 1H), 7.40-7.26(m, 7H), 2.92-2.69 (m, 16H), 1.34-1.20 (m, 24H), 0.27 (s, 9H).

Compound **17** was prepared following the synthetic procedure for the fragment A. The following amounts of reagents were used: compound **15** (5.2 g, 6.6 mmol), KOH (1.3 g, 24 mmol). The product was purified by column chromatography (silica gel, Hexane:$CHCl_3$=1:1) to give compound **17** (4.6 g) in 99% yield. Data for compound **17**: ^1H NMR ($CDCl_3$, 250 MHz) δ 7.43-7.36 (m, 8H), 3.32 (s, 1H), 2.92-2.69 (m, 16H), 1.56-1.24 (m, 24H).

Compound **18** was prepared following the synthetic procedure for compound **5**. The following amounts of reagents were used: compound **16** (2.0 g, 2.3 mmol), compound **17** (2.0 g, 2.6 mmol), $Pd(PPh_3)_4$ (0.040 g, 0.04 mmol) and CuI (0.007 g, 0.04mmol) in 60 mL of Toluene:*i*-Pr_2NH (v/v 7:3). An attempt to purify the product by column chromatography (silica gel, $CHCl_3$)

gave crude compound **18** (100 mg). Data for compound **18**: ^{1}H NMR ($CDCl_3$, 250 MHz) δ 7.46-7.37 (m, 16H), 2.93-2.66 (m, 32H), 1.37-1.14 (m, 48H), 0.31 (s, 9H).

Fragment **B** was prepared following the synthetic procedure for the fragment A. The following amounts of reagents were used: compound **18** (88 mg, 0.062 mmol), KOH (10 mg, 0.2 mmol). An attempt to purify the product by column chromatography (silica gel, $CHCl_3$) gave crude fragment **B** (40 mg). Data for fragment B: ^{1}H NMR ($CDCl_3$, 250 MHz) δ 7.43-7.35 (m, 16H), 3.31 (s, 1H), 2.93-2.68 (m, 32H), 1.33-1.21 (m, 48H).

Compound **19** was prepared following the synthetic procedure for compound **5**. The following amounts of reagents were used: compound **16** (0.8 g, 0.97 mmol), fragment A (0.3 g, 1.1 mmol), $Pd(PPh_3)_4$ (0.017 g, 0.015 mmol) and CuI (0.003 g, 0.015mmol) in 20 mL of Toluene:*i*-Pr_2NH (v/v 7:3). The product was purified by column chromatography (silica gel, Hexane:$CHCl_3$ 90:10) to give compound **19** (500 mg) in 56% yield. Data for compound 1**9**: ^{1}H NMR ($CDCl_3$, 400 MHz) δ 7.48-7.34 (m, 18H), 6.88 (d, *J* = 8.4 Hz, 2H), 5.88-7.58 (m, 1H), 5.03-4.93 (m, 2H), 3.98 (t, *J* = 6.4 Hz, 2H), 2.92-2.79 (m), 2.07-0.87 (m), 0.28 (s, 9H).

Compound **20** was prepared following the synthetic procedure for the fragment A. The following amounts of reagents were used: compound **19** (500 mg, 0.52 mmol), KOH (87 mg, 1.6 mmol). The product was purified by column chromatography (silica gel, Hexane:$CHCl_3$=80:20) to give compound **20** (427 mg) in 92% yield. Data for compound **20**: ^{1}H NMR ($CDCl_3$, 250 MHz) δ 7.49-7.39 (m, 18H), 6.89 (d, *J* = 8.4 Hz, 2H), 5.92-5.75 (m, 1H), 5.08-4.92 (m, 2H), 3.97 (t, *J* = 6.5 Hz, 2H), 3.33 (s, 1H), 2.91-2.85 (m), 2.10-0.87 (m).

Compound **21** was prepared following the synthetic procedure for compound **5**. The following amounts of reagents were used: compound **20** (0.053 g, 0.06 mmol), the fragment C

(0.029 g, 0.06 mmol), $Pd(PPh_3)_4$ (2 mg, 0.002 mmol) and CuI (0.35 mg, 0.002mmol) in 6 mL of Toluene:*i*-Pr_2NH (v/v 7:3). The product was purified by column chromatography (silica gel, Hexane:EtOAc=80:20) to give compound **21** (39.6 mg) in 53% yield. Data for compound **9**: ^1H NMR ($CDCl_3$, 250 MHz) δ 8.76 (d, *J* = 8.8 Hz, 2H), 8.61 (d, *J* = 8.1 Hz, 2H), 7.81-7.34 (m, 21H), 7.13 (s, 1H), 6.90 (d, *J* = 8.8 Hz, 2H), 5.89-5.80 (m, 1H), 5.05-4.94 (m, 2H), 4.56 (t, *J* = 6.5 Hz, 2H), 4.34 (m, 4H), 4.00 (t, J = 6.5 Hz, 2H), 2.93-2.87 (m), 1.82-0.88 (m).

Compound **22**. The mixture of compound **21** (39.6 mg, 0.032 mmol) and PTSA (10 mg, 0.015 mmol) are dissolved in a mixture of acetone (5 mL) and $CHCl_3$ (5mL) and stirred at rt for 24 h. Five drops of conc. aqueous $NaHCO_3$ were added before drying over Na_2SO_4. Organic solvents were removed under reduced pressure. Resulting crude product was subjected to column chromatography (silica gel, Hexane:$CHCl_3$=50:50) to give compound **22** (20 mg) in 51% yield. Data for compound **22**: ^1H NMR ($CDCl_3$, 250 MHz) δ 11.77 (s, 1H), 8.99 (d, *J* = 8.8 Hz, 2H), 8.79 (d, *J* = 8.2 Hz, 2H), 7.83-7.35 (m, 22H), 6.89 (d, *J* = 8.1 Hz, 2H), 5.92-5.83 (m, 1H), 5.03-4.90 (m, 2H), 3.99 (t, *J* = 6.4 Hz, 2H), 2.88 (m), 2.12-0.86 (m).

Compound **23** was prepared following the synthetic procedure for compound **5**. The following amounts of reagents were used: compound **18** (380 mg, 0.27 mmol), the fragment A (88 mg, 0.33 mmol), $Pd(PhCN)_2Cl_2$ (3.1 mg, 0.015 mmol) as a replacement for $Pd(PPh_3)_4$, P(t-Bu)$_3$(0.2 ml of 0.1 M solution in dioxane) and CuI (1 mg, 0.008mmol) in 5 mL of Dioxane:*i*-Pr_2NH (v/v 98:2). An attempt to purify the product by column chromatography (silica gel, EtOAc) gave crude compound **23** (77 mg). Data for compound **23**: ^1H NMR ($CDCl_3$, 250 MHz) δ 7.41-7.34 (m, 18H), 6.88-6.80 (m, 2H), 5.89-5.72 (m, 1H), 5.06-4.93 (m, 2H), 3.96 (t, *J* = 6.4 Hz, 2H), 2,97-2.60 (m), 2.10-0.83 (m), 0.28 (s, 9H).

Compound **24** was prepared following the synthetic procedure for the fragment A. The following amounts of reagents were used: compound **23** (77 mg, 0.05 mmol), KOH (10.5 mg, 0.19 mmol). The product was purified by column chromatography (silica gel, Hexane:EtOAc=95:5) to give compound **24** (59 mg) in 80% yield. Data for compound **24**: ^{1}H NMR ($CDCl_3$, 250 MHz) δ 7.48-7.36 (m, 18H), 6.88 (d, *J* = 8.2 Hz, 2H), 5.88-5.77 (m, 1H), 5.03-4.92 (m, 2H), 3.98 (t, *J* = 6.5 Hz, 2H), 3.32 (s, 1H), 2.93-2.76 (m), 2.06-2.01 (m), 1.82-1.76 (m), 1.43-0.85 (m).

Compound **26**-**34** were synthesized following the literature procedures.[22]

Compound **35** was prepared following the synthetic procedure for compound **5**. The following amounts of reagents were used: compound **34** (0.10 g, 0.08 mmol), the fragment A (0.05 g, 0.17 mmol), $Pd(PPh_3)_4$ (0.9 mg, 0.002 mmol) and CuI (0.45 mg, 0.002mmol) in 5 mL of Toluene:*i*-Pr_2NH (v/v 7:3). The product was purified by column chromatography (silica gel, Hexane:EtOAc=80:20) to give compound **35** (88 mg) in 78% yield. Data for compound **9**: ^{1}H NMR ($CDCl_3$, 300 MHz) δ 7.49-7.33 (m, 10H), 6.90 (d, *J* = 8.9 Hz, 2H), 5.88-5.78 (m, 1H), 5.05-4.94 (m, 2H), 3.99 (t, *J* = 6.5 Hz, 2H), 2.90-2.65 (m), 2.09-0.87 (m), 0.30 (s, 9H).

Compound **39**. Compound **37** (164 mg, 0.615 mmol) and compound **38** (0.23 ml, 1.3 mmol) were dissolved in DCM (4mL) at 0ºC. The mixture was stirred for 1 h and solvents was evaporated under reduced pressure. The residue was subjected to column chromatography (silica gel, $CHCl_3$:MeOH 98:2) to give compound **39** (181 mg) in 72% yield. Data for compound **9**: ^{1}H NMR ($CDCl_3$, 250 MHz) δ 7.80 (d, *J* = 8.3 Hz, 2H), 7.62 (d, J = 8.3 Hz, 2H), 6.49 (s, 1H), 3.47 (q, *J* = 7.5 Hz, 2H), 1.77 (m, 2H), 0.74 (t, *J* = 8.7 Hz, 2H).

Compound **40**. Compound **39** (90 mg, 0.22 mmol) and silica microspheres (254 mg, 0.33 μm, Bang Laboratories, Inc.) were mixed with toluene (10 mL) and refluxed for 4 h. The surface modified silica particle were collected via centrifugation and washed a few timeswith acetone after sonication.

Compound **41** was prepared following the synthetic procedure for the fragment A. The following amounts of reagents were used: compound **10** (750 mg, 2.1 mmol), KOH (0.35 g, 6.3 mmol). The product was purified by column chromatography (silica gel, Hexane) to give compound **41** (596 mg) in quantatitive yield. Data for compound **9**: ^{1}H NMR ($CDCl_3$, 250 MHz) δ

Compound **42** was prepared following the synthetic procedure for compound **5**. The following amounts of reagents were used: compound **41** (85 mg, 0.3 mmol), compound **40** (50 mg), $Pd(PPh_3)_4$ (1 mg, 0.001 mmol) and CuI (0.2 mg, 0.001mmol) in 5 mL of Toluene:*i*-Pr_2NH (v/v 7:3). The reaction was carried out at 60ºC for 24 h. The fragment C was added thereafter and resulting mixture was stirred for 36 h. After centrifugation, compound **43** was obtained as a solution fraction.

Compound **51**. A mixture of compound **50** (20 g, 77 mmol), NBS (28.3 g, 0.16 mol) and benzoyl peroxide (0.010 g) in benzene (380 mL) was refluxed for 8 h. The solvent was removed under reduced pressure. The pure product (23 g) was purified by recrystallization in 73% yield. Data for compound **51**: ^{1}H NMR ($CDCl_3$, 250 MHz) δ 7.67 (s, 2H), 4.52 (s, 4H).

Compound **52**. Compound **51** (2.0 g, 4.7 mmol), Na_2SO_3 (1.5 g, 11.9 mmol) and TBAB (0.10 g, 0.28 mmol) were mixed in water (50 mL) and ethanol (50 mL) and refluxed for 72 hrs. The solvents were removed under reduced pressure and the crude product was recrystallized

from water (20 mL) to give compound **52** (1.7 g) in 77% yield. Data for compound **52**: ^{1}H NMR (D_2O, 250 MHz) δ 7.62 (s, 2H), 4.21 (s, 4H).

Compound **53** was prepared following the synthetic procedure for compound **5**. The following amounts of reagents were used: compound **51** (0.513 g, 1.94 mmol), TIPS-acetylene (862 mg, 4.7 mmol), $Pd(PPh_3)_4$ (65.4 mg, 0.06 mmol) and CuI (10.8 mg, 0.06 mmol) in 8 mL of Toluene:*i*-Pr_2NH (v/v 7:3). The reaction was carried out at 85ºC. The product was purified by column chromatography (silica gel, Hexane) to give compound **53** (0.90 g) in 99% yield. Data for compound **53**: ^{1}H NMR (Acetone-d_6, 250 MHz) δ 7.39 (s, 2H), 2.83 (s, 6H), 2.40 (s, 6H), 1.16 (s, 36H).

Compound **60** was synthesized following the literature procedures.[21]

Compound **61**. Compound **60** (200 mg, 0.65 mmol), TBDMSCl (196 mg, 1.3 mmol) and imidazole (110 mg, 1.6 mmol) were dissolved in DMF (12 mL) and stirred for 24 h under N_2 atmosphere at rt. Mixture was poured into water (100 mL) and extracted with $CHCl_3$ (3×100 mL). The organic layer was washed with water and brine and dried over Na_2SO_4. Solvents were removed under reduced pressure and the residue was subjected to column chromatography (silica gel, Hexane:EtOAc=50:50) to give compound **61** (151 mg) in 55% yield. Data for compound **61**: ^{1}H NMR (Acetone-d_6, 300 MHz) δ 7.67 (s, 1H), 7.58 (d, J = 8.5 Hz, 1H), 7.20 (s, 1H), 6.97 (d, J = 8.5 Hz, 1H), 1.91 (s, 6H), 1.03 (s, 9H), 0.32 (s, 6H).

REFERENCES

1. a) Shirakawa, H.; Louis, E. J.; Macdiarmid, A. G.; Chiang, C. K.; Heeger, A. J. *J. Chem. Soc. Chem. Comm.* **1977**, *16*, 578-580. b) www.nobelprize.org.

2. a) Brusic, V.; Angelopoulos, M.; Graham, T. *J. Electrochem. Soc.* **1997**, *144*, 436-442. b) Yu, G.; Wang, J.; McElvain, J.; Heeger, A. J. *Adv. Mater.* **1998**, *10*, 1431. c) Horowitz, G. *Adv. Mater.* **1998**, *10*, 365-377. d) Sirringhaus, H.; Tessler, N.; Friend, R. H. *Science* **1998**, *280*, 1741-1744. e) Bao, Z. *Adv. Mater.* **2000**, *12*, 227-230. f) Xu, H.; Wu, H. P.; Fan, C. H.; Li, W. X.; Zhang, Z. H.; He, L. *Chin. Sci. Bull.* **2004**, *49*, 2227-2231. g) Roncali, J. *Chem. Soc. Rev.* **2005**, *34*, 483-495. h) Dini, D. *Chem. Mater.* **2005**, *17*, 1933-1945. i) Lam, J. W. Y.; Tang, B. Z. *Acc. Chem. Res.* **2005**, *38*, 745-754. j) Bobacka, J. *Electroanal.* **2006**, *18*, 7-18. k) Tse, C. W.; Man, K. Y. K.; Cheng, K. W.; Mak, C. S. K.; Chan, W. K.; Yip, C. T.; Liu, Z. T.; Djurisic, A. B. *Chem.-Eur. J.* **2007**, *13*, 328-335. l) Frampton, M. J.; Anderson, H. L.*Angew. Chem. Int. Ed.* **2007**, *46*, 1028-1064.

3. a) Bharathan, J.; Yang, Y. *Appl. Phys. Lett.* **1998**, *72*, 2660-2662. b) Dodabalapur, A. *Mater. Today* **2006**, *9*, 24-30.

4. a) Zhou, Q.; Swager, T. M. *J. Am. Chem. Soc.* **1995**, *117*, 12593-12602. b) Swager, T. M. *Acc. Chem. Res*.; **1998**; *31*, 201-207. c) McQuade, D. T.; Pullen, A. E.; Swager, T. M. *Chem. Rev*. **2000**, *100*, 2537-2574.

5. Street, G. B. In *Handbook of Conducting Polymers*; Skotheim, T. A., Ed.; Marcel Dekker: New York, 1986; Chapter 8, pp 265-291.

6. Marsella, M. J.; Swager T. M. *J. Am. Chem. Soc.* **1993**, *115*, 12214-12215.

7. Swager, T. M.; Gil, C. J.; Wrighton, M. S. *J. Phys. Chem.* **1995**, *99*, 4886-4893.

8. a) Greenham, N. C.; Moratti, S. C.; Bradley, D. D. C.; Friend, R. H.; Holmes, A. B. *Nature* **1993**, *365*, 628-30. b) Goldfinger, M. B.; Swager, T. M. *J. Am. Chem. Soc.* **1994**, *116*, 7895-6.

9. Förster, T. *Ann. Phys.* **1948**, *2*, 55.

10. a) Zimmerman, H. E.; Lapin, Y. A.; Nesterov, E. E.; Sereda, G. A. *J. Org. Chem.* **2000**, *65*, 7740-7746. b) Murphy, C. B.; Zhang, Y.; Troxler, T.; Ferry, V.; Martin, J.; Jones, W. E., Jr. *J. Phys. Chem. B* **2004**, *108*, 1537-1543. c) List, E. J. W.; Leising, G. *Synth. Met.* **2004**, *141*, 211-218.

11. a) Silva, A. P. de; Gunaratne, H. Q. N.; Gunnlaugsson, T.; Huxley, A. J. M. McCoy, C. P.; Rademacher, J. T.; Rice, T. E. *Chem. Rev.* **1997**, *97*, 1515-1566. b) Eggins, B. R. *Chemical sensors and biosensors.* Wiley: West Sussex, UK, 2002. c) Sauer, M. *Angew. Chem. Int. Ed.* **2003**, *42*, 1790-1793.

12. a) Special issue on "*Luminescent sensors"*. *Coord. Chem. Rev.* **2000**, *205*, 1-232. b) Rurack, K.; Resch-Gender, U. *Chem. Soc. Rev.* **2002**, *31*, 116-127.

13. James, D.; Scott, S. M.; Ali, Z.; O'Hare, W. T. *Microchim. Acta* **2005**, *149*, 1-17.

14. a) Valdes-Aguilera, O.; Neckers, D. C. *Acc. Chem. Res.* **1989**, *22*, 171-177. b) Megelski, S.; Lieb, A.; Pauchard, M.; Drechsler, A.; Glaus, S.; Debus, C.; Meixner, A. J.; Calzaferri, G. L. *J. Phys. Chem. B* **2001**, *105*, 25-35.

15. Yang, J.-S.; Swager, T. M. *J. Am. Chem. Soc.* **1998**, *120*, 11864-11873.

16. a) Flink, S.; van Veggel, F. C. J. M.; Reinhoudt, D. N. *Adv. Mater.* **2000**, *12*, 1315-1328. b) Tully, D. C.; Fréchet, J. M. J. *Chem. Comm.* **2001**, 1229-1239. c) Lee, M.; Kim, T.-I.; Kim, K.-H.; Kim, J.-H.; Choi, M.-S.; Choi, M.-J.; Koh, K. *Anal. Biochem.* **2002**, *310*, 163-170. d) Umar, A. A.; Salleh, M. M.; Yahaya, M. *Sensors and Actuators B* **2004**, *101*, 231-235. e) Zhang, S.; Song, F.; Echegoyen, L. *Eur. J. Org. Chem.* **2004**, 2936-2934. f) Beer, P. D.; Cormode, D. P.; Davis, J. J. *Chem. Commun.* **2004**, 414-415.

17. a) Crego-Calama, M.; Reinhoudt, D. N. *Adv. Mater.* **2001**, *13*, 1171-1174. b) Basabe-Desmonts, L.; Beld, J.; Zimmerman, R. S.; Hernando, J.; Mela, P.; García Parajó, M. F.; van Hulst, N. F.; van den Berg, A.; Reinhoudt, D. N.; Crego-Calama, M. *J. Am. Chem. Soc.* **2004**, *126*, 7293-7299.

18. Rusin, O.; St. Luce, N. N.; Agbaria, R. A.; Escobedo, J. O.; Jiang, S.; Warner, I. M.; Dawan, F. B.; Lian, K.; Strongin, R. M. *J. Am. Chem. Soc.* **2004**, *126*, 438-439.

19. Sonogashira, K. *J. Organomet. Chem.* **2002**, *653*, 46-49.

20. Hundertmark, T.; Littke, A. F.; Buchwald, S. L.; Fu, G. C. *Org. Lett.* **2000**, *2*, 1729-1731.

21. Corey, P. F.; Trimmer, R. W.; Biddlecom, W. G. *Angew. Chem. Int. Ed.* **1991**, *30*, 1646-1648.

22. Ziener, U.; Godt, A. *J. Org. Chem*. **1997**, *62*, 6137-6143.

APPENDIX: CHARACTERIZATION DATA

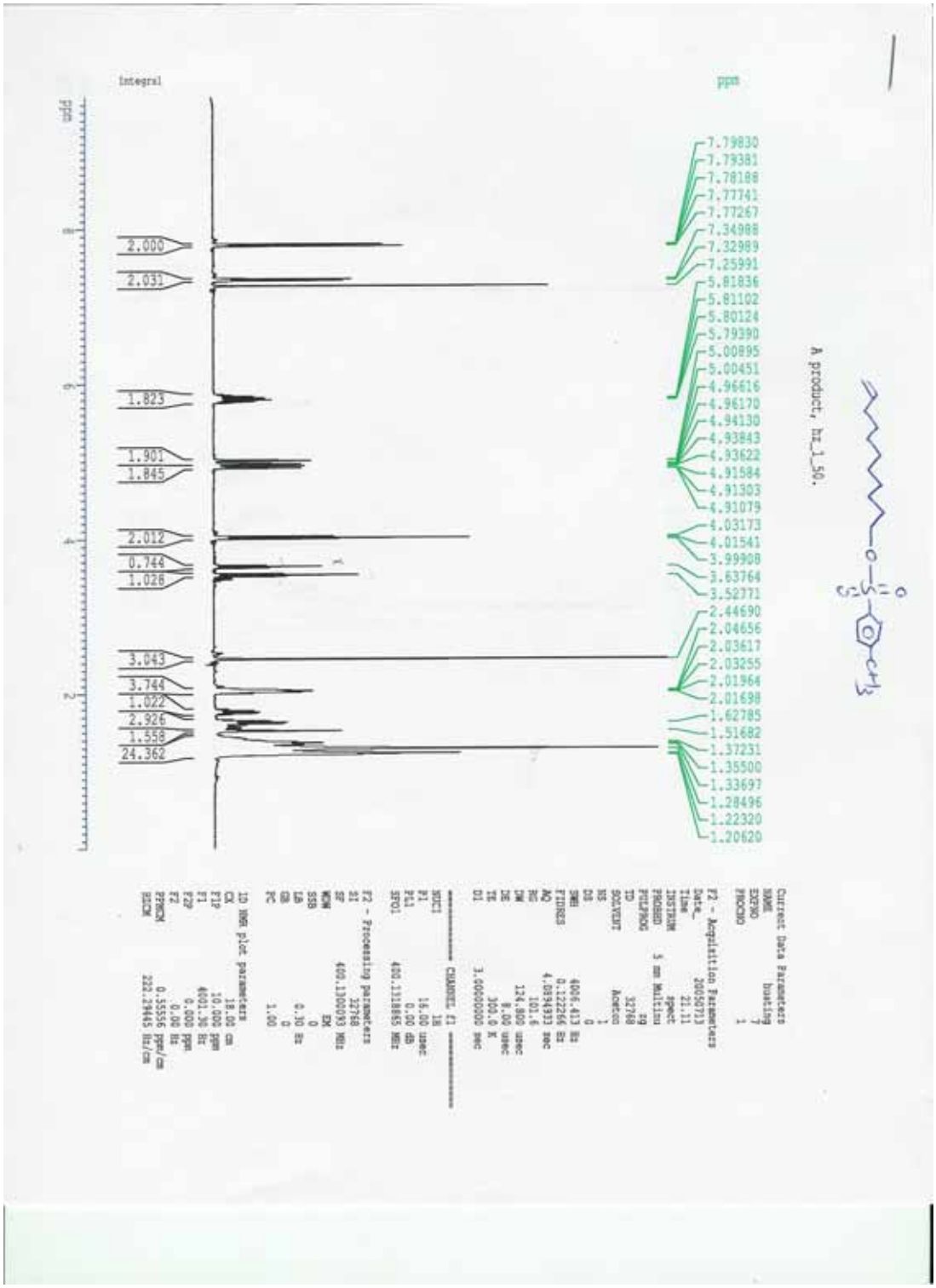

Figure A1. ^{1}H NMR of Compound **3**.

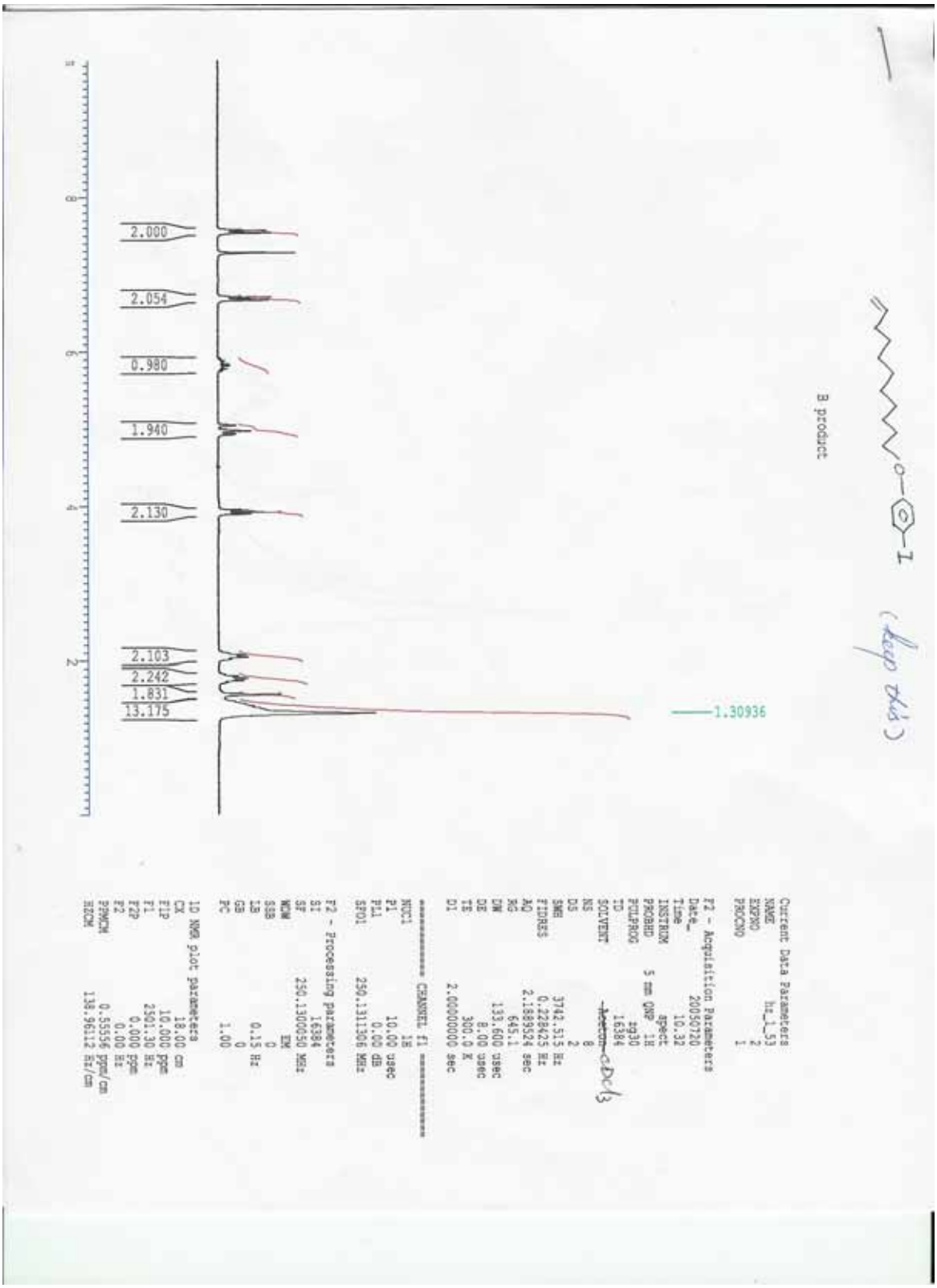

Figure A2. ^{1}H NMR of Compound **4**.

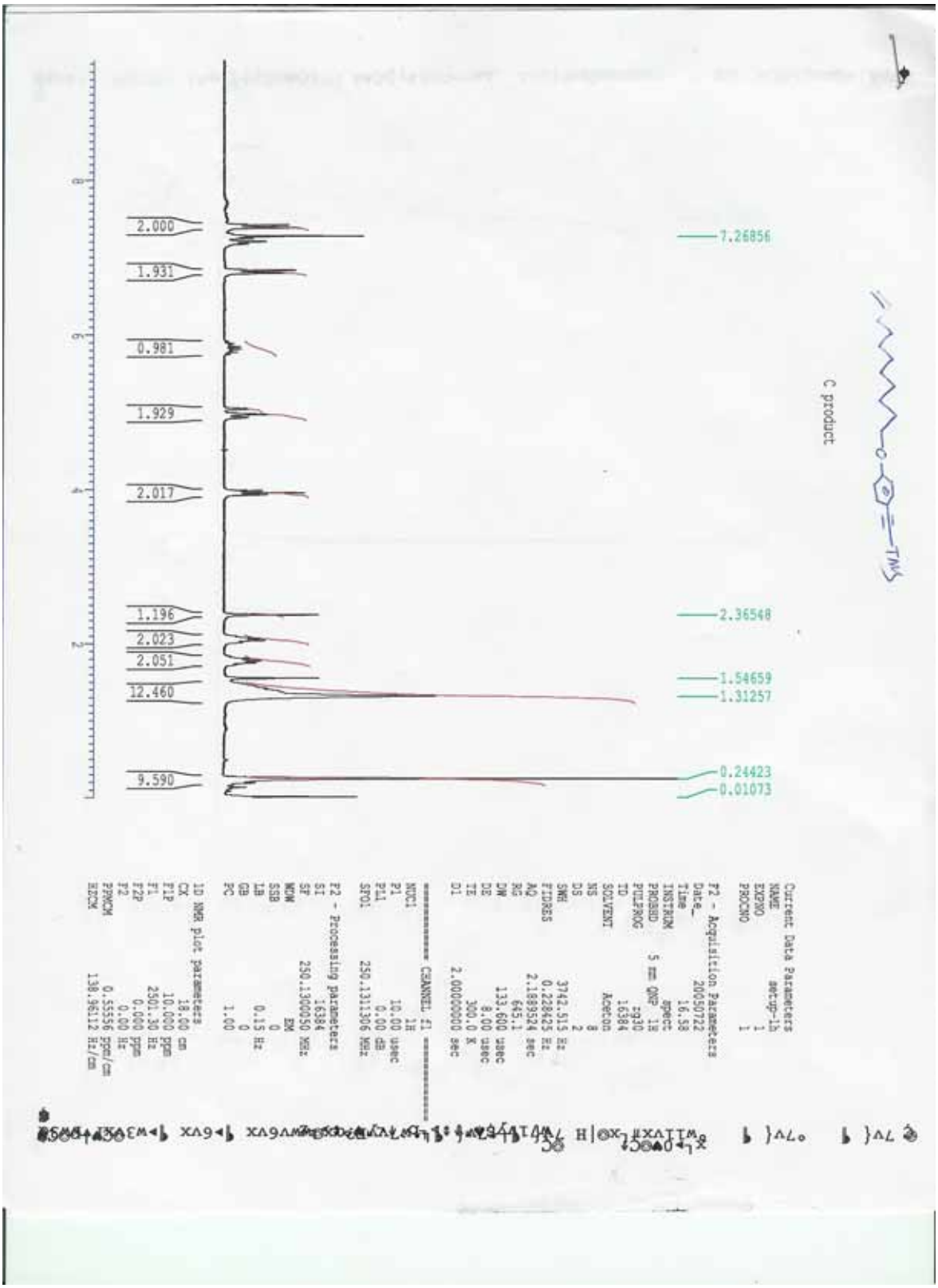

Figure A3. ^{1}H NMR of Compound **5**.

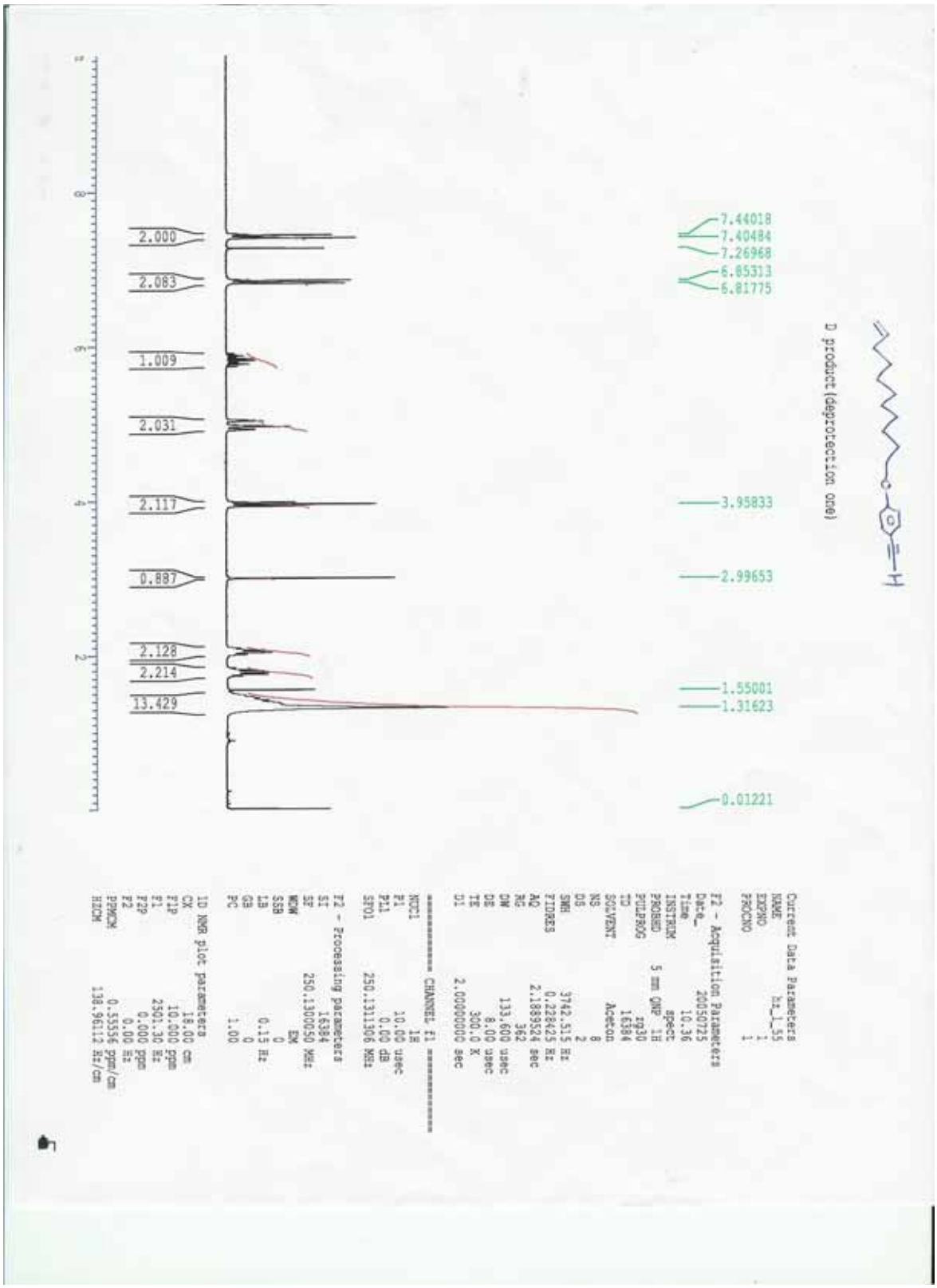

Figure A4. ^{1}H NMR of the fragment **A**.

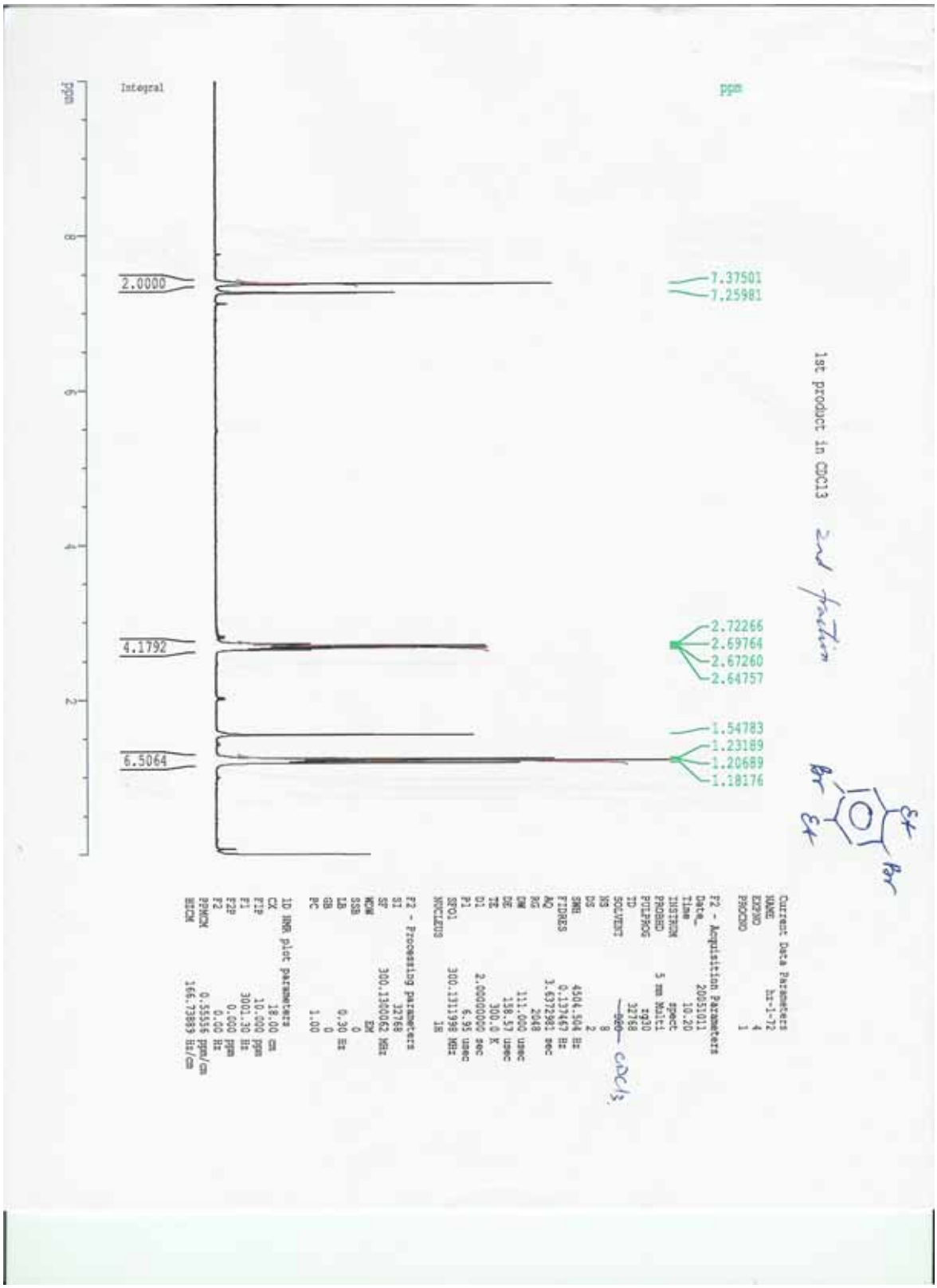

Figure A5. ^{1}H NMR of Compound **7**.

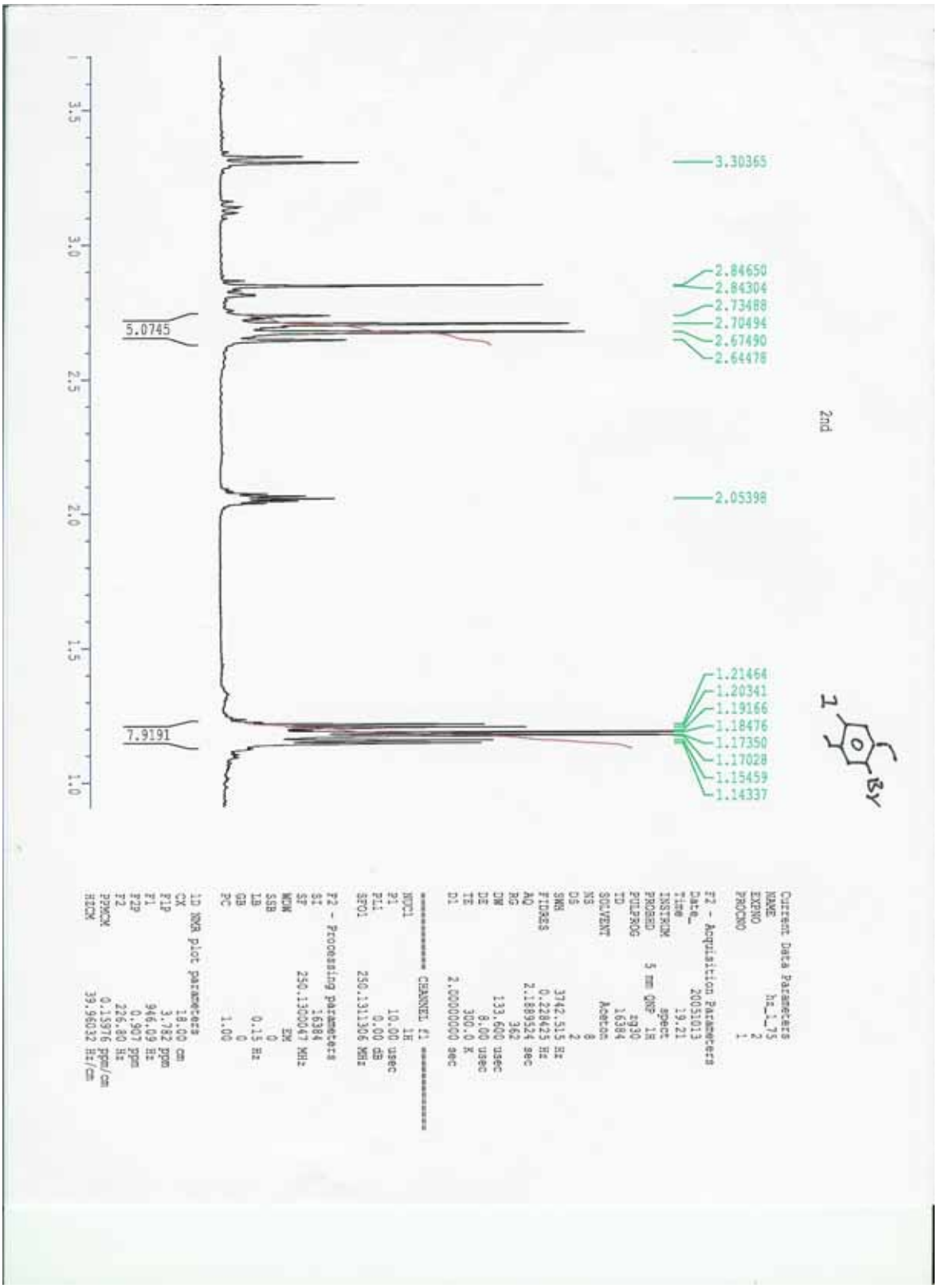

Figure A6. ^{1}H NMR of Compound **8**.

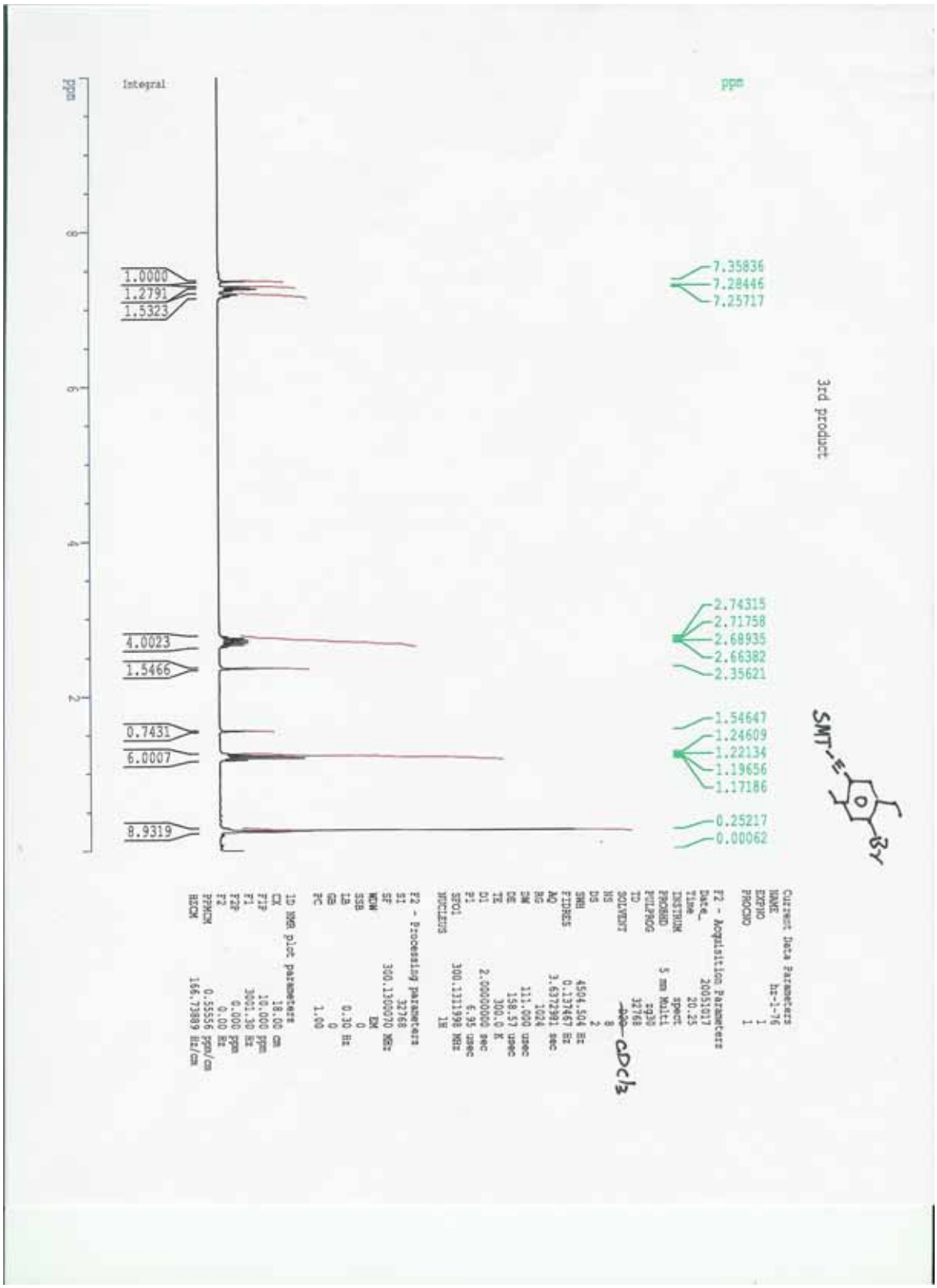

Figure A7. ^{1}H NMR of Compound **9**.

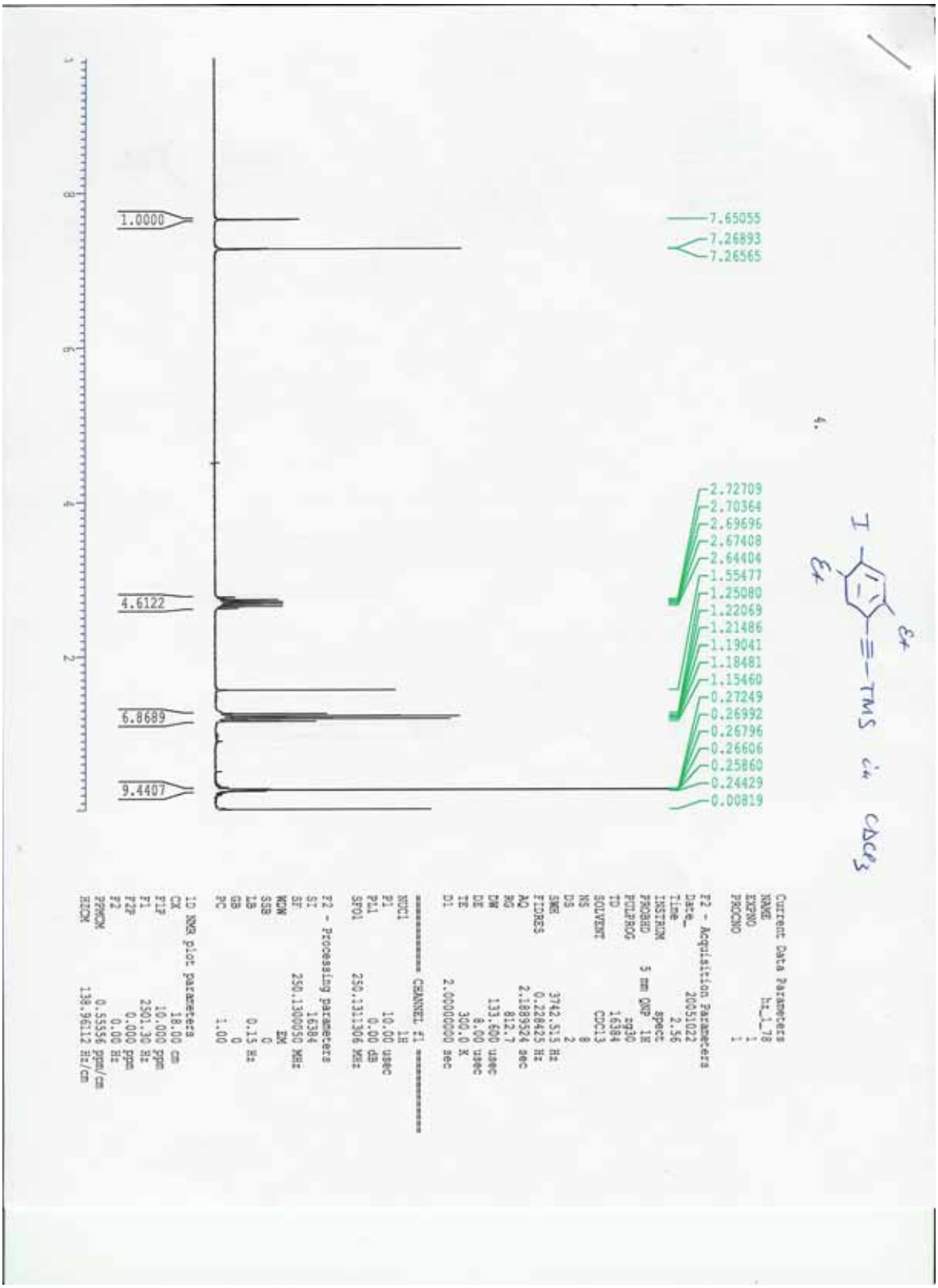

Figure A8. ^{1}H NMR of Compound **10**.

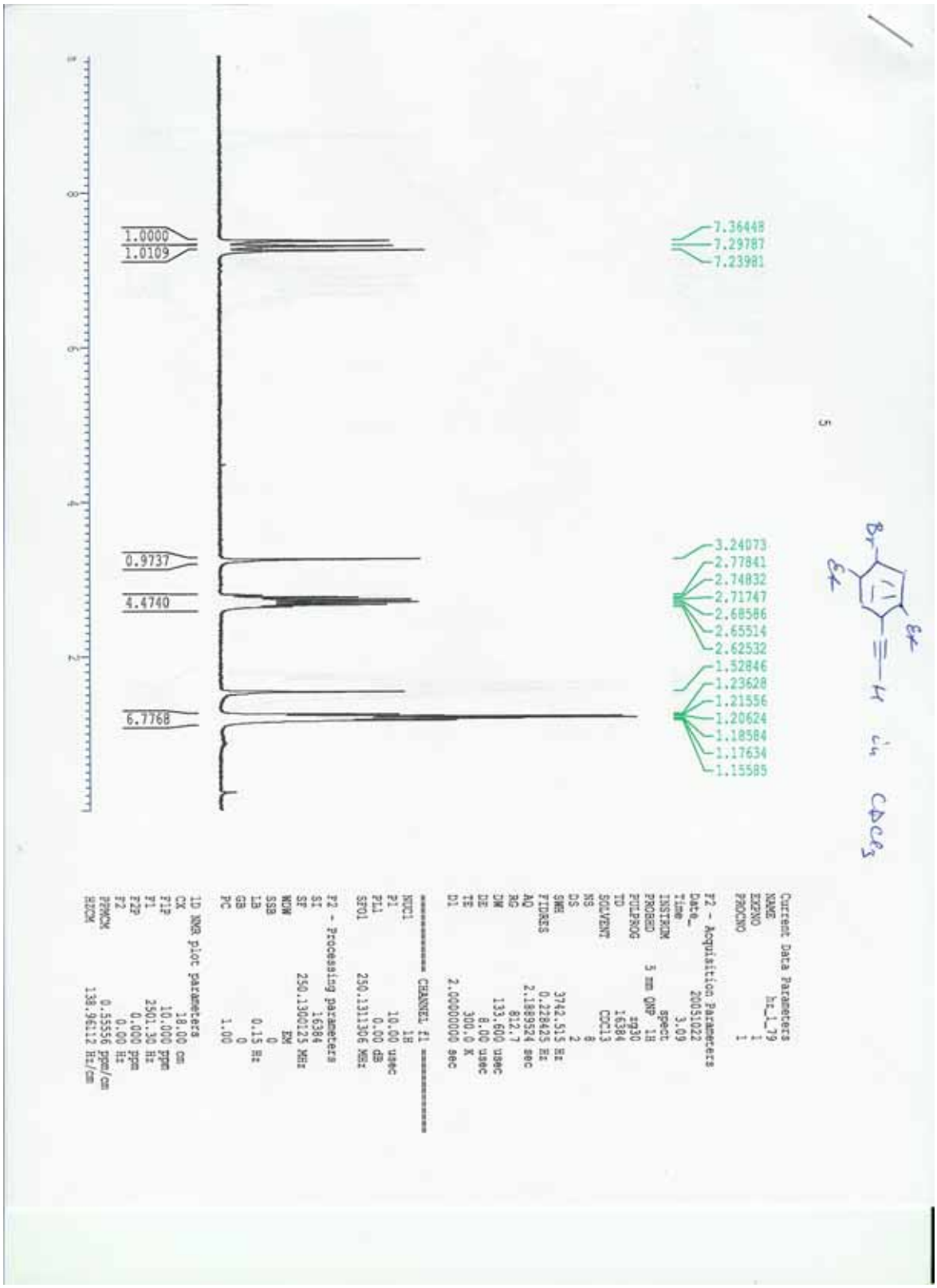

Figure A9. ^{1}H NMR of Compound **11**.

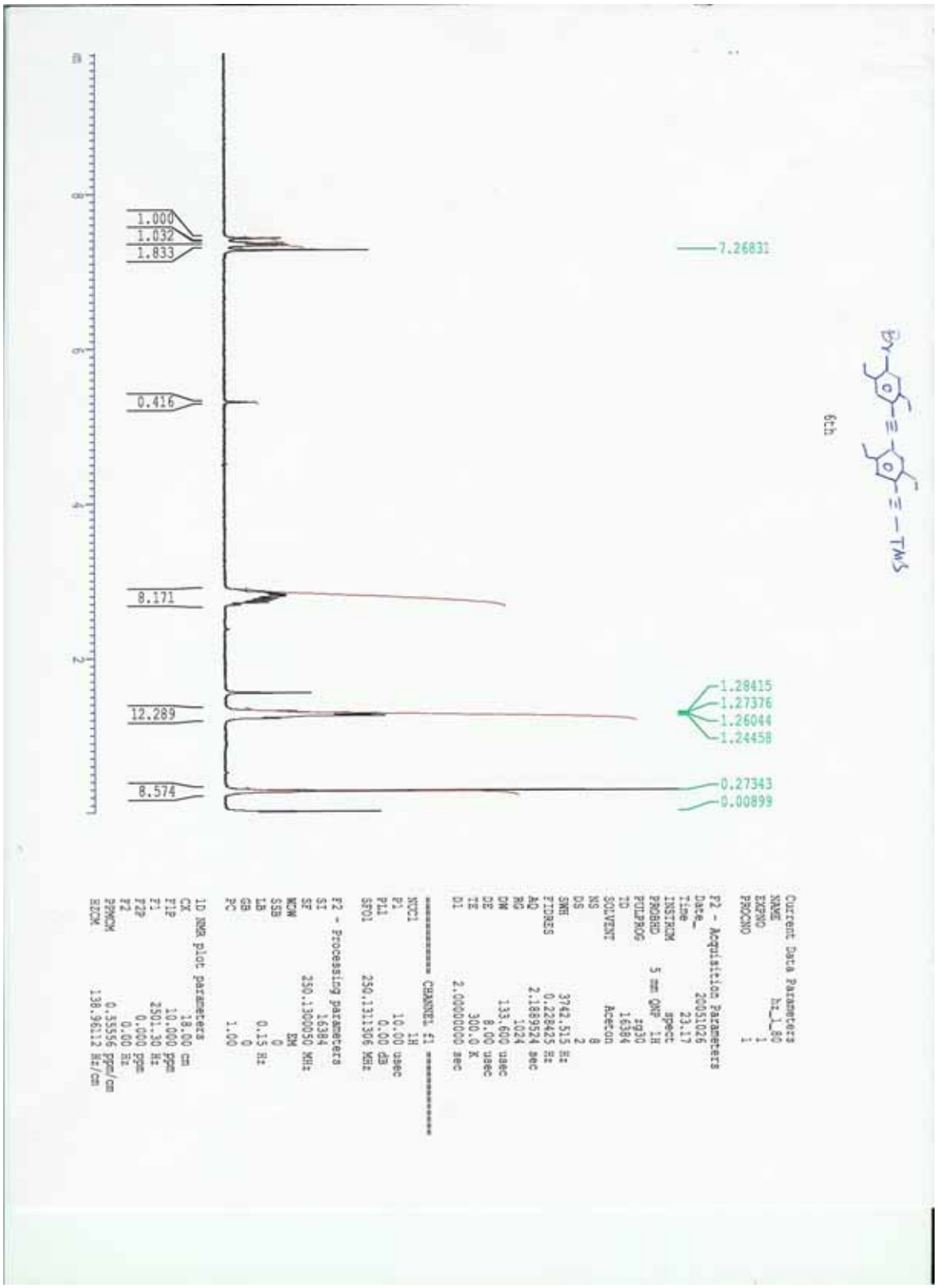

Figure A10. ^{1}H NMR of Compound **12**.

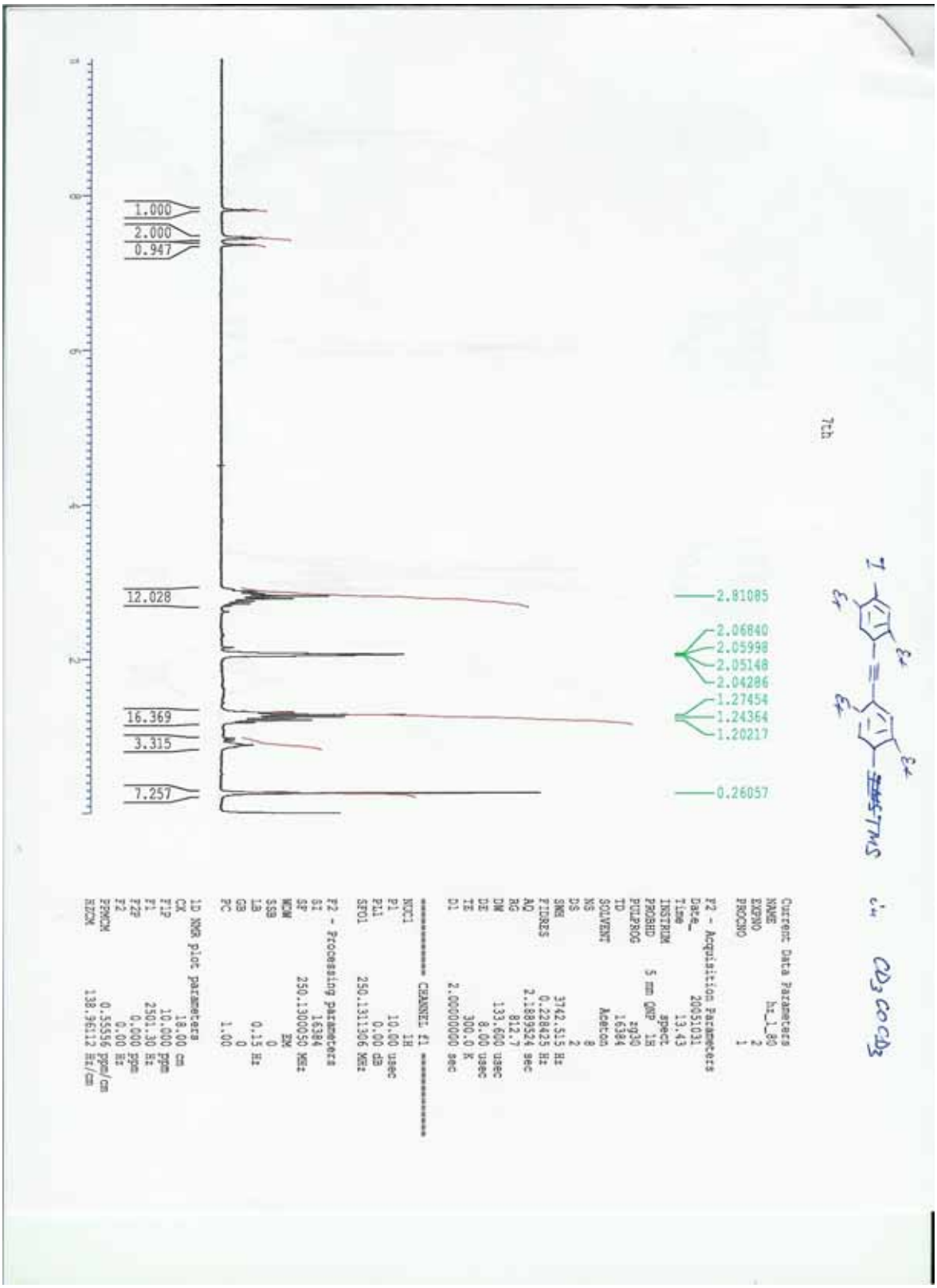

Figure A11. ^{1}H NMR of Compound **13**.

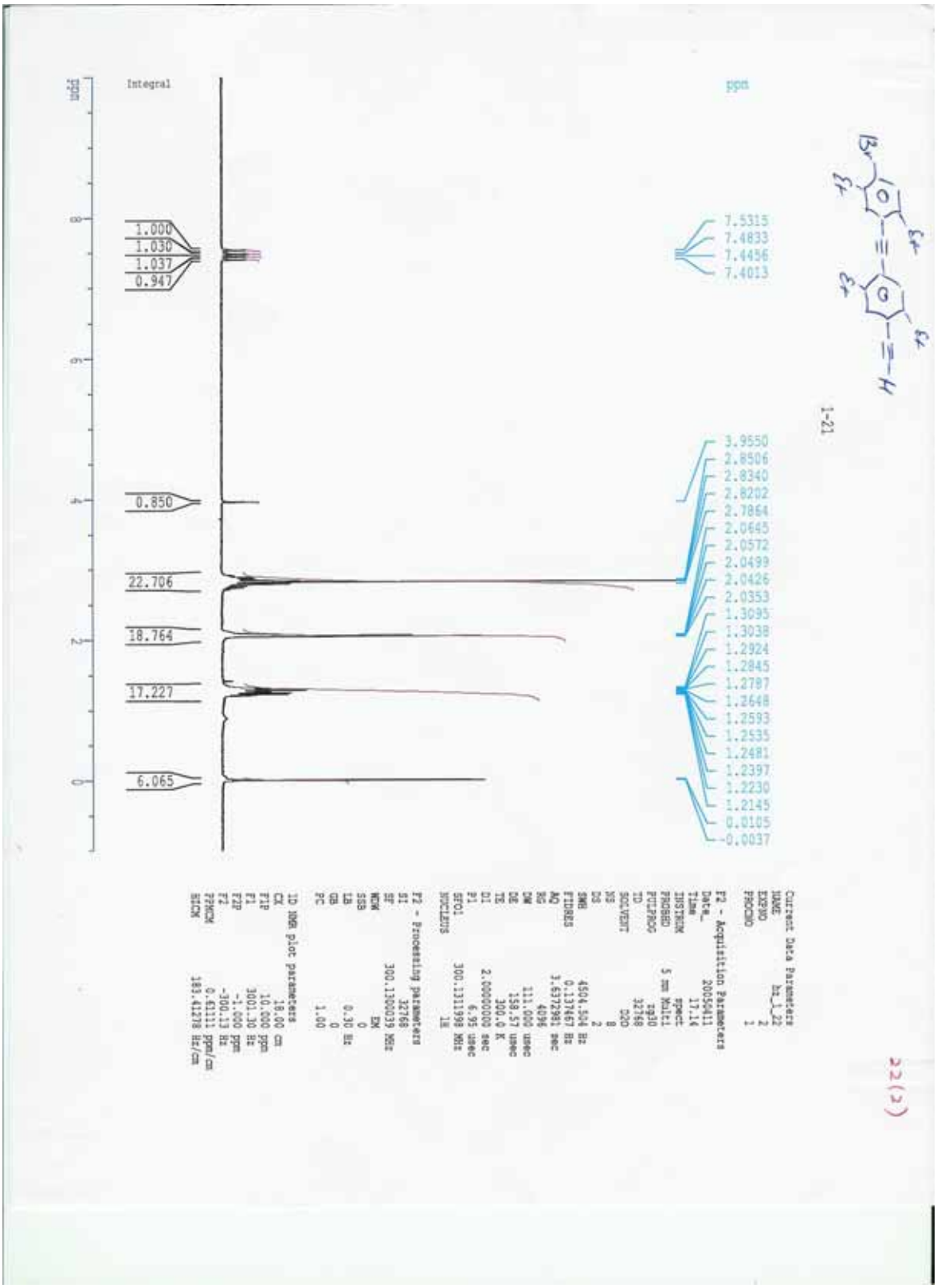

Figure A12. ^{1}H NMR of Compound **14**.

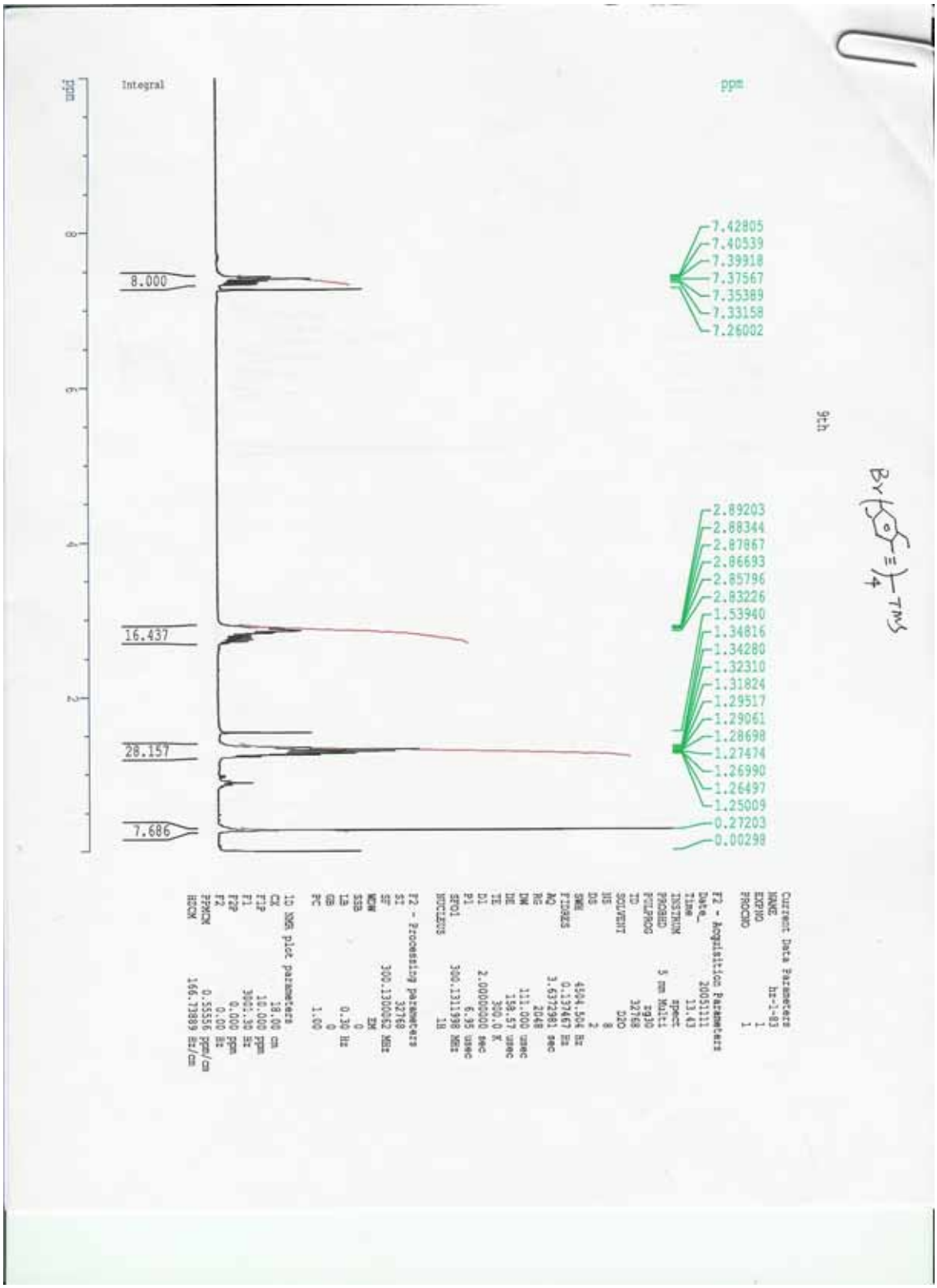

Figure A13. ^{1}H NMR of Compound **15**.

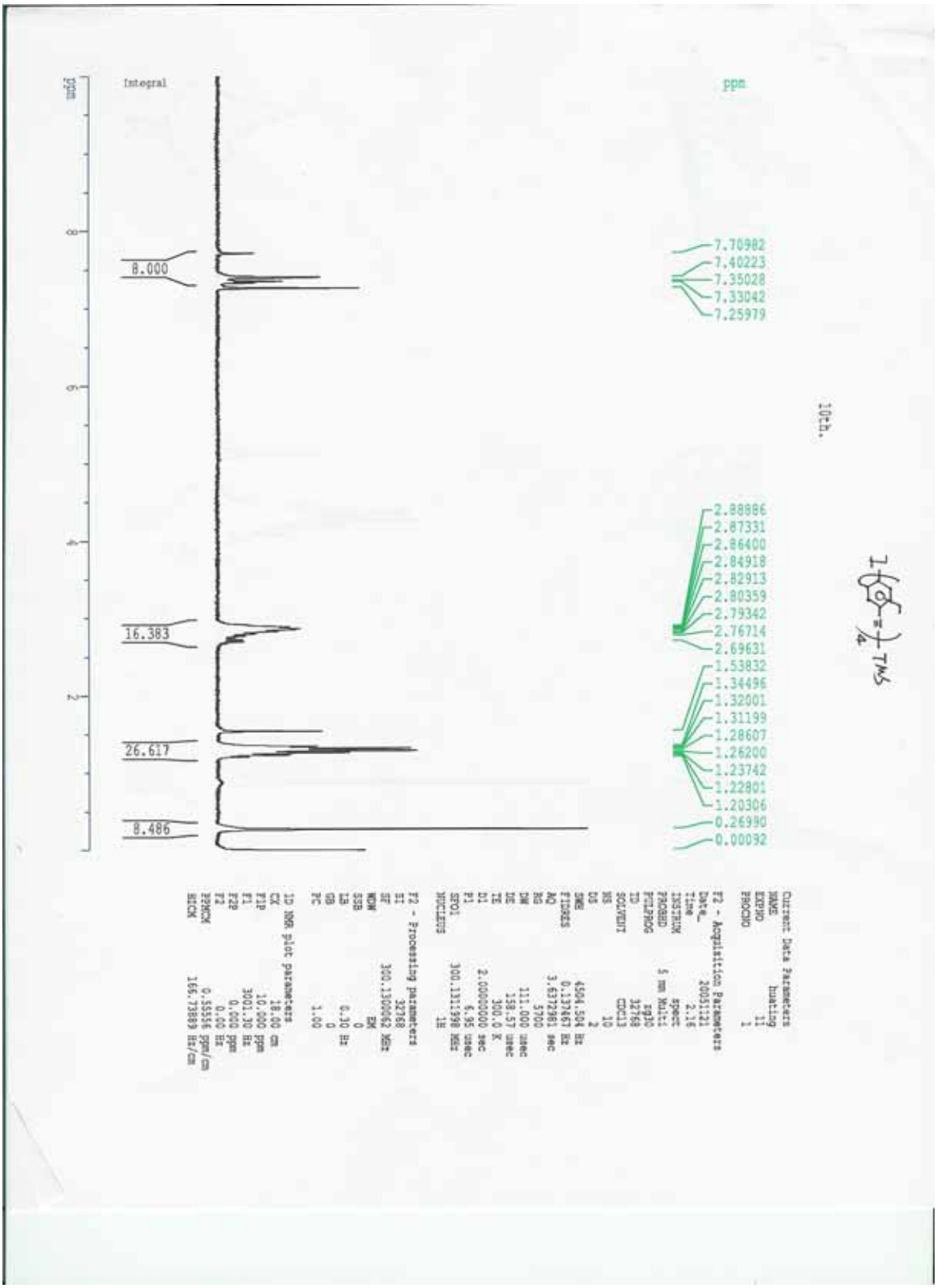

Figure A14. ^{1}H NMR of Compound **16**.

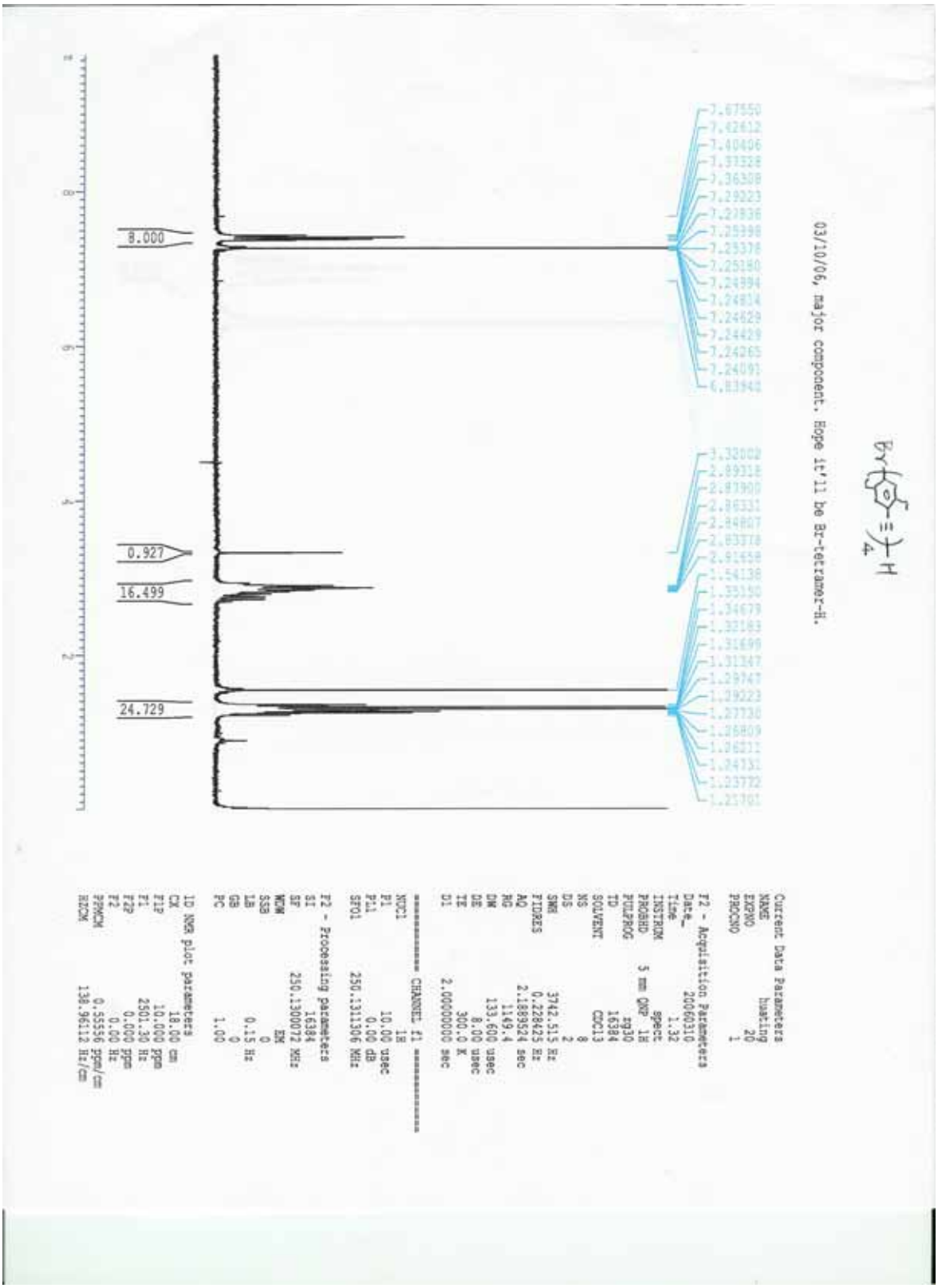

Figure A15. ^{1}H NMR of Compound **17**.

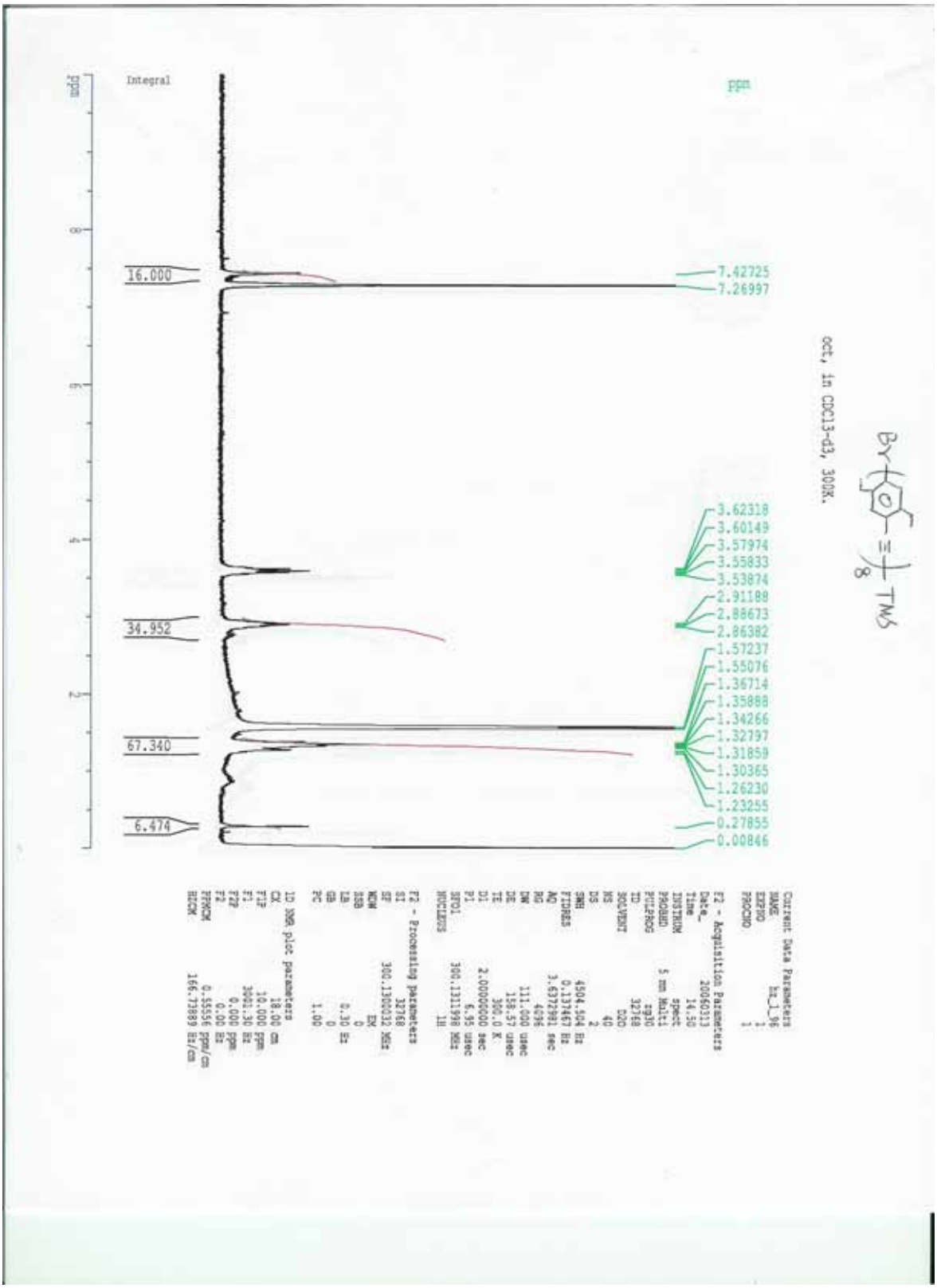

Figure A16. ^{1}H NMR of Compound **18**.

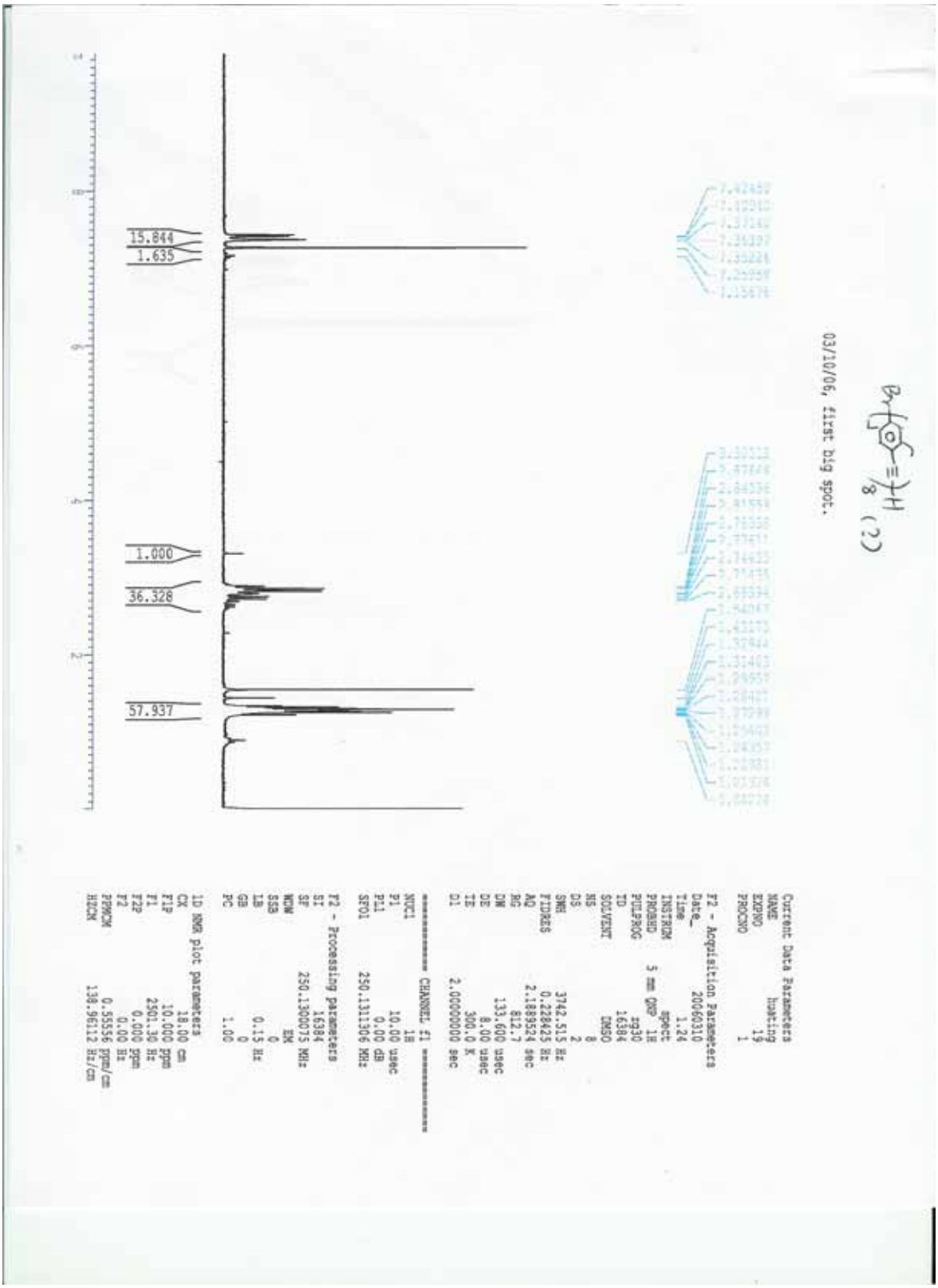

Figure A17. ^{1}H NMR of the fragment **B**.

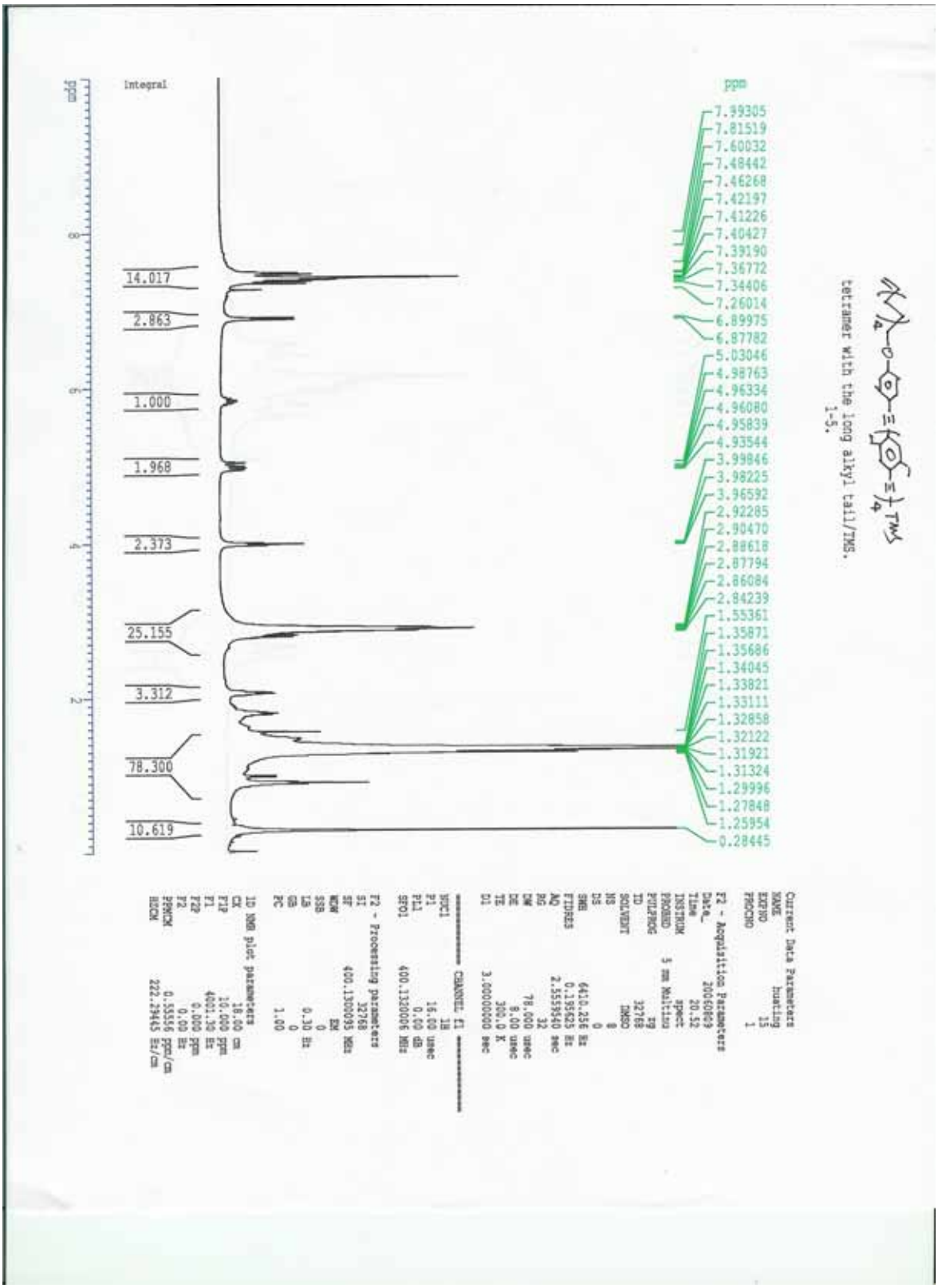

Figure A18. ^{1}H NMR of Compound **19**.

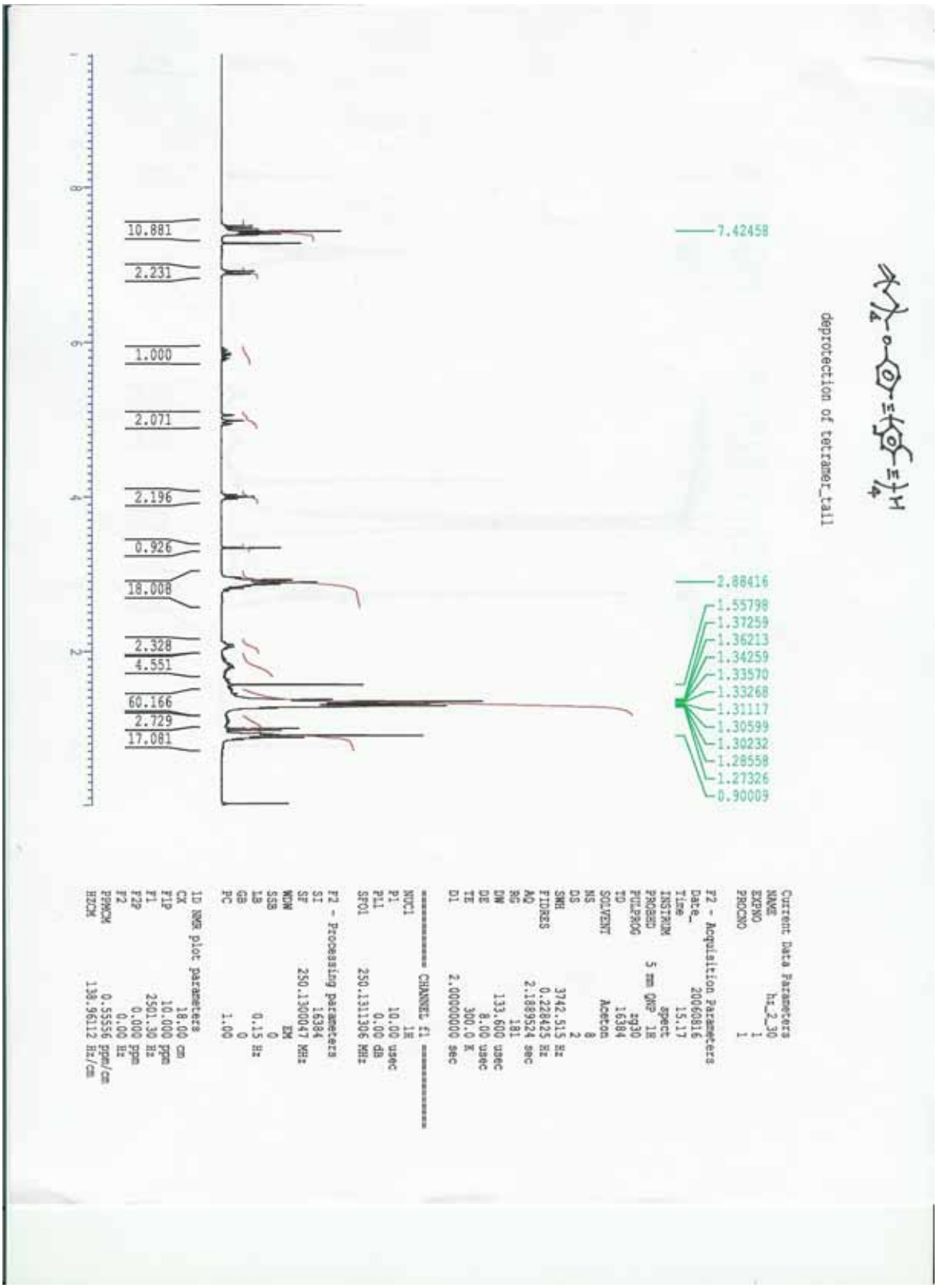

Figure A19. ^{1}H NMR of Compound **20**.

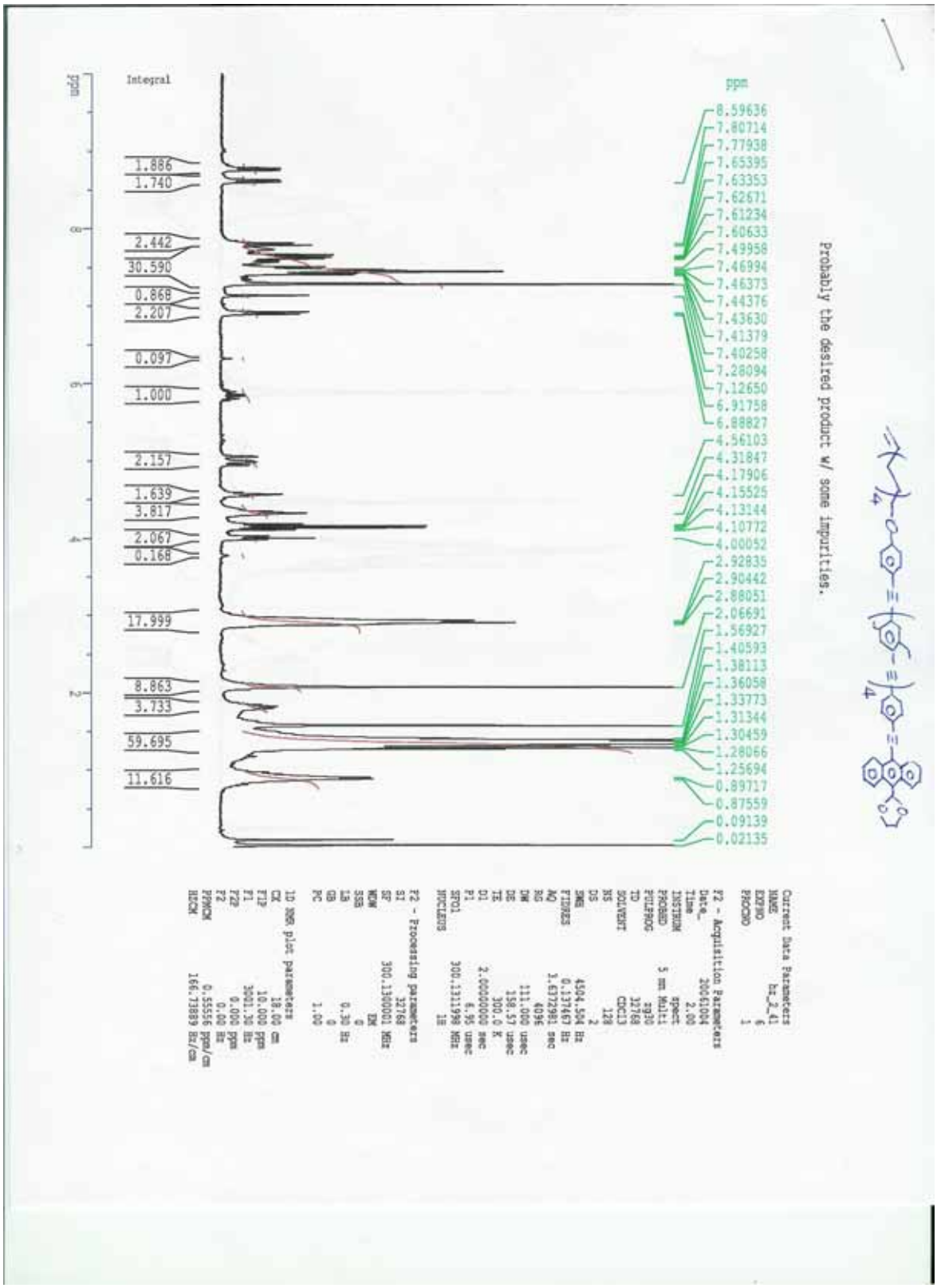

Figure A20. ^{1}H NMR of Compound **21**.

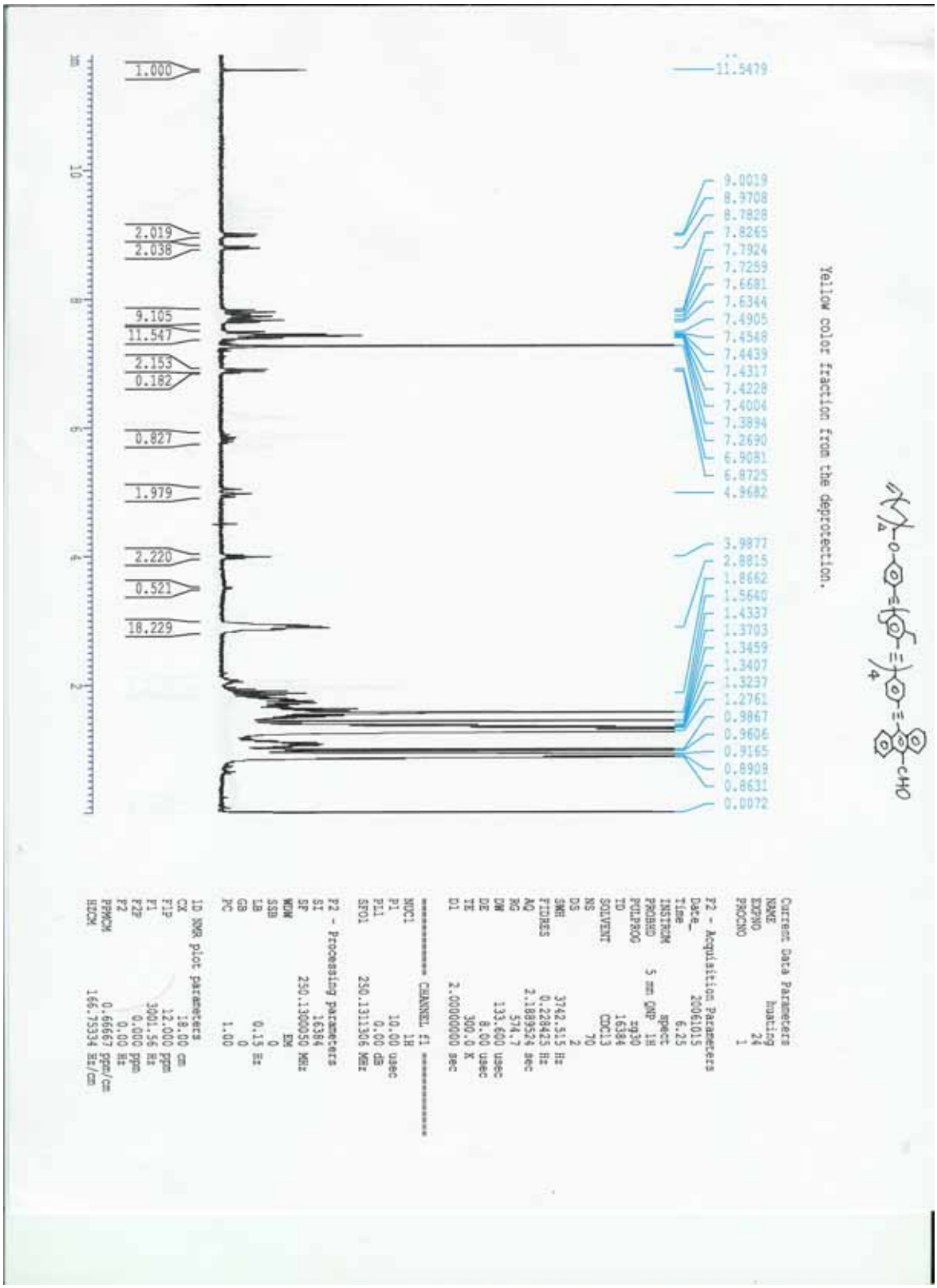

Figure A21. ^{1}H NMR of Compound **22**.

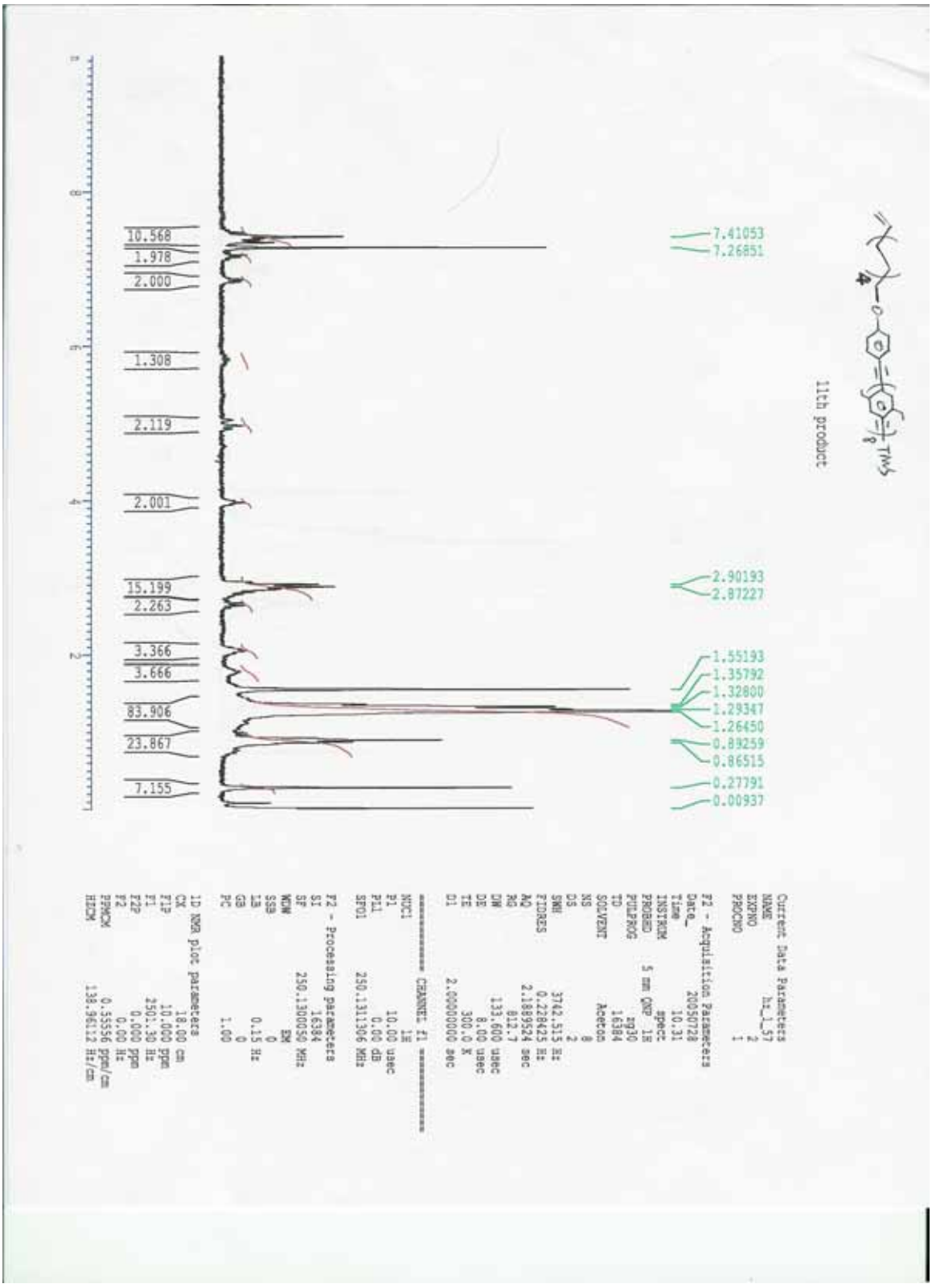

Figure A22. ^{1}H NMR of Compound **23**.

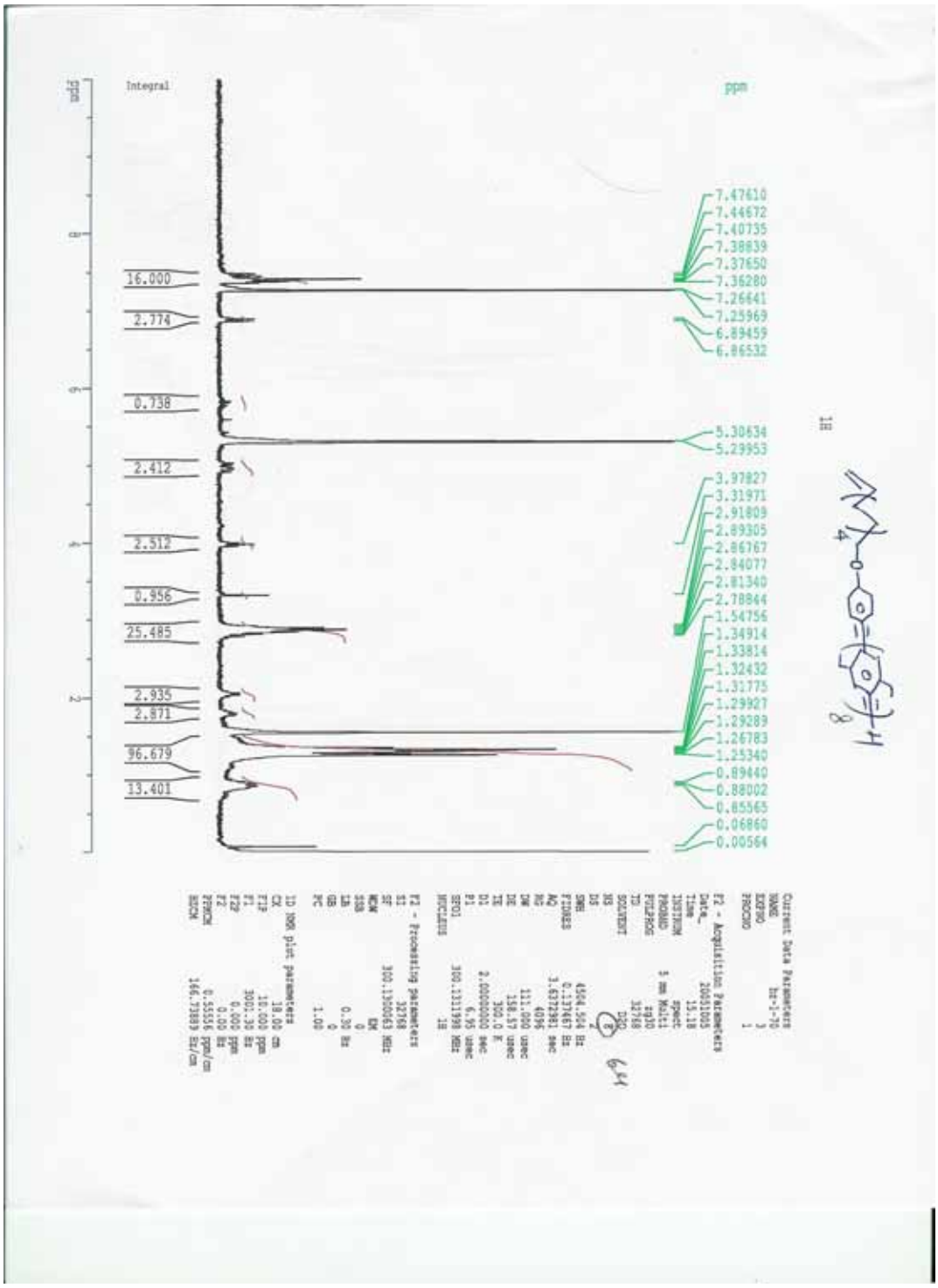

Figure A23. ^{1}H NMR of Compound **24**.

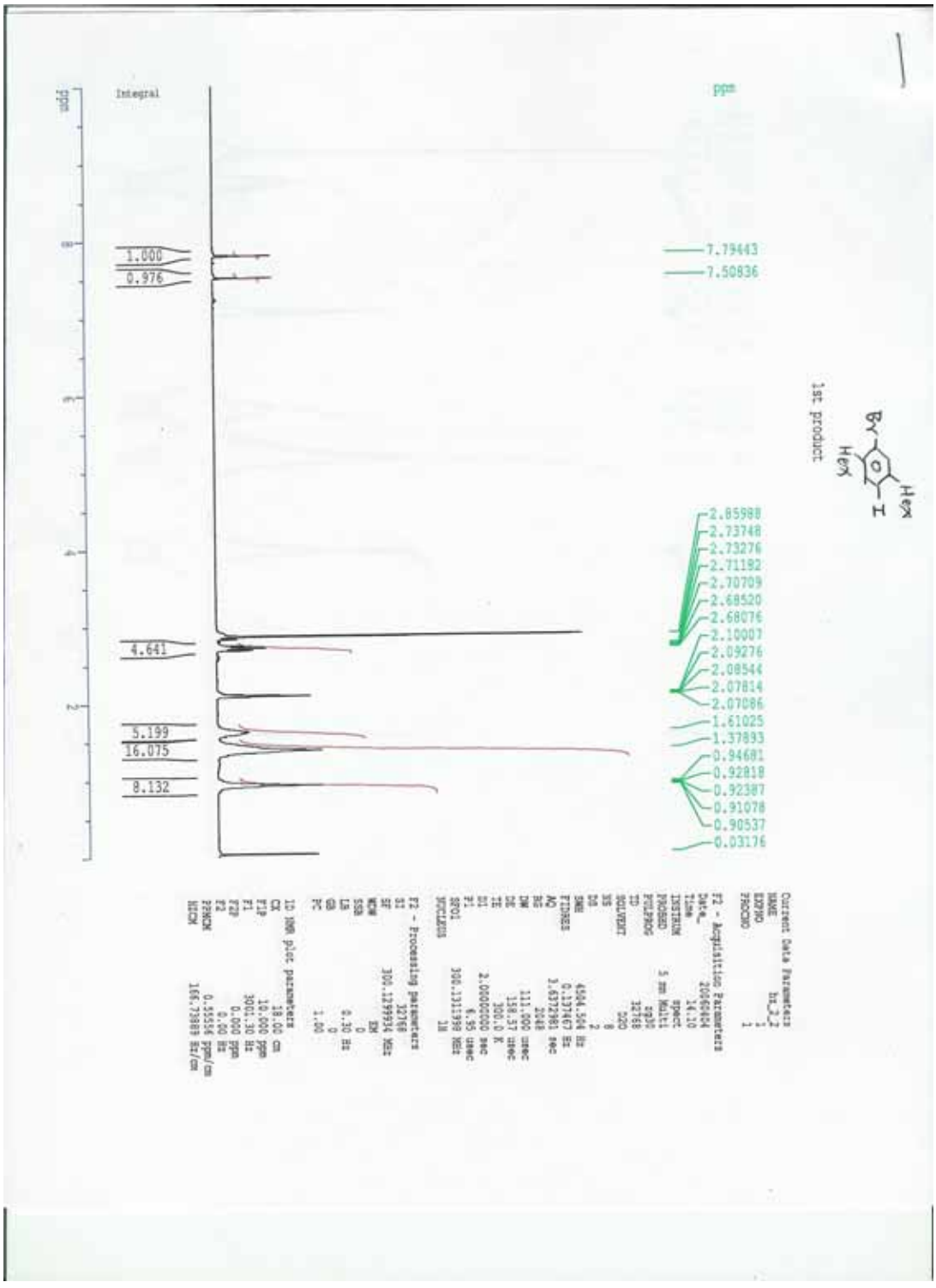

Figure A24. ^{1}H NMR of Compound **26**.

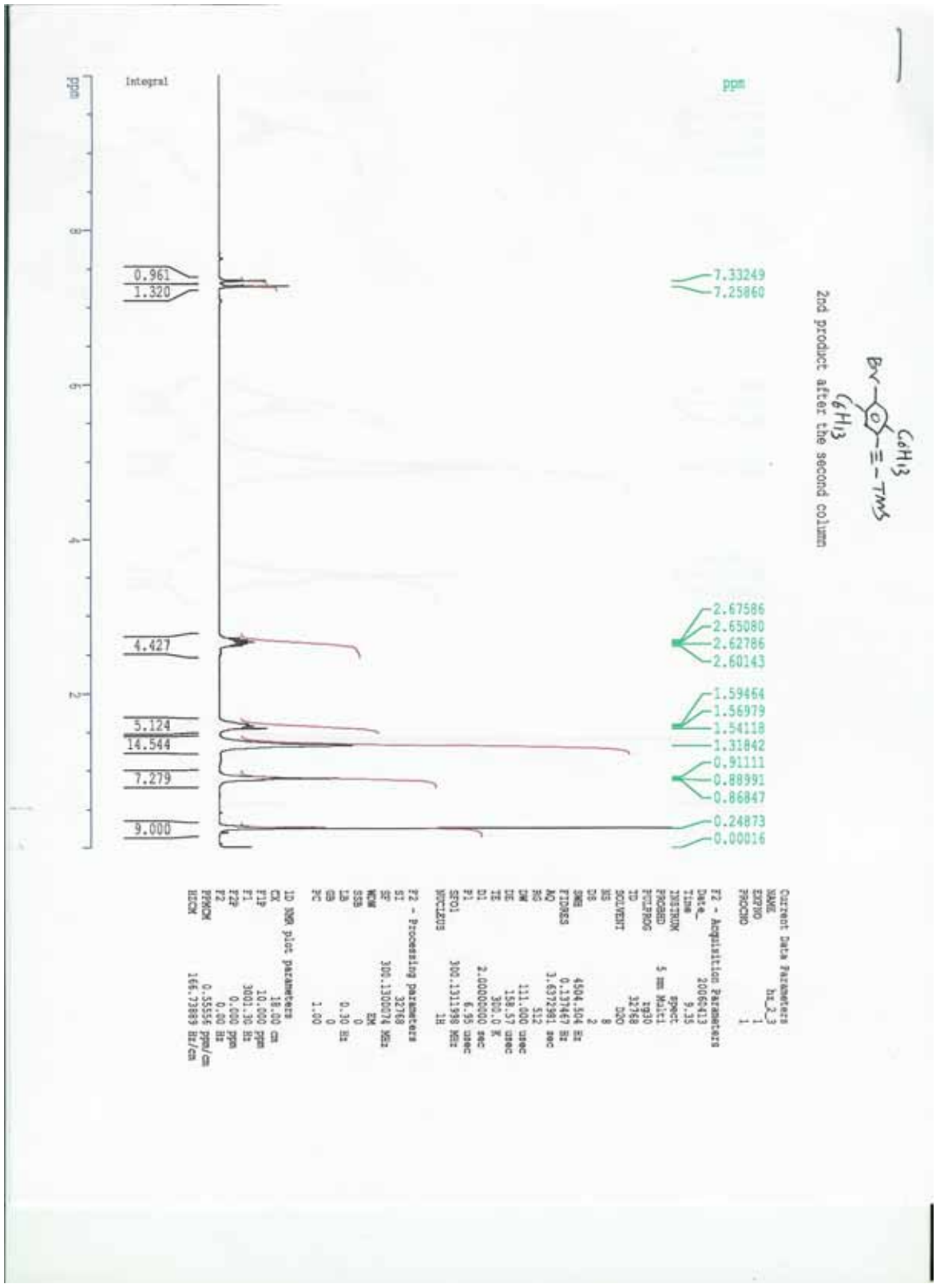

Figure A25. ^{1}H NMR of Compound **27**.

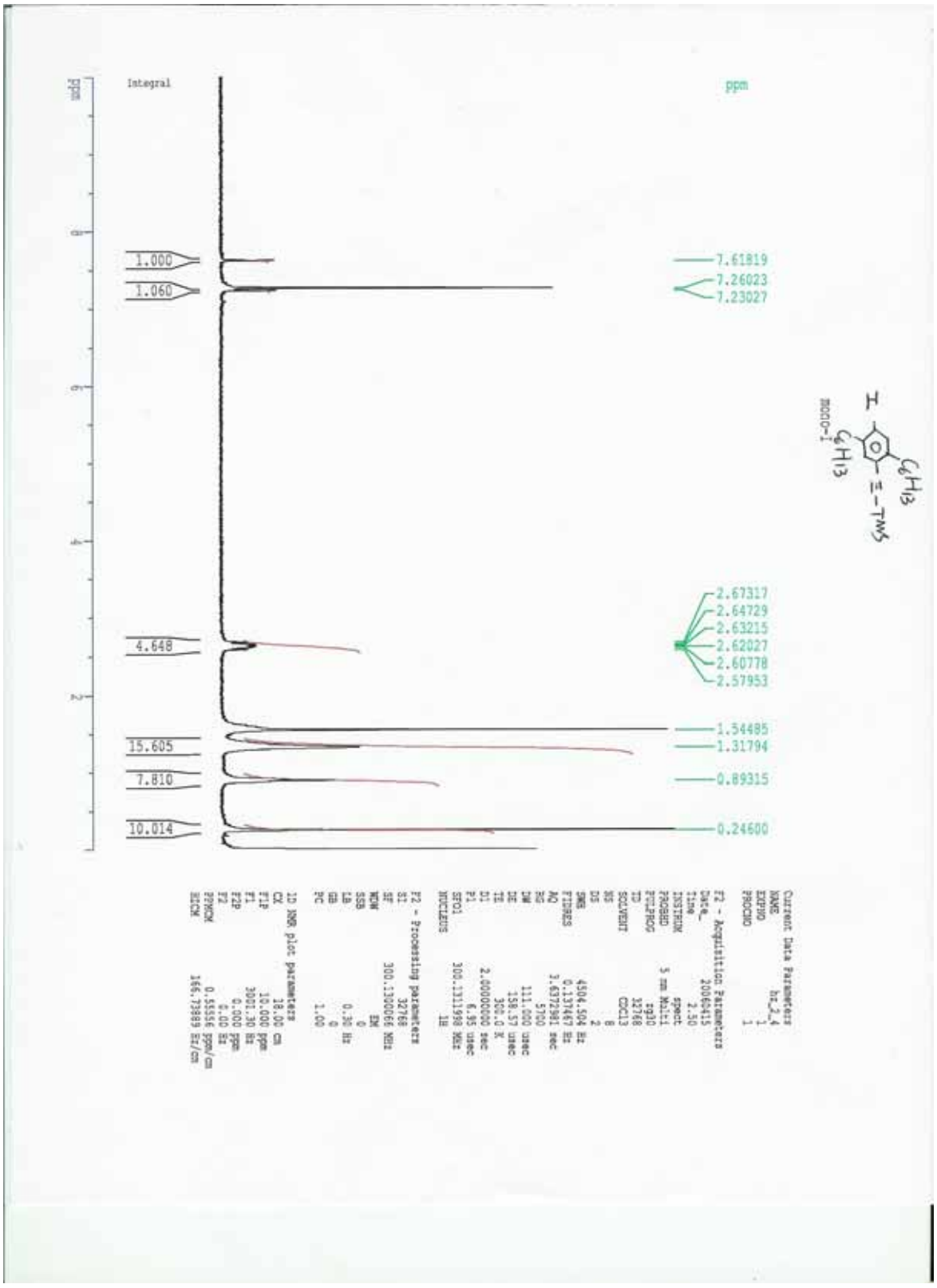

Figure A26. ^{1}H NMR of Compound **28**.

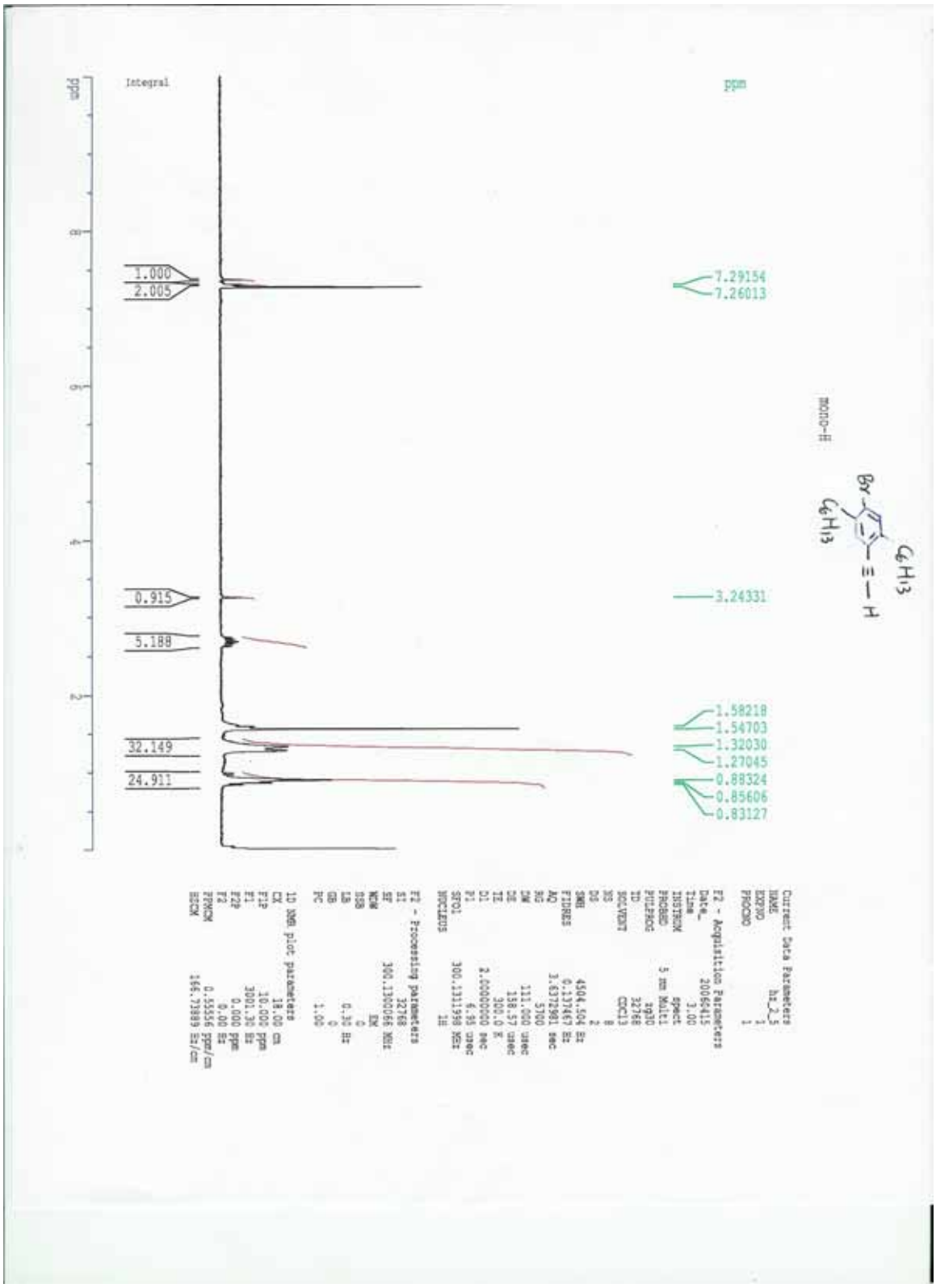

Figure A27. ^{1}H NMR of Compound **29**.

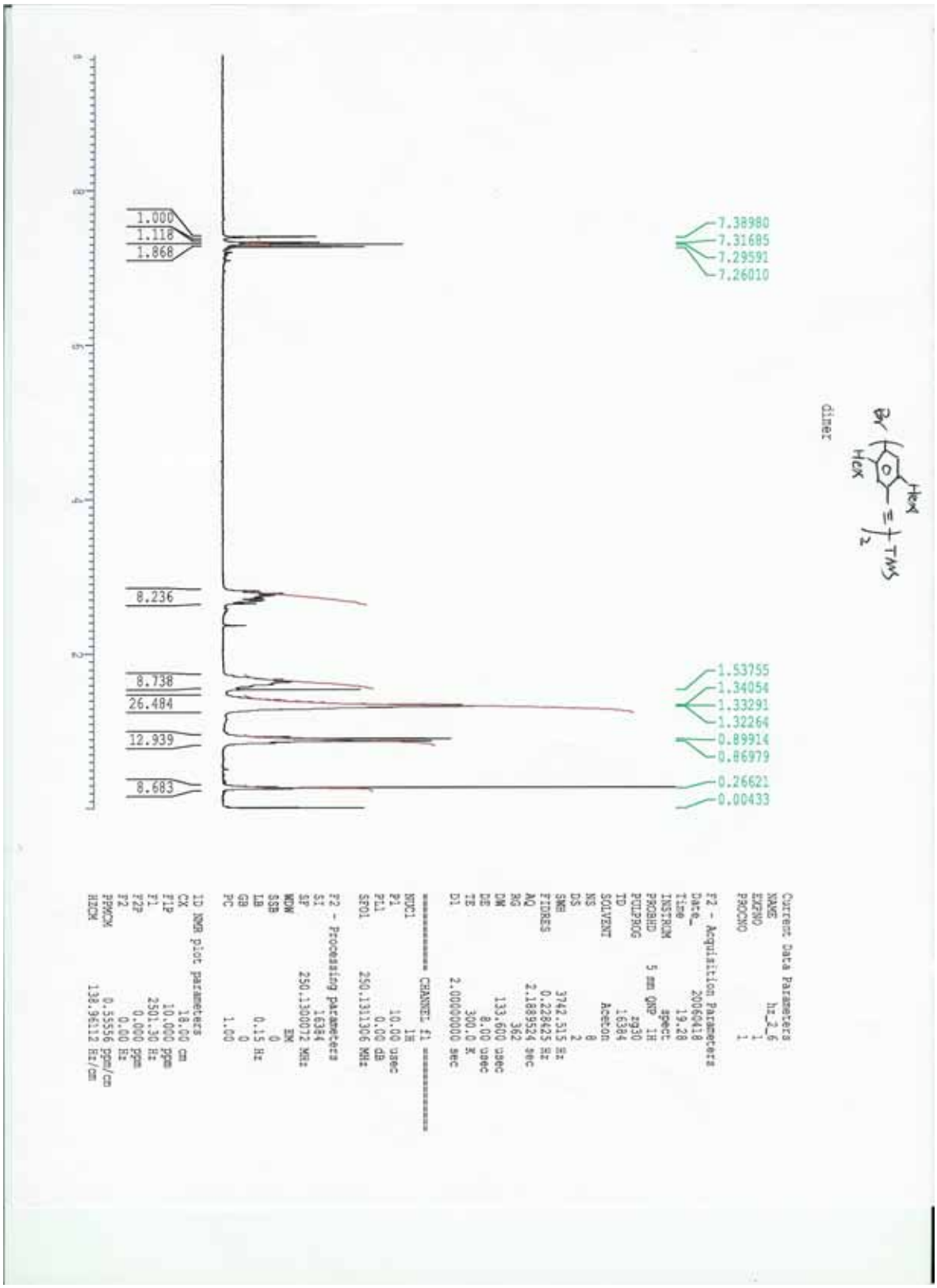

Figure A28. ^{1}H NMR of Compound **30**.

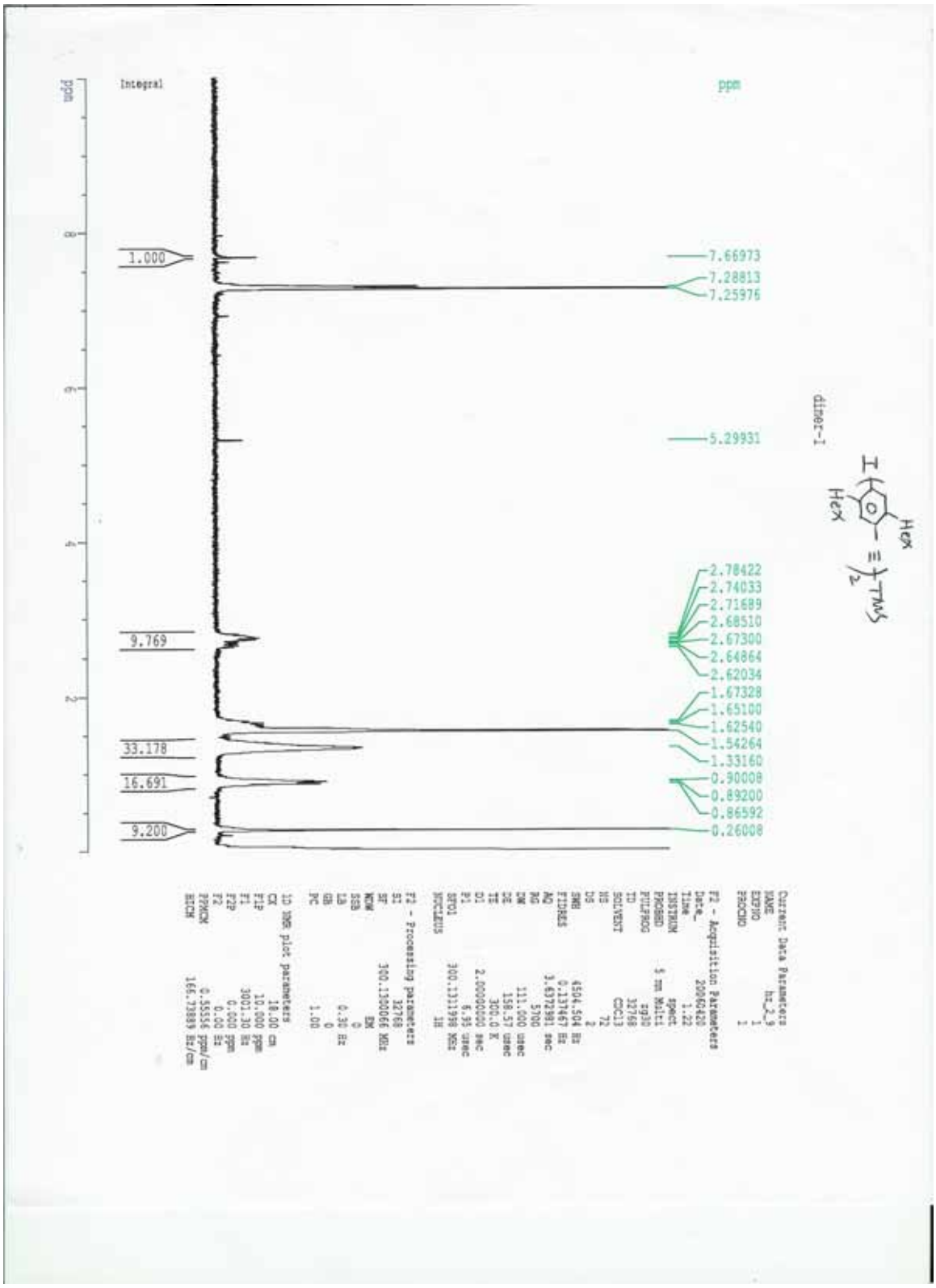

Figure A29. ^{1}H NMR of Compound **31**.

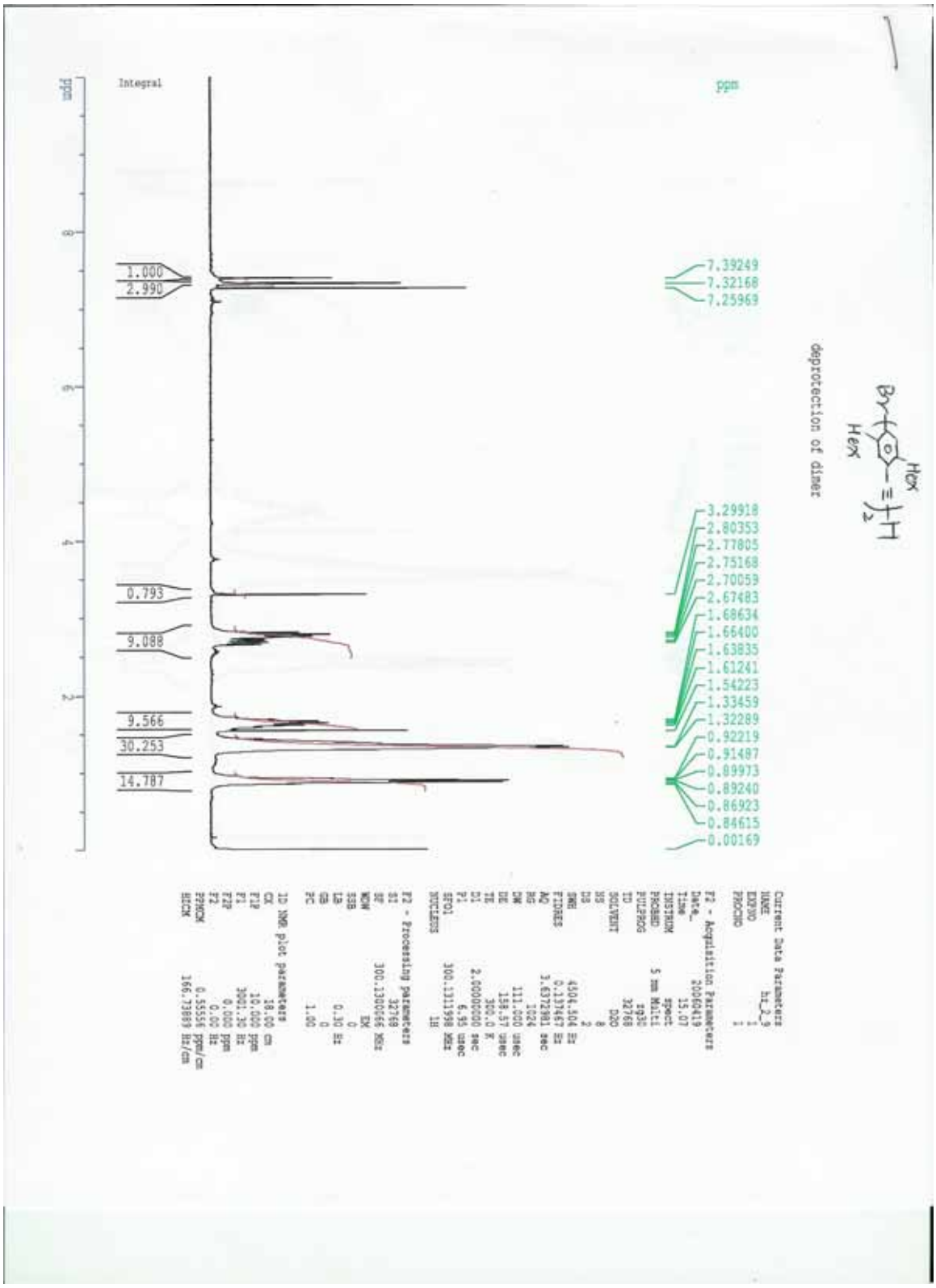

Figure A30. ^{1}H NMR of Compound **32**.

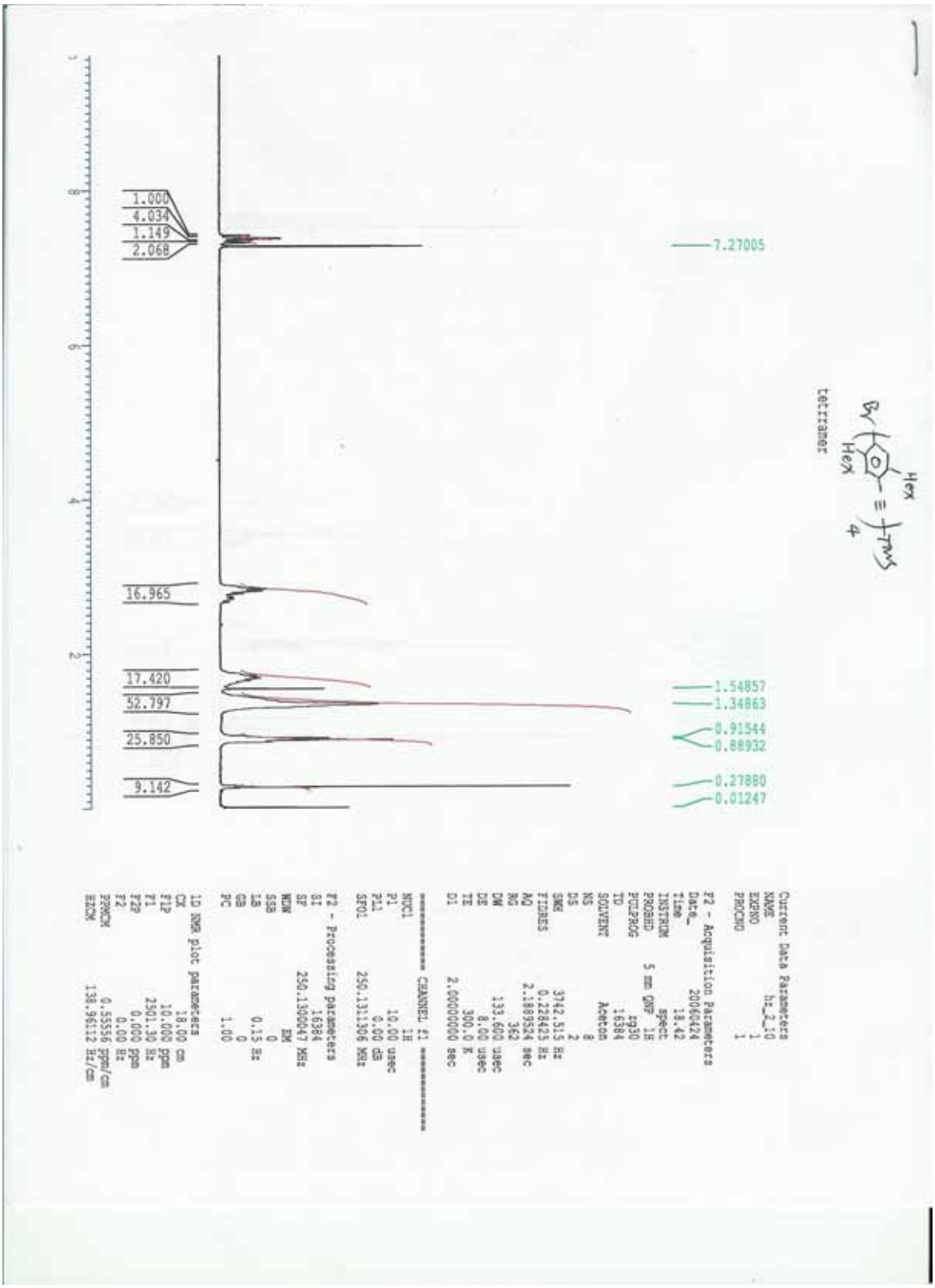

Figure A31. ^{1}H NMR of Compound **33**.

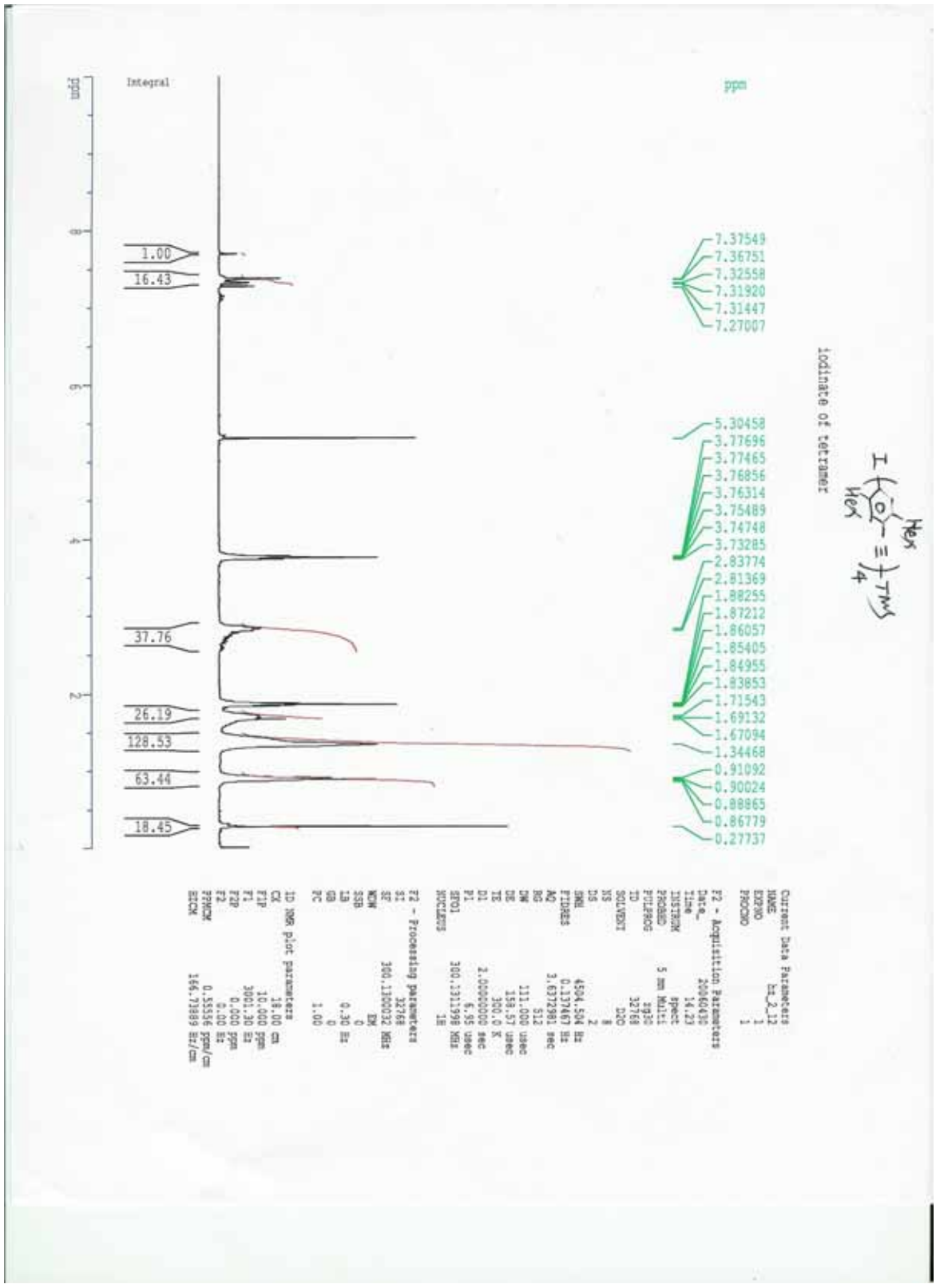

Figure A32. ^{1}H NMR of Compound **34**.

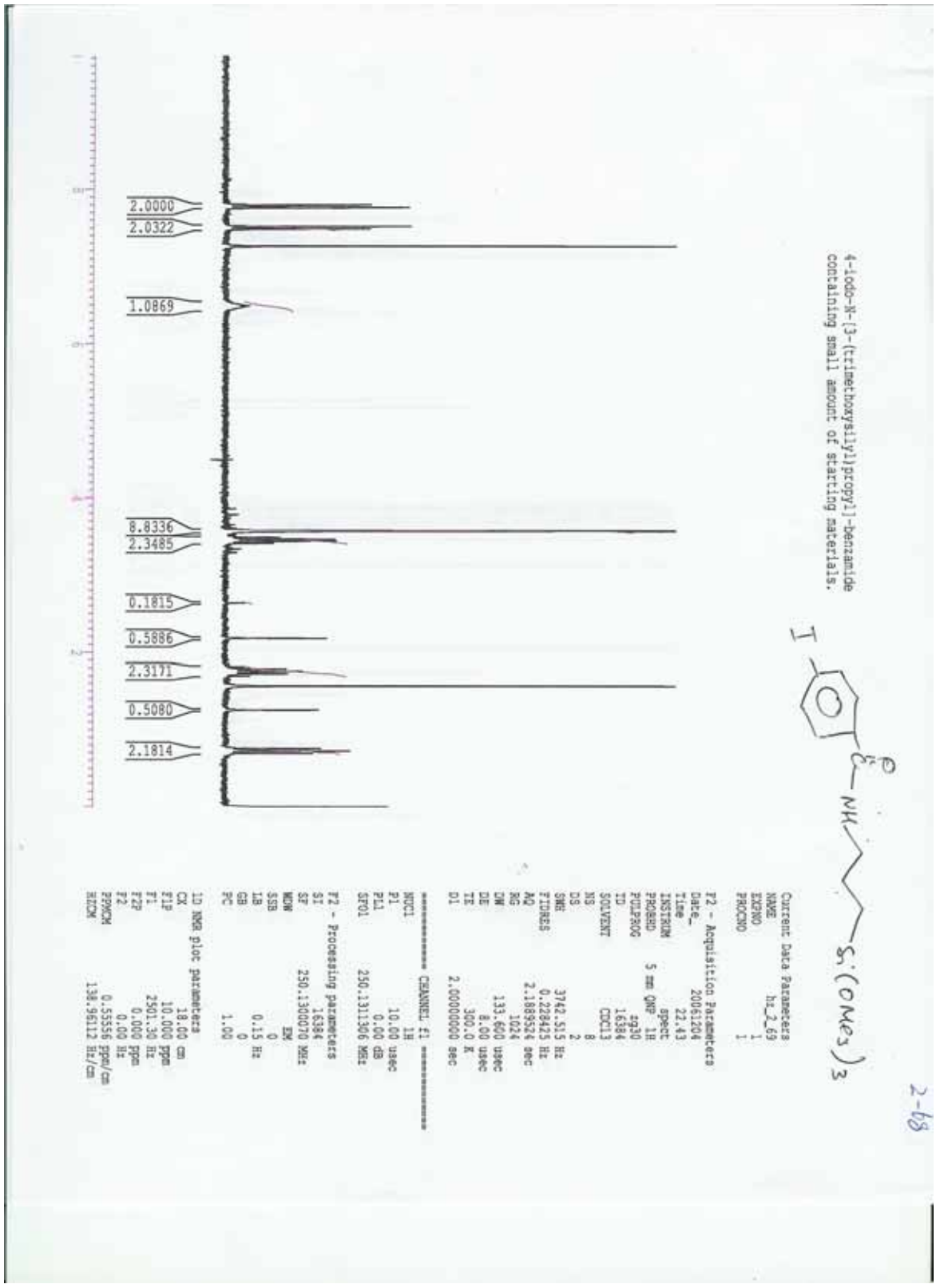

Figure A33. ^{1}H NMR of Compound **39**.

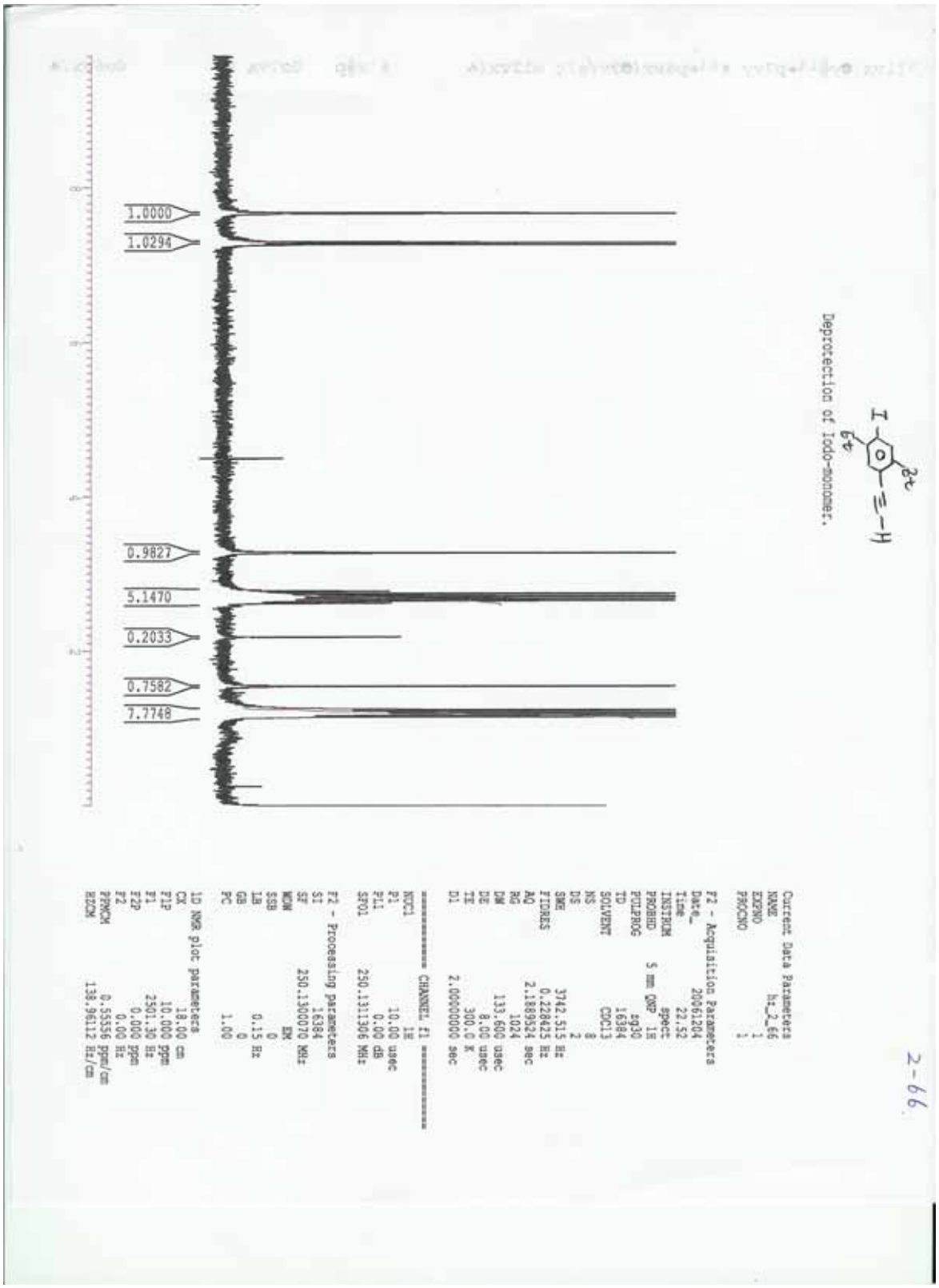

Figure A34. ^{1}H NMR of Compound **41**.

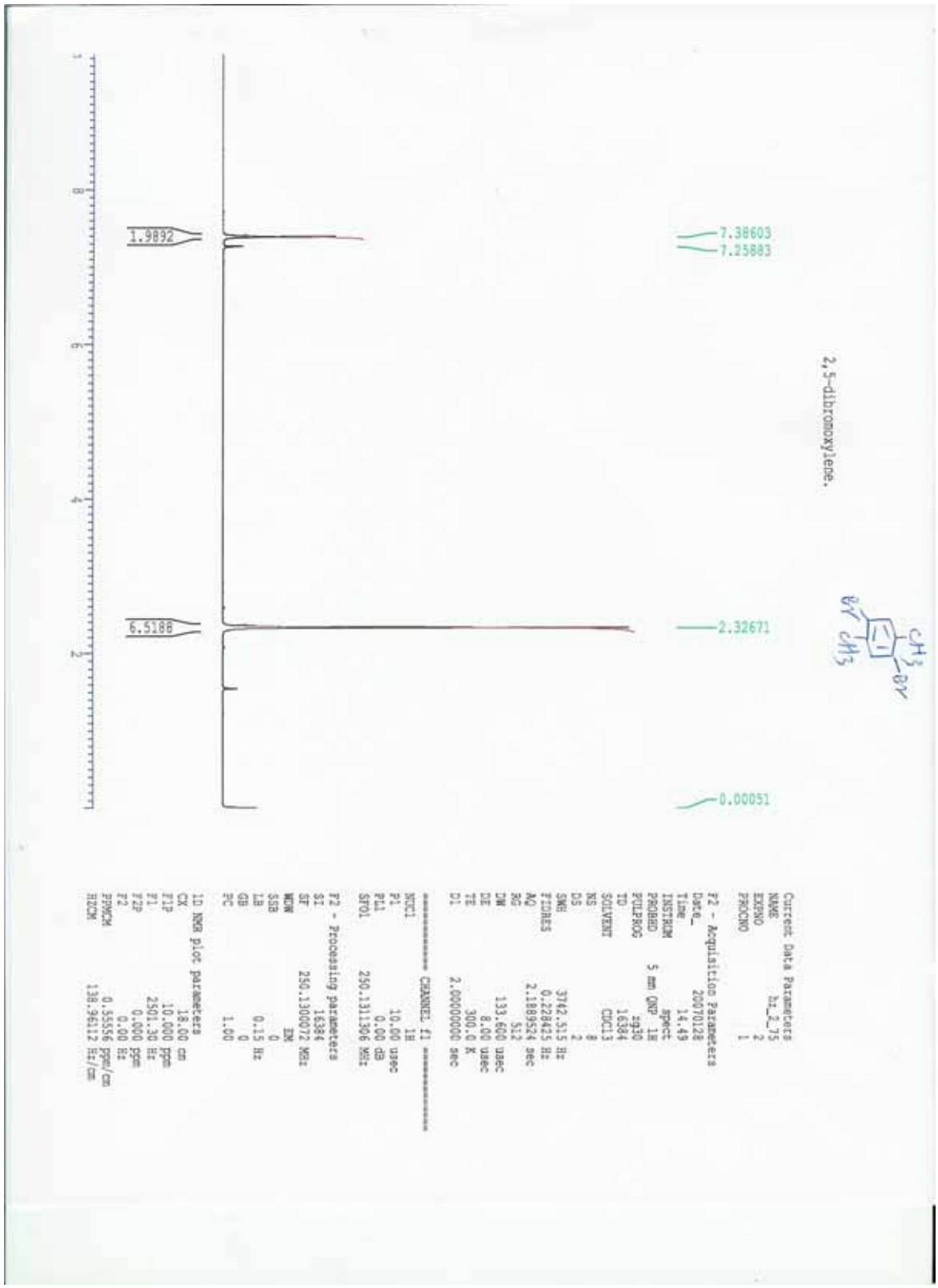

Figure A35. ^{1}H NMR of Compound **50**.

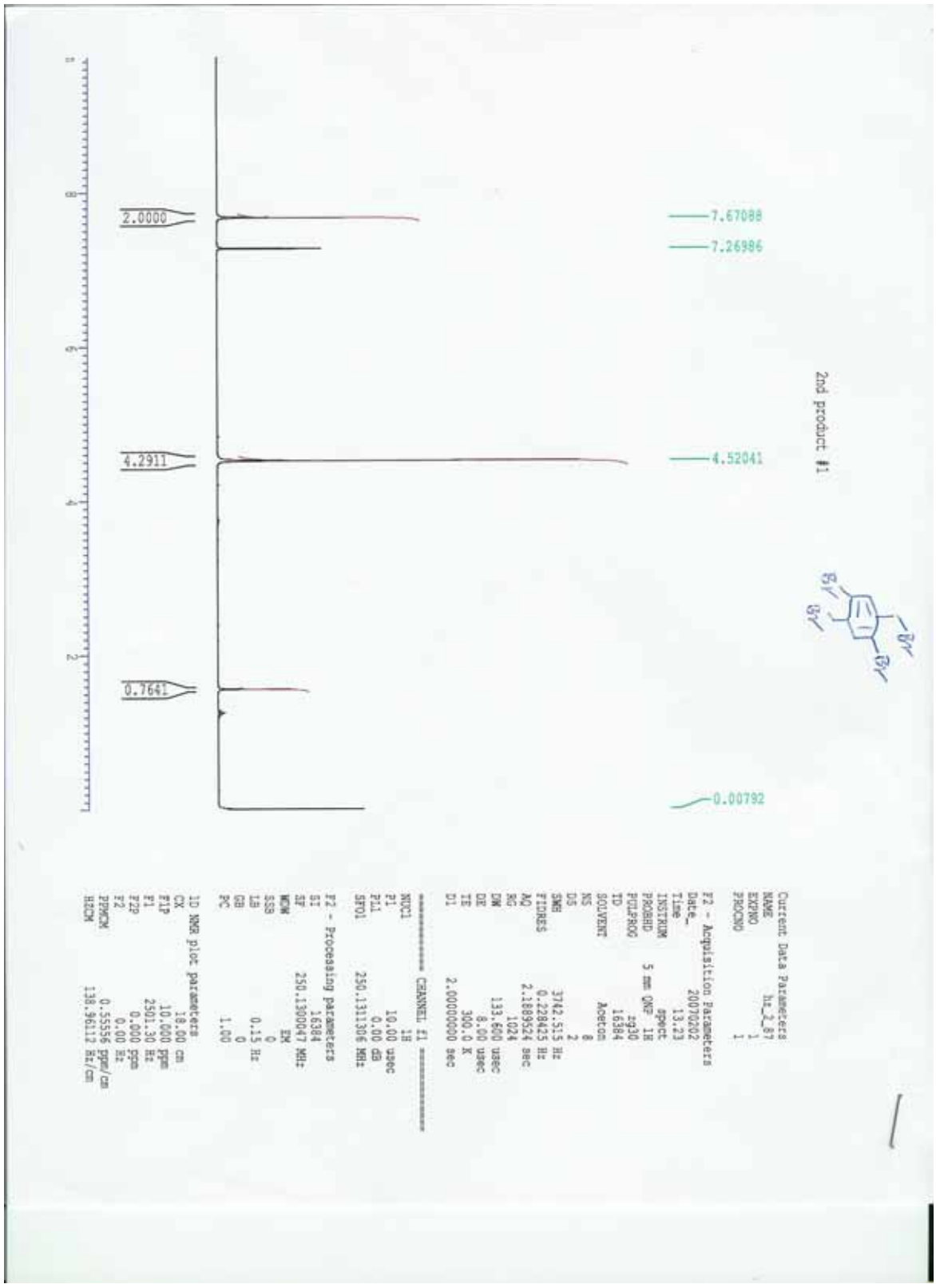

Figure A36. ^{1}H NMR of Compound **51**.

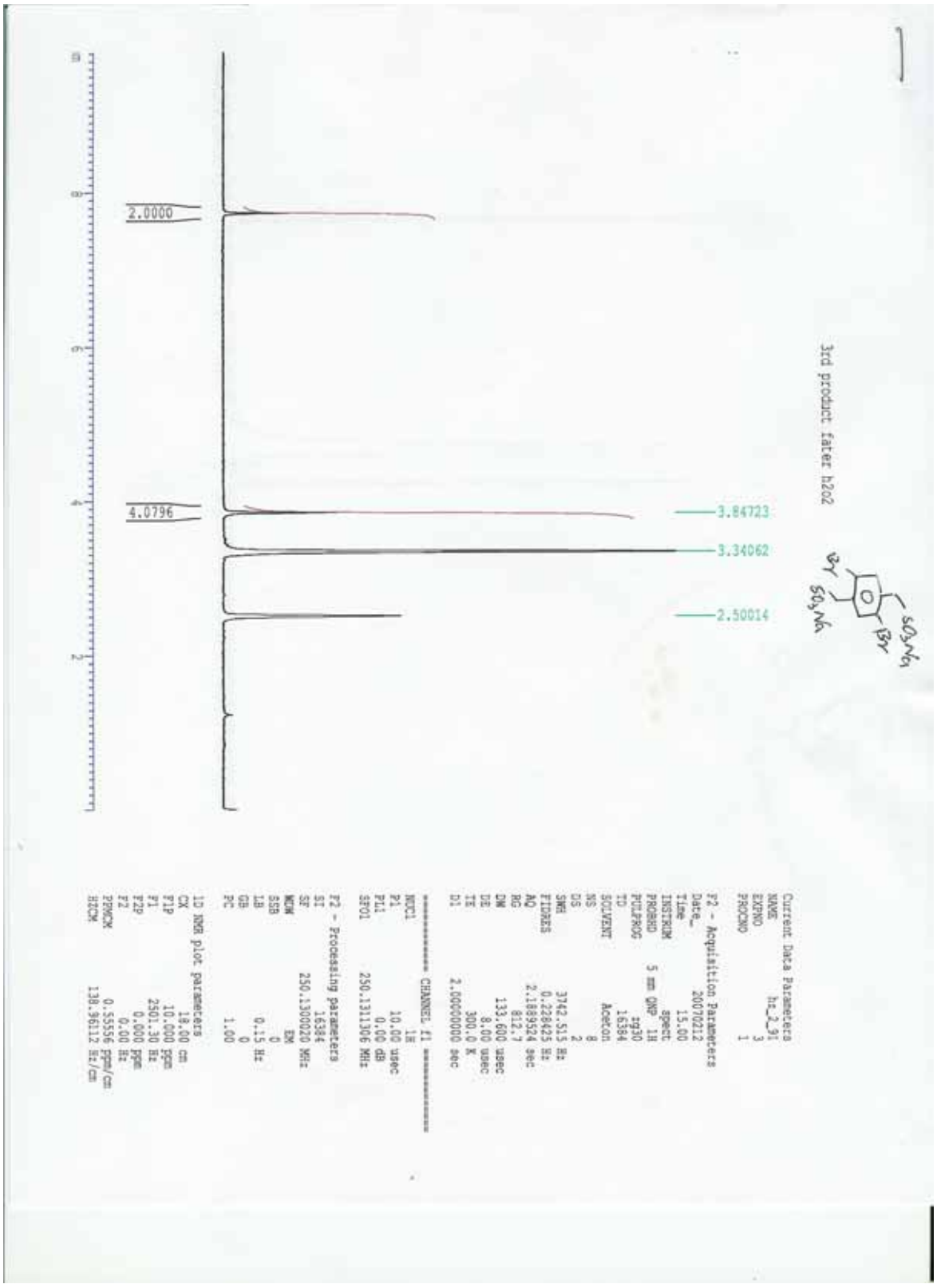

Figure A37. [1]H NMR of Compound **52**.

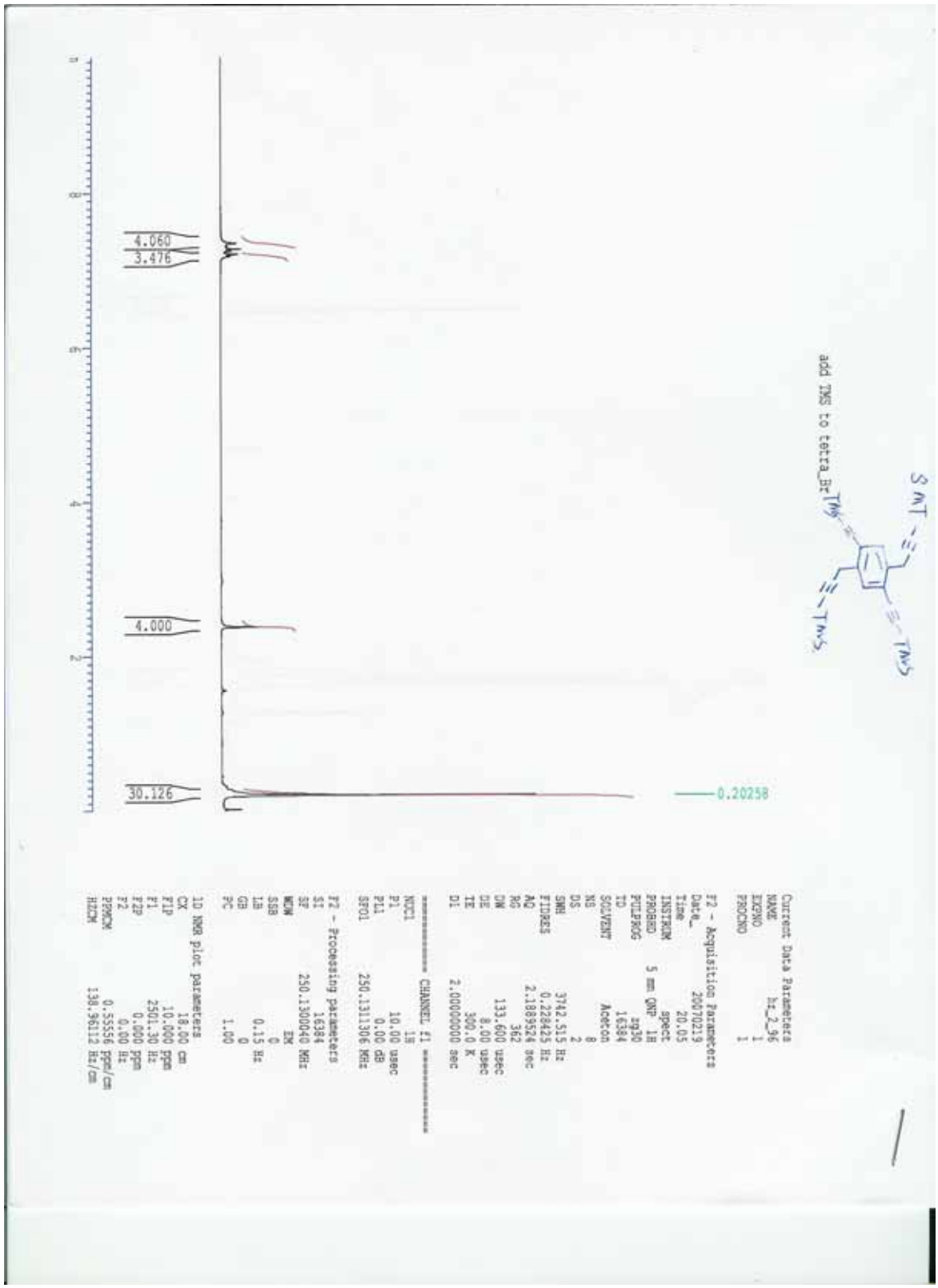

Figure A38. ^{1}H NMR of Compound **53**.

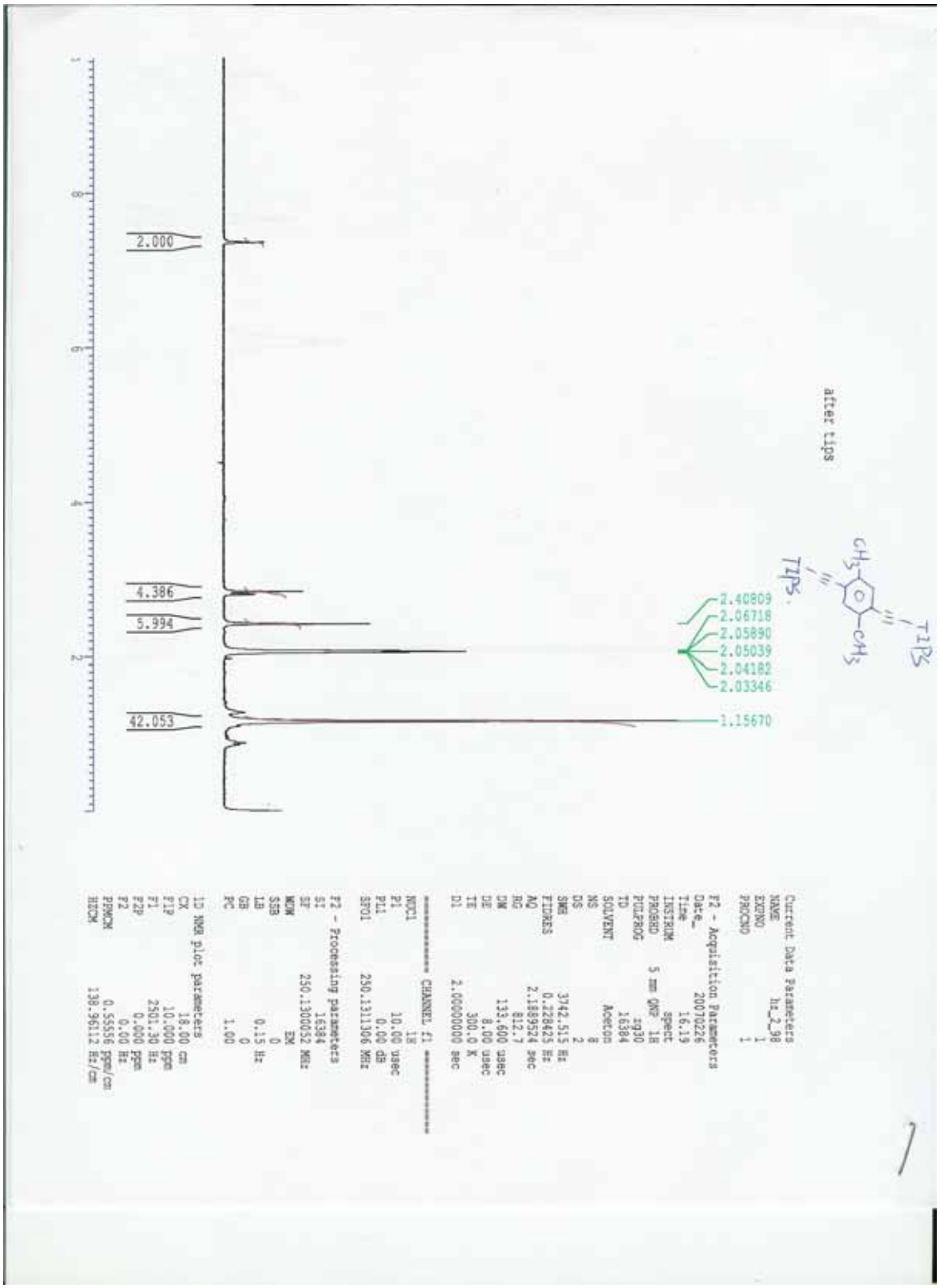

Figure A39. ^{1}H NMR of Compound **54**.

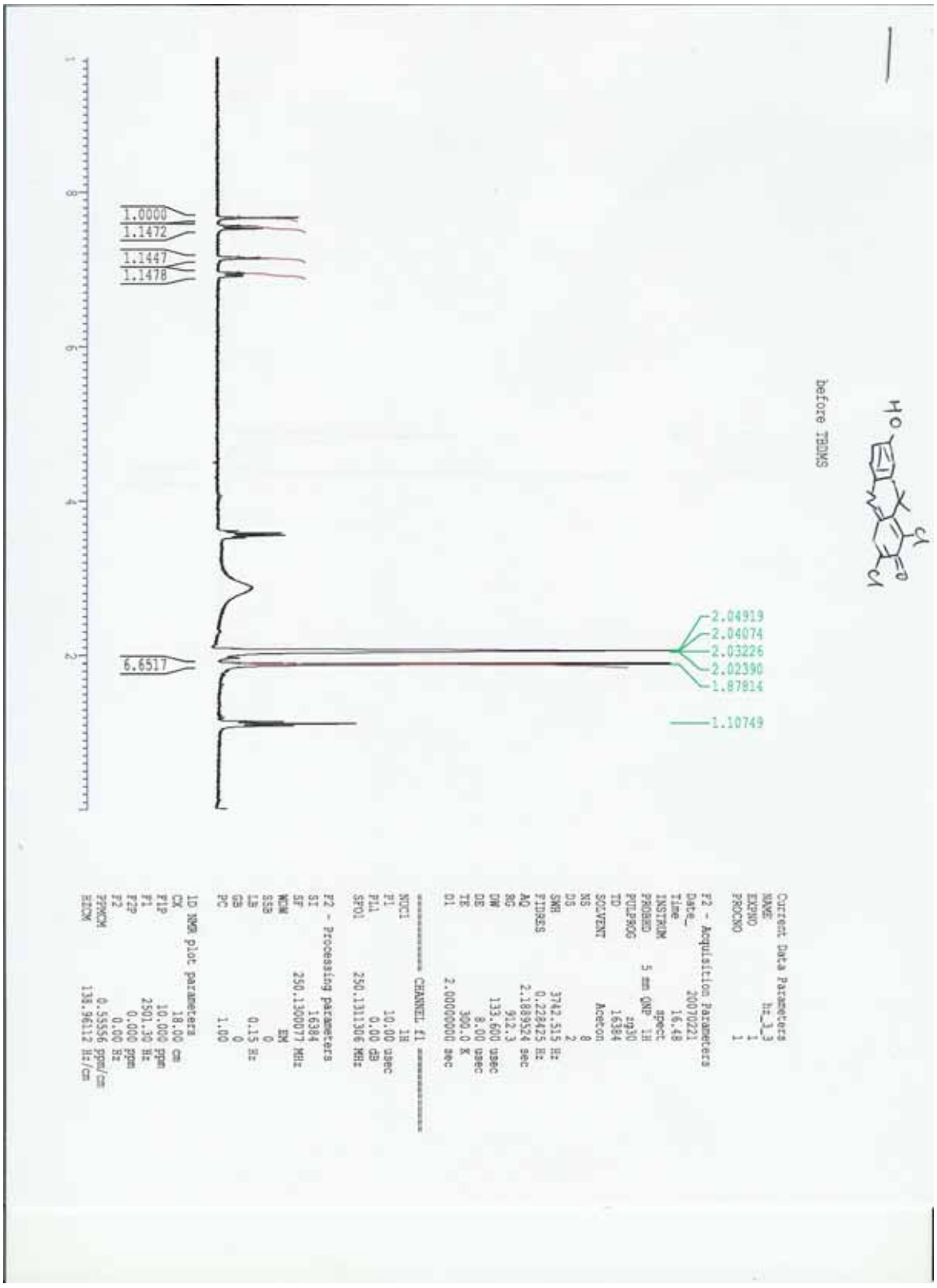

Figure A40. ^{1}H NMR of Compound **60**.

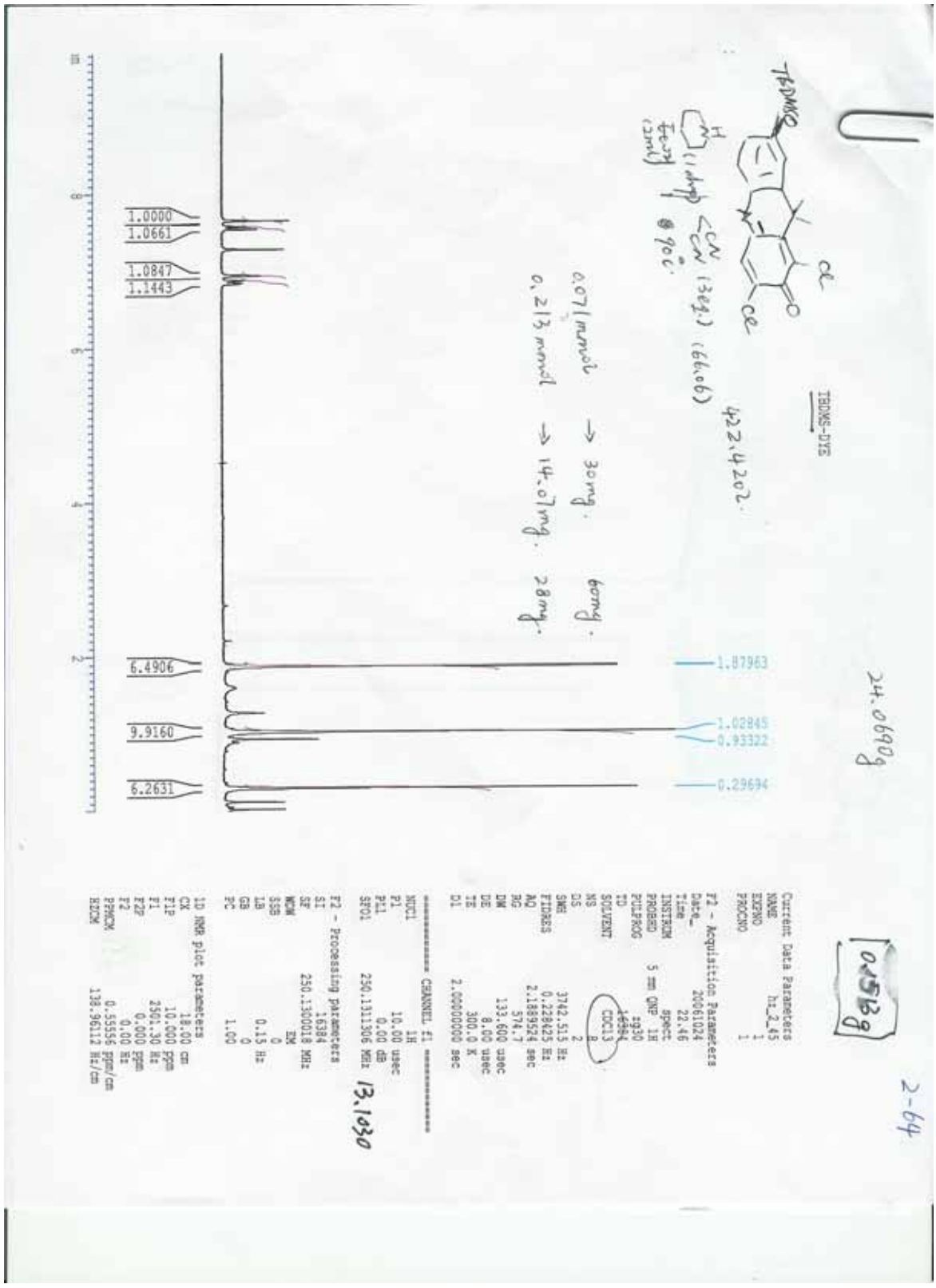

Figure A41. ^{1}H NMR of Compound **61**.

VITA

Huating Zhang was born in Xinzhou, Shanxi Province, the People's Republic of China, on October 16, 1978. She entered the Pharmaceutical Department of Shanxi Medical University in September 1997, where she received a Bachelor of Science degree in July, 2001. She joined the Department of Chemistry of the Louisiana State University in September, 2004. She will receive a Master of Science degree in chemistry in May 2007.